Transmission Line Parameters Estimation for Series Compensated Lines, Mutually Coupled Lines, and Short Length Lines Using Synchrophasor Measurements

A Dissertation

Presented in Partial Fulfillment of the Requirements for the

Degree of Doctor of Philosophy

with a

Major in Electrical Engineering

in the

College of Graduate Studies

University of Idaho

by

Ahmed M. Momen

Major Professor: Brian K. Johnson, Ph.D.

Committee Members: Herbert L. Hess, Ph.D.; Ahmed Abdel-Rahim, Ph.D.;

Abel Rahman Khatib, Ph.D.

Department Administrator: Joseph D. Law, Ph.D.

May 2019

Authorization to Submit Dissertation

This dissertation of Ahmed M. Momen, submitted for the degree of Doctor of Philosophy with a major in Electrical Engineering and titled "Transmission Line Parameters Estimation for Series Compensated Lines, Mutually Coupled Lines, and Short Length Lines Using Synchrophasor Measurements," has been reviewed in final form. Permission, as indicated by the signatures and dates given below, is now granted to submit final copies to the College of Graduate Studies for approval.

Major Professor: _____ Date: _____
Brian K. Johnson, Ph.D.

Committee Members: _____ Date: _____
Herbert L. Hess, Ph.D.

_____ Date: _____
Ahmed Abdel-Rahim, Ph.D.

_____ Date: _____
Abel Rahman Khatib, Ph.D.

Department Administrator: _____ Date: _____
Joseph D. Law, Ph.D.

Abstract

The accuracy of transmission line parameters' values is crucial for many power system applications such as power flow, relay settings, fault location, and voltage stability. Currently, there are many methods to estimate line parameters for both transposed and untransposed lines, but most of them consider only positive sequence parameters. Only a few published methods estimate positive sequence parameters for a series compensated line or for lines that are mutually coupled for part of thier length and operated at different voltage levels.

Most power systems in the world use phasor measurement units (PMUs) for data collection to at least a limited extent. Synchrophasor technology is used in this research to collect time synchronized measurements of voltages and currents as phasors at both ends of the line under test. This research develops a new method to estimate line parameters for a series compensated line. The errors in synchrophasor measurements resulting from low-frequency oscillation caused by the series capacitor response to a fault, was treated as bad data. The estimation was performed by creating different cases of unbalanced currents in the system and then using a Least Trimmed Square (LTS) estimator to detect and reject the bad data. Then, positive, negative, and zero sequence parameters were estimated using the weighted least square method. A comparison between Chi-squared approach, a conventional method to detect bad data, and the LTS has also been done.

The work also presents a new method to estimate the line parameters for mutually coupled lines operated at different voltages. Two separate sets of equations have been built to convert the non-linear equations to linear equations. One set of equations estimates the shunt capacitance and the second set estimates the series and mutual impedance of the targeted lines. The method is based on taking one of the lines out of service and creating different states of unbalanced conditions elsewhere in the system. The accuracy of current transformers introduces a challenge for estimating parameters for a shorter line. The LTS is used again to detect and reject the sensor measurements error for line with different ratios

of inductive reactance to resistance (X/R).

Initial simulations are performed using alternate transient program (ATP) to simulate the power system. Testing with two commercial synchrophasor units, a Real Time Digital Simulator (RTDS), a phasor data concentrator (PDC), and a GPS satellite-synchronized clock, is also used to validate the performance of the new method for series compensated lines. PSCAD/EMTDC simulation is used to validate the developed estimation method for the mutually coupled lines. The ability of the proposed methods to estimate line parameters will be evaluated along with assessing what would be needed to apply these techniques in practice.

Acknowledgements

Firstly, I would like to express my sincere gratitude to my advisor Prof. Brian Johnson for the continuous support of my Ph.D study and related research, for his patience, motivation, and immense knowledge. His guidance helped me in all the time of research and writing of this dissertation. I could not have imagined having a better advisor and mentor for my Ph.D study.

Besides my advisor, I would like to thank the rest of my dissertation committee: Prof. Hess, Prof. Abdel-Rahim, and Prof. Khatib, for their insightful comments and encouragement.

In addition, I would like to express my special appreciation and thanks to Dr. Yacine who helped and supported me.

I would like to thank my wife, Tahani, who has encouraged me and patiently allowed me to pursue this endeavor. None of this would have been possible without the support of her and my kids, Mohammed, Yazid, Moad, Motasm, Rakan, and Kenda.

Last but not the least, I would like to thank my family: my parents and to my brothers and sister for supporting me spiritually throughout writing this dissertation and my life in general.

Dedication

To my Mom Mabroka and my Dad Mohammed

To my wife Tahani and my kids

To my brothers and sisters

To the soul of my brother Momen

Table of Contents

List of Tables

List of Figures

List of Abbreviations

LFO	...	Low Frequency Oscillation
CT	...	Current Transformer
CCVT	...	Coupling Capacitor Voltage Transformer
LTS	...	Least Trimmed Squares
PMU	...	Phasor Measurement Unit
PSCAD	...	Power System Computer Aided Design
EMTDC	...	Electromagnetic Transients for DC
LCC	...	Line Constants Calculation
RSCAD	...	Real Time Simulation Computer Aided Design Software
GPS	...	Global Positioning Satellite System
PDC	...	Phasor Data Concentrator
HMI	...	Human Machine Interface
Mbps	...	Megabits Per Second
SEL	...	Schweitzer Engineering Laboratories

Chapter 1: Introduction

Having accurate line parameter information for power transmission lines is essential for many reasons. Distance relays use impedance information of the lines for proper zone settings. Inaccurate impedance information can lead to incorrect settings, resulting in under-reach/over-reach in response to faults. State estimation software uses line parameters for estimating the system states and operators use the results to make decisions that can impact system stability. A model with faulty parameters can lead to erroneous estimates of the state of the system. Another use of line parameters is in the location of faults in a transmission system. Fault locating algorithms use positive and zero sequence network information for locating faults. As such, it is essential that a line parameter estimation algorithm be accurate [1].

The line constants calculation method has been used for a long time by most utilities to compute transmission line parameters. This approach is based on equations that consider tower geometry, conductor type, earth resistance, line length, and conductor sag [2]. However, the accuracy of the line constants method could be off because of the difficulty in modeling different tower configurations, the actual geometric route of the line, conductor sag, ambient temperature, terrain variations, variations in earth resistivity, and mutual coupling with other lines. The accuracy of the estimation of line parameters is essential for modeling the power system, because the mismatch between reality and model-based expectations can degrade reliability and efficiency. Inaccurate models have contributed to a few major North American power outages, including for example, the August 10, 1996 WSCC outage. To prevent large-scale system events resulting from inaccurate models, the North American Electricity Reliability Corporation (NERC) has adopted reliability standards for periodic model validation and calibration. The standards are known as (MOD-032-1) and (MOD-033-1), which are applied to verify and assure the appropriate responses of power system models during system disturbances [3].

Installation of phasor measurements units (PMUs) has increased in North America in

the past decade. A PMU provides time stamped phasor values for voltage and current measurements from anywhere on a power system. These time stamped measurements are referred to synchronized phasor measurements or synchrophasors [4]. For the application at hand their outputs can be used to compute the line parameters accurately [5]. The measurements include precise voltage, current, power and phase angles measured at both ends of a line [6]. The development deployment of PMUs and their applications in wide-area measurement systems (WAMS) will provide synchronized measurements for parameter identification. PMU-based model validation and calibration are an accepted and cost-effective way to satisfy the requirements of NERC Reliability Standards MOD-032-1, and MOD-033-1 [3].

In order to increase the power capacity of transmission lines, series capacitors (SC) are installed on some transmission lines, which changes their effective line impedance. Series capacitors help improve system stability and reduce the voltage drop during disturbances. Installing a series capacitor costs between 15 and 30 percent of the cost installing a new line [7]. On the other hand, adding series capacitors introduces many challenges for line protection. For some fault locations, the effective impedance of the line between the relay and the fault will be capacitive, which leads to voltage inversions and possibly current inversions. In addition, the transient response at the onset of the fault includes low-frequency oscillations which affects the quality of the effective line impedance calculation which can cause a distance relay to misoperate as well complicating locating the fault [8]. One of the objectives of this research is to accurately estimate zero and positive sequence impedances for a series compensated line whether the line is transposed or untransposed. Both lumped and distributed parameter models will be used in an electromagnetic transients program simulation for testing and comparison.

To increase the amount of transferred power, utilities often either build a new transmission line or add a series capacitor on an existing line. If adding series capacitors is not enough to meet the required transferred power, building a new line is another option. Utilities take advantage of the existing right-of-way to avoid the cost and trouble of getting a new right

of way. Many lines share the same right-of-way, sometimes on the same tower. There are several different options for parallel line configurations [9]. The first case is when two lines are running parallel at the same voltage from one bus to the next bus as shown in Figure 1.1

In the second case, as the lines leave the bus, they are parallel for part of the distance. They leave the substation together, and they are of the same voltage, same circuit, and following the same right-of-way for a distance, but they ultimately have different destinations as shown in Figure 1.2

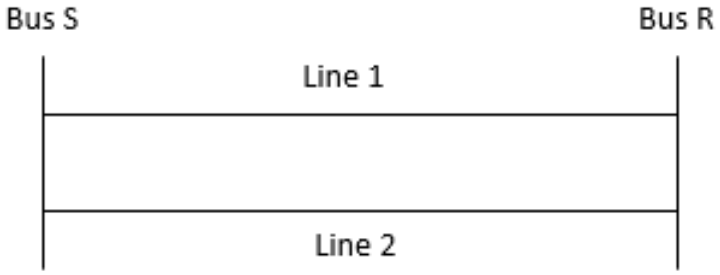

Figure 1.1: Parallel transmission line bused at both ends where both line are electrically and magnetically coupled

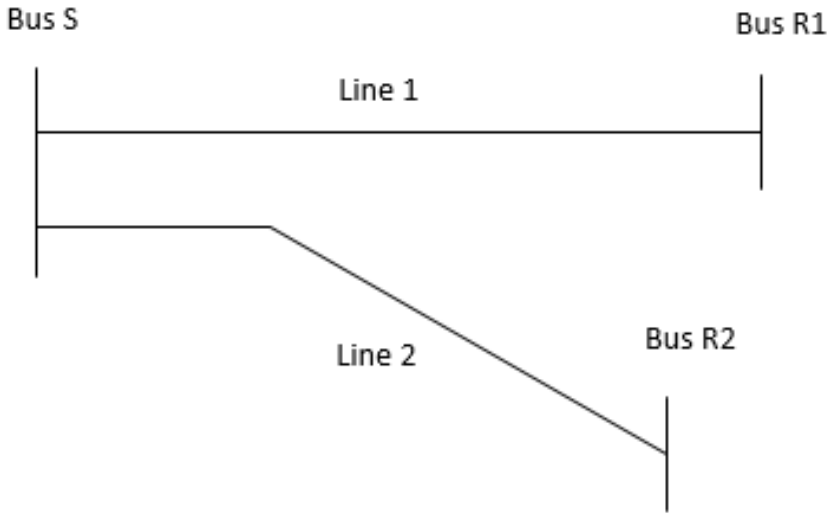

Figure 1.2: Parallel transmission line bused at one end where both lines are electrically and magnetically coupled

Another option is when different transmission lines have different voltages. They may not be parallel for the entire length of either line between the substations, but they are going to be in parallel with each other for a some distance. Parallel lines are mutually coupled, which means a ground fault in one line induces voltage drop and current flow in the other line. Mutual coupling must be accounted for when calculating line parameters since the mutual coupling factors are required for many applications using line parameters. The PMU data reflect these effects and can be used to calculate the full set of parameters. This research focuses on the third case of mutual coupling. Fig.1.3 shows the representation of a case with a single line to ground fault on line 1, which induces a zero sequence current in the other line flowing in the opposite direction. The induced zero sequence current impacts the quality of PMUs measurements [10].

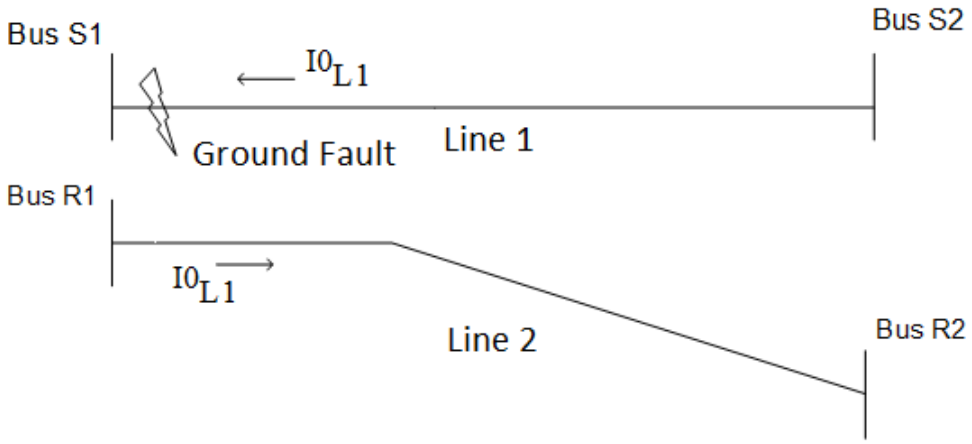

Figure 1.3: Parallel Transmission Line With Lines that are Magnetically and Capactivily Coupled but not Electrically Coupled

A second objective of this theses is to develop a method to estimate line parameters of mutually (magnetically and capacitively) coupled lines that are not electrically coupled and are parallel for part of the distance.

Error in the current transformer output (CT) presents a challenge for estimating the parameters, especially in cases with shorter lines. Since a zero sequence unbalance in the system is needed for the estimation purposes, a nearby fault which could cause the CT to saturate. Including the measurements during the saturation in the estimation calculation

leads to inaccurate values. These CT errors complicate angle measurements which leads to error in line parameter estimation. C-class protection CTs can have an error of up to 3% steady state conditions, which can also cause challenges for parameter estimation for shorter length. In this research a new method was developed to detect and reject the errors in the data whether they are from the CT saturation or not.

1.1 Objectives

1. Develop a method to estimate line parameters using measurement data from faults occurring on series compensated lines or elsewhere in the system, and provide a method to overcome the effects of the transient response of series compensated line to the fault on the estimation.
2. Develop a method to estimate the parameters for lines that are mutually coupled, including cases that are magnetically and capactively coupled but not electrically coupled.
3. Develop a method to overcome measurement errors in PTs, and CTs, to accurately estimate the line parameters, especially for shorter lines.

A general overview of low frequency oscillations, mutually coupled lines, and short length line sensitivity to CT error is discussed in Chapter 2. Also Chapter 2 gives a literature review of the state of the art in line parameter estimation from the research community. Chapter 3 gives a general review of the transmission line parameter calculations and the impacts of their accuracy on power system. Synchronized phasor measurements technologies are described in Chapter 4. Chapter 5 is an accepted paper in IEEE Transactions on Power Delivery, which presents a method to estimate parameters for series compensated line in presence of LFO [11]. The chapter also gives a comparison between a classical Weighted Least Squares (WLS) approach and the proposed Least Trimmed Squares (LTS) approach. The proposed method is validated using hardware-in-the-loop simulation for both transposed

and untransposed lines. New methods for mutually coupled lines that are parallel for part of distance and magnetically and capacitively coupled but not electrically coupled are developed in Chapter 6. One method is applied for two mutually coupled lines that are each transposed and the another method is applied for two mutually coupled lines that are each untransposed. Chapter 7 is a paper that was presented at Innovative Smart Grid Technologies (ISGT) conference discussing the effect of CT saturation and the impact of line X over R ratio on parameter estimation for a short length line [12]. A new method based on LTS is developed and validated with PSCAD simulation. Chapter 8 presents a summary, conclusions, and recommendations for future work.

Chapter 2: Literature Review

2.1 Past Work and Problem Description

Several methods have previously been proposed to identify transmission line parameters using phasor measurement units (PMUs). The concept of synchronized phasor measurements was introduced in 1980 [4]. PMU technology and wide area measurement systems (WAMS) opened a new way to estimate transmission line parameters from live measurements [13]. PMUs provide precise, time synchronized voltage, current, and power measurements at a different location in a power system. The availability of PMUs in a wide area network gives an opportunity for live parameter estimation [14]. The Newton-Raphson method was utilized to solve non-linear equations to calculate line parameters using measurements data collected from PMUs [15].

The author of [16] proposed a non-iterative algorithm to determine positive sequence parameters under steady-state load conditions. Positive sequence parameters were calculated using voltage and current measurements from PMUs at both ends of the line. In [17], unfaulted data from PMUs was used to determine the positive sequence line parameters after rejecting bad data. Four methods to estimate line parameters were presented in [18]. The methods were based on using a number of PMU measurements and then linear and non-linear regression approaches were used to estimate the line parameters. Application of the Total Least Squares (TLS) method to estimate line parameters was proposed in [19]. The authors proposed a moving window technique using voltage, current, as well as active and reactive power measurements from PMUs and to estimate the positive sequence parameters to build an equivalent π model for the line.

The author of [20] uses the least squares method to solve linear equations to estimate the line parameters for both a compensated line and an uncompensated line. The estimation was performed under steady state conditions. An optimal estimator was used for detecting and identifying the measurement error. The effect of low frequency oscillation as a response for the series capacitor during faults has not been considered in the reviewed literature and the

estimation was only done for positive sequence parameters. In [20], the chi-squares method was utilized for detecting bad data. The Chi-squares approach can only detect measurements with current errors but not measurements with voltage errors. A traveling wave technique was used in [21] for estimating parameters of a series compensated line. The method utilized synchronized time-domain data recorded at the terminal of the line. The method was able to accurately estimate the line parameter for any lines with different series devices. However, only the positive sequence parameters were estimated and detection, and correction of bad measurements was not considered.

In [22] the currents and the voltages were measured by a PMU at one end of compensated line and the measurements at the other end were obtained from the SCADA system. The authors used a nonlinear weighted least squares error approach for the estimation. The estimation was performed for transposed line only and the measurement error detection has not been considered. In [23] the positive sequence parameters of series compensated line were estimated. The author of [23] utilized the measurements from the PMUs at both ends of the line. An optimal estimator was used to detect measurements error in voltage and current.

Only a few of the papers addressed estimating parameters for series compensated lines. The few papers which considered series compensated lines estimated only the positive sequence series impedance, and they did not estimate the shunt capacitance impedance. The shunt capacitance is very important for setting some protection elements such as a line current differential element. Another issue with the series compensated line is the low-frequency oscillation if there is a fault close to the capacitor. The low-frequency oscillation interacts with the voltage and the current at both ends of the compensated line and is only partially attenuated by the digital filter in the PMUs, which leads to inaccurate line parameter estimation. The authors of [24] considered the effect of low-frequency oscillation (LFO) on the line parameter estimation and used a conventional Chi-square method to detect and reject the measurements affected by the LFO as bad data. However, the paper estimated only

the positive sequence impedance and ignored the zero sequence impedance. Also, it did not estimate the shunt capacitance for the compensated line.

Many different methods have been proposed in the past to estimate the line parameters for mutually coupled lines. The authors of [25] used different loading conditions to calculate positive sequence parameters. External ground faults were simulated to estimate the zero-sequence parameters. The authors stated that the required number of generated faults should be at least equal the number of lines for which the parameters are to be estimated. The singularity feature is used to check whether the solution is acceptable or not. The transmission lines were bused at one end and had different destinations. In [26] the sequence impedances were calculated for double circuit transmission lines bused at both ends where each line was transposed. One line was disconnected, and the unbalanced state was created from an external ground fault. Both zero-sequence series impedance and zero-sequence shunt capacitance were calculated in [27]. The lines were parallel for the entire distance, and wide area measurements system (WAMS) provided the voltage and current measurements. The telegraph equations were used for the estimation. The authors of [28] utilized the least squares method to solve a set of equations to estimate the zero sequence parameters of double circuit transmission lines including zero sequence mutual coupling. The lines were bused at both ends and parallel for the whole distance. A chi-square method was used to detect bad data from the PMUs.

The papers listed above did not consider cases when the coupling was present only for a part of the lines length, and cases where the lines were not electrically coupled. The parameter estimation of mutually coupled lines that are not electrically connected has been done in [29]. The author used orthogonal distance regression for estimating the zero sequence impedance. However, the estimation was done only for transposed lines.

The sensitivity of the parameter estimation to current transformer (CT) errors in short lines presents a challenge for estimating line parameters [30]. Depending on a number of measurements, the author of [31] applied four different methods to estimate the short line

parameters. The least squares method and Jacobian methods were used in the estimation to reduce the measurement noise. The method did not consider the CT error effects on the estimation. The authors of [32] proposed a repeated estimation method to reduce the effect of PMU measurement noise on parameter estimation. Two different types of noise were considered, systematic and random. The study was for a medium line model, but it did not consider the impact of CT saturation on the estimation. A nonlinear estimation method was used in [17] to create an optimal estimator of line parameters. The unbiased noise from the PMUs was considered and eliminated as bad data. The method was applied to a transposed line and only a positive sequence transmission line model was considered. In [33] the parameters for both transposed and untransposed lines were determined for the long line models. The methods discussed above were applied for either a long line or a medium line model parameters but they did not consider a short line with the CT error.

2.2 Problem Overview

2.2.1 Series Compensated Line Parameters Estimation

The power demand is increasing all over the world. To meet that demand, the transmission systems need increased transfer capacity. One way to increase capacity is to apply series compensation on transmission lines. Installing a series capacitor increases the transfer capacity power of a transmission line. The power transfer equation is shown in (2.1). Adding the series capacitor (SC) reduces the effective reactance of the line, which increases the power transfer.

$$P = \frac{|V_S|.|V_R|}{X_L - X_C} sin(\delta) \tag{2.1}$$

Where:

V_S is the sending end voltage

V_R is the receiving end voltage

X_L is the series inductive reactance of the line

(δ) is the phase angle between V_S and V_R

X_C is the series capacitor

Also installing series capacitors can improve power system stability. Typically installing series capacitors costs between 15 to 30 percent of the cost of building a new line [7]. On the other hand, the presence of series capacitors presents challenges for transmission line protection, with the potential to cause voltage, and in some cases current inversions as well as creating low-frequency oscillations during faults occurring close to the capacitor. These behaviors also impact the quality of line parameters estimation. There are two options for the location of the series capacitor in the line. The first option is to install the capacitor at one end of the line and this is a typical location, because of the available space in the substation. Having the capacitor at one end of the line will reduce the installation cost but presents some protection problems. Another option is to install capacitor at one end of a

line. The other option is to install the capacitor at the middle of the line, which increases the cost of the installation but reduces the protection problems. Figure (2.1) shows the transmission line with SC at one end of the line.

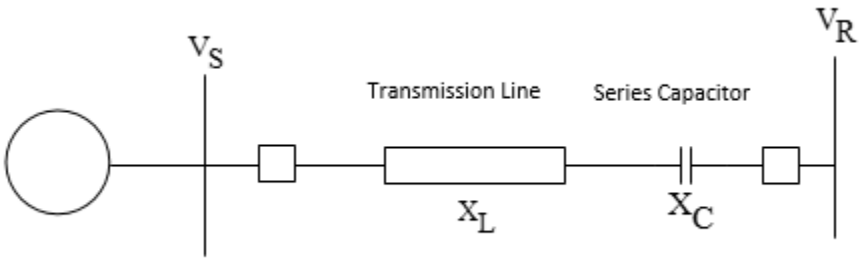

Figure 2.1: Transmission line with series capacitors at one end.

This research focuses on the impact of low-frequency oscillation on the line parameter estimation. The natural frequency of the response of a series compensated line during a fault can be determined from equation (2.2), where f is the power system frequency and X_L is the line reactance. If the fault is at remote end of the line, which means $X_L > X_C$, the RLC circuit produces a decaying low-frequency resonance in the fault current, which superimpose 60 Hz component with natural frequency of series RLC circuit, which is often less than 60Hz.

$$f_e = \frac{1}{2\pi\sqrt{LC}} = f\sqrt{\frac{X_C}{X_L}} \tag{2.2}$$

The resulting low-frequency envelope around the 60Hz response will impact the V_{rms} measurement and the I_{rms} measurement as well. Typically digital relays use cosine filters with low pass anti-aliasing filter, which gets rid of high-frequency natural response but not the low-frequency response. The filter is designed to reject direct current DC along with decaying dc offsets as well. However, the natural frequency of the RLC circuit is between DC and $60Hz$, which is going to be attenuated by the cosine filter and amplified by the low pass filter [8]. The LFO impacts V_{rms} and I_{rms} such that the fault trajectory of a distance element will appear to spiral in impedance plane which leads to inaccurate line parameter

estimation. For example, if there is a line without series capacitor SC and a fault occurs at the remote end of that line, the impedance trajectory as samples from the digital filters of a mho relay are processed will move from the load impedance toward the fault impedance in a straight line as shown in Figure 2.2.

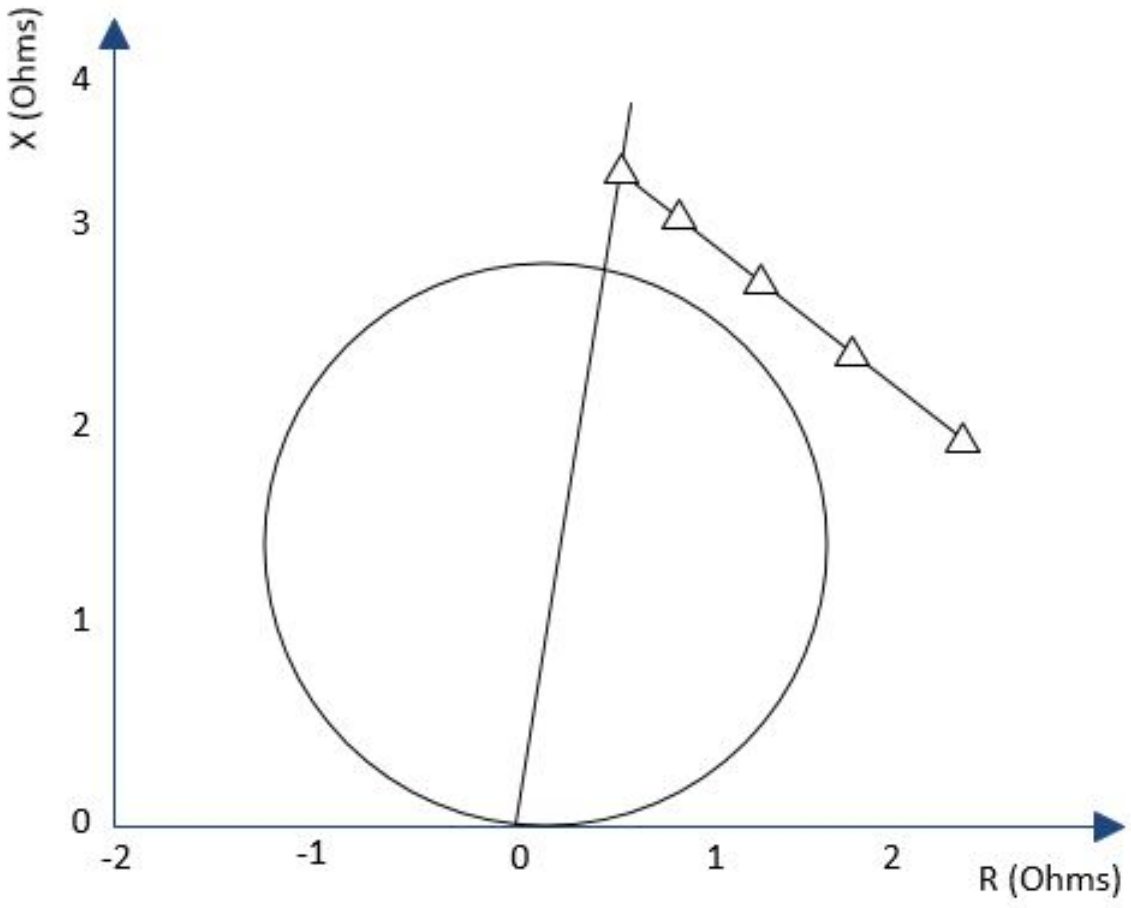

Figure 2.2: Mho relay response for line without series capacitor

This is not the case if a series capacitor is added on the line. The capacitor will lower the effective reactance of the line, and when the target from the relay comes in, it is going to tend to spiral into the fault point as shown in Figure 2.3. Note that the zone 1 circle was set shorter due to the series capacitor. The *rms* voltages and currents will vary with time due to the low frequency oscillation.

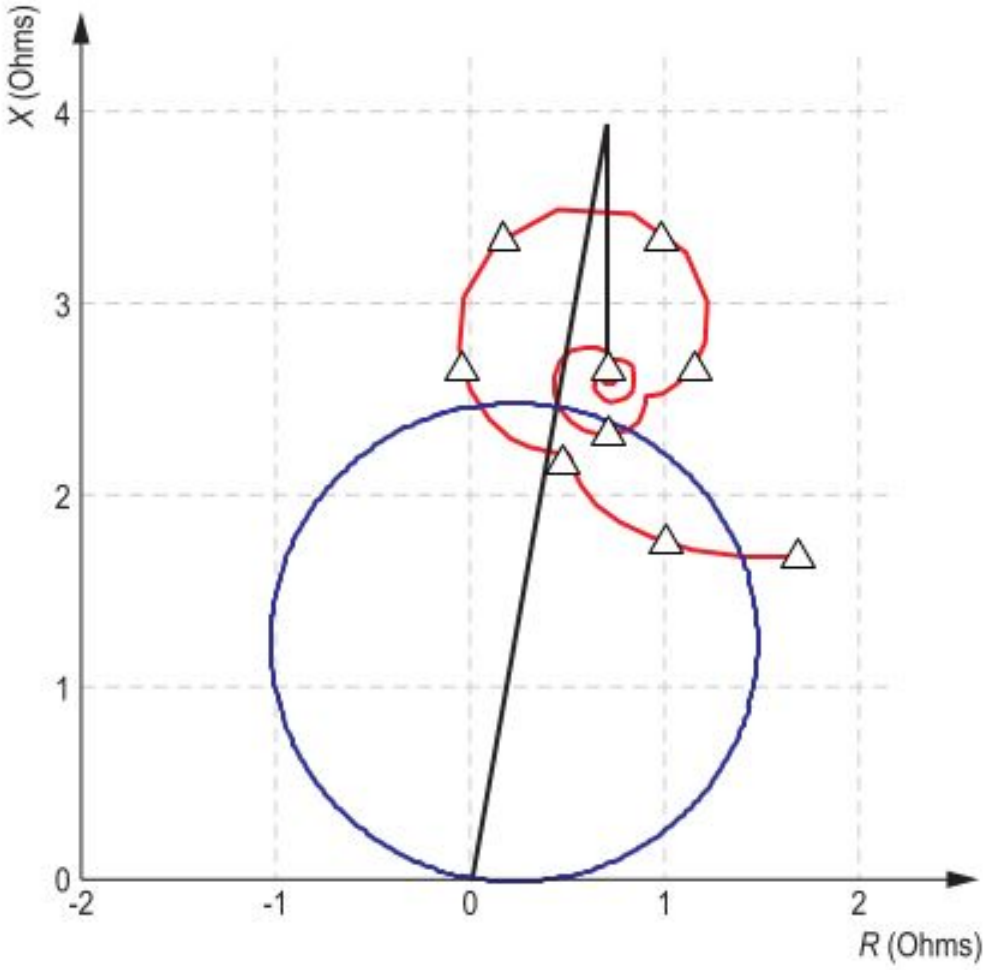

Figure 2.3: Mho relay response for line with series capacitor
[8]

2.2.2 Mutually Coupled Line Parameters Estimation

Two transmission lines, and sometimes more, may share the same right of way because of the cost and difficulties with getting a new right of way. In the case of balanced positive-sequence current, the sum of the flux linkages due to the balanced currents will be nearly zero once they get outside of the phase conductors, because they are 120° out of phase. Thus, positive- and negative-sequence type mutual coupling is very weak and is typically neglected. Zero-sequence flux linkages are always going to add, and the zero mutual coupling could be as high as 50%-70% of the zero sequence self-impedance Z_0 [34].

A ground fault in one of the lines induces zero sequence current in the unfaulted line (or lines) in the opposite direction. Most of the parameter estimation methods are based on the current and voltage measurements at both ends of the targeted line. The mutual zero-sequence current impacts the accuracy of the line current and terminal voltage measurements. The line parameter estimation must correctly calculate these inductive and capacitive mutual coupling terms from these voltages and currents so protection engineers can account for them setting relays.

There are many types of configurations of parallel lines as mentioned in Chapter 1. This research focuses on case with two lines that a parallel for part of the line length and are not electrically coupled as shown in Figure 2.4.

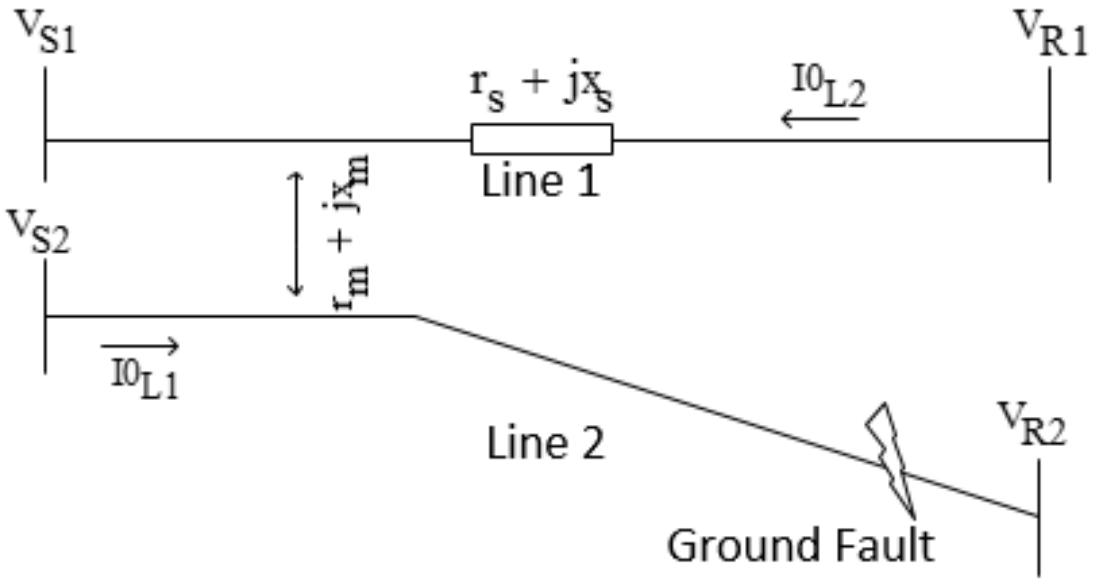

Figure 2.4: Parallel transmission line with different voltages

While positive-positive, negative-negative, positive-negative, positive-zero, and negative-zero coupling varies with transpositions, the zero mutual term always exists whether the lines are transposed or untransposed [35]. However, the magnitude may change depending on the geometry and voltage level [35]. Equation (2.3) represents the sequence impedance matrix for two fully individually transposed lines. In this case the set of the equations to

solve for parameter identification is linear with five unknowns.

$$Z_{transposed-seq} = \begin{bmatrix} Z_{00} & 0 & 0 & Z_{00m} & 0 & 0 \\ 0 & Z_{11} & 0 & 0 & 0 & 0 \\ 0 & 0 & Z_{22} & 0 & 0 & 0 \\ Z_{00m} & 0 & 0 & Z_{00'} & 0 & 0 \\ 0 & 0 & 0 & 0 & Z_{11'} & 0 \\ 0 & 0 & 0 & 0 & 0 & Z_{22'} \end{bmatrix} \tag{2.3}$$

In case only one line is transposed, equations (2.4) and (2.5) represent the phase and the sequence impedance matrices respectively. The equation results used to perform the estimation are now non-linear with eight unknowns, which can not be solved by any linear method such least squares (LS) and total least squares (TLS) [29]. The unbalanced condition needed to produce measurement data for the estimation would be a ground fault. However, some lines may go years without experiencing faults, so relying on internal line faults to provide unbalanced conditions for parameter estimation is not a practical approach.

$$Z_{phase} = \begin{bmatrix} Z_{aa} & Z_{ab} & Z_{ac} & Z_{aa'} & Z_{ab'} & Z_{ac'} \\ Z_{ab} & Z_{bb} & Z_{bc} & Z_{ba'} & Z_{bb'} & Z_{bc'} \\ Z_{ac} & Z_{bc} & Z_{cc} & Z_{ca'} & Z_{cb'} & Z_{cc'} \\ Z_{a'a} & Z_{a'b} & Z_{a'c} & Z_{a'a'} & Z_{a'b'} & Z_{a'b'} \\ Z_{b'a} & Z_{b'b} & Z_{b'c} & Z_{a'b'} & Z_{a'a'} & Z_{a'b'} \\ Z_{c'a} & Z_{c'b} & Z_{c'c} & Z_{a'b'} & Z_{a'b'} & Z_{a'a'} \end{bmatrix} \tag{2.4}$$

$$Z_{012} = \begin{bmatrix} Z_{00} & Z_{02} & Z_{01} & Z_{00'} & 0 & 0 \\ Z_{10} & Z_{11} & Z_{12} & 0 & 0 & 0 \\ Z_{20} & Z_{21} & Z_{22} & 0 & 0 & 0 \\ Z_{0'0} & 0 & 0 & Z_{0'0'} & 0 & 0 \\ 0 & 0 & 0 & 0 & Z_{1'1'} & 0 \\ 0 & 0 & 0 & 0 & 0 & Z_{2'2'} \end{bmatrix} \tag{2.5}$$

2.2.3 Short Line Length Parameter Estimation

Sections 2.2.1 and 2.2.2 discussed two factors that impact the parameter estimation accuracy. Another significant factor is current transformer CT and voltage transformer VT errors. These effects are more pronounced for shorter lines. In addition these are often sources of measurement noise in the PMUs' instrumentation channel [32]. The impact of measurements error is more pronounced for shorter lines because the total series impedance and shunt capacitance terms are smaller. The error can have a more significant impact on resistance or line angle calculation for lines with high ($\frac{X}{R}$). The PMUs' instrumentation channel can be defined as the equipment between the PMU and the phase conductor, including current transformers, voltage transformers, attenuators, and the signal cable. The PMUs' instrumentation channel is shown in Figure 2.5.

CT saturation is a common source of error in current transformers for cases with large fault currents or slowly decaying dc offsets. CT saturation is expected as a transient response to close-in faults with high X over R ratios . For the purposes of this work, saturation can lead to a significant error in current measurements coming from PMUs, negatively impacting the accuracy of line parameter estimation [37]. Figure 2.6 shows a CT equivalent circuit model referred to the secondary side. Ideally, all the secondary current should go through the burden Z_b. The magnetizing branch will start to saturate because of the change in the permeability due to large level of flux. Increasing flux will decrease the permeability, which

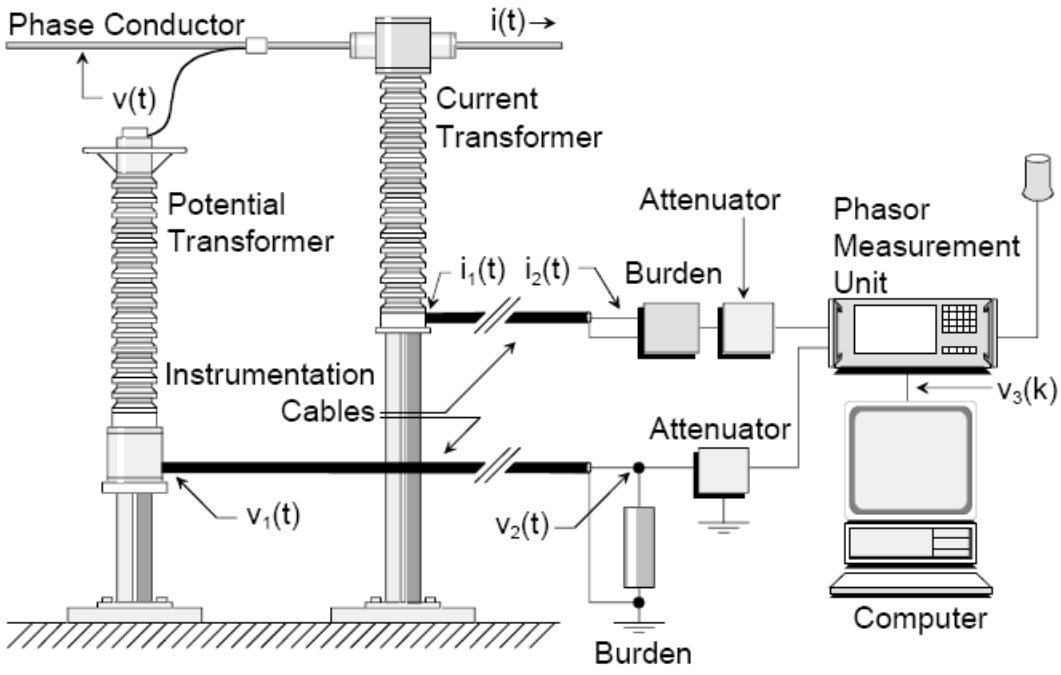

Figure 2.5: Typical potential and current instrumentation channels [36]

means decreasing the inductance of the magnetizing branch, so some of the ratio current(the primary current referred to secondary) ($\frac{I_P}{n}$) goes through it instead of to the burden for part of the sinusoidal cycle. I_P is primary current of the CT and n is the transformer turns ratio.

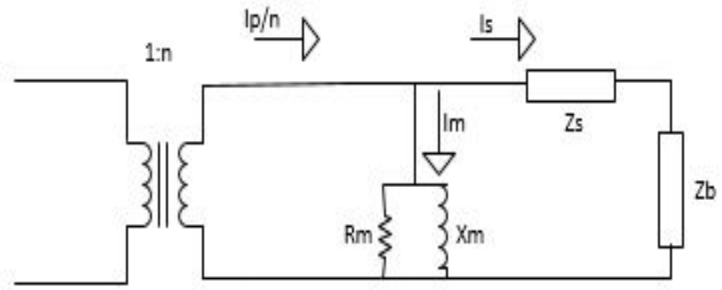

Figure 2.6: Current transformer model with impedances referred to secondary side

Equation (2.6) shows the relation between the permeability and the inductance of the magnetizing branch.

$$L_m = {N_s}^2.(\frac{\mu.A}{l}) \tag{2.6}$$

Where L_m is the inductance of the magnetizing branch, A is the cross section area of the core, l is the length of the flux path, and μ is the permeability.

Often, faults happen near voltage maximum, which tends to reduce the dc offset. However, if a fault happens near minimum voltage, there could be a large dc offset, increasing unidirectional flux, which leads the CT to saturate. Also, if the system has high X over R ratio (meaning low resistance relative to inductance) the dc offset takes longer to decay, and saturation may be more likely to happen [37].

In summary, the impedance of short length line is a small, the sensitivity to measurements error is significant and so an error can impact the accuracy of parameter estimation. In this research saturation in a current transformer CT will be considered as a cause of sensor error. Two cases with different X over R ratios will be considered.

Chapter 3: Transmission Line Parameters

The transmission line is a conductor, but that does not mean it is only a resistance, R. There is an inductance, L, combined with the resistance. Computed at system frequency, they are the line impedance as shown in equation (3.1) for a single phase impedance.

$$Z = R + jX_L \tag{3.1}$$

There is also shunt line admittance ,Y, as shown in equation (3.2) which represents the shunt conductance and the capacitive susceptance of the transmission line. The conductance component G is the leakage current in the insulators. It is complicated to determine the conductance because it changes with atmospheric conditions. The conductance can be neglected because it is very small compared to the susceptance component. The imaginary component of admittance is the susceptance B which represents the capacitive susceptance. [38].

$$Y = G + jB \tag{3.2}$$

Transmission line models use series resistance, series inductance, shunt capacitance, and mostly neglect the shunt conductance. The symbols and units for each parameter are listed in the Table 3.1 [30]

Table 3.1: Line parameters symbols and units

Quantity	Symbol	Unit
Resistance	R	Ohm (Ω)
Inductance	L	Henry (H)
Capacitance	C	Farad (F)
Conductance	G	Siemens (S or Ω^{-1})

3.1 Resistance

The resistance of transmission line is usually small compared to line reactance, though it is still the main cause of power loss in a transmission line. The AC resistance can be calculated based on its direct current resistance. Direct current flows are uniformly distributed over the conductor cross-section area and the dc resistance of the conductor can be determined by the following equation (3.3):

$$R = \frac{\rho * \ell}{A} \tag{3.3}$$

ρ is the resistivity of the conductor.

A is the cross-section area of the conductor.

ℓ is the length of the conductor.

On the other hand, the AC current is nonuniformaly distributed over the conductor cross-section area which means the effective resistance of the conductor is going to be higher due to the skin effect. The change in the resistance of the line could cause a mismatch between the real parameters and the line model parameters. Any significant mismatch between model-based expectations and real behavior of the system could negatively affect reliability, efficiency and security. Inaccurate system models were one of the reasons for several power outages in North America, such as the blackout in August 1996 [39]. To prevent large-scale system events resulting from inaccurate models, reliability standards for model validation were adopted by the North American Electricity Reliability Corporation (NERC). The standards used to insure modeling accuracy are (MOD-032-1) and (MOD-033-1) [3].

Most of transmission lines use Aluminum Conductor Steel Reinforced conductors (ACSR). In ACSR strands of steel wire are surrounded by twisted aluminum strands which increases the actual length of the conductor by 2%. Also, the temperature has a considerable impact on the resistivity of the conductor. There is a linearly proportional relationship between temperature and resistance, with the resistance increasing with increasing temperature as

shown in Figure 3.1 [38]. The relation between the temperature and the resistance can be written as :

$$\frac{R_2}{R_1} = \frac{T + t_2}{T + t_1} \tag{3.4}$$

R_1, R_2 are the resistances of the conductor at temperatures t_1 and t_2, respectively, in degree Celsius, and T is a constant. Values of the constant T in degrees Celsius for different materials are as follows:

T= 234.5 for annealed copper of 100% conductivity.

T= 241 for hard-drawn copper of 97.3% conductivity.

T= 228 for hard-drawn aluminum of 61% conductivity .

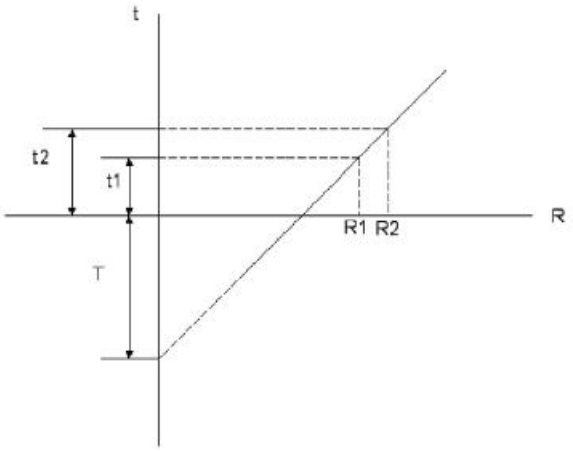

Figure 3.1: Resistance of a metallic conductor as a function of temperature [38]

3.2 Inductance

The transmission line is a conductor without any coils, which could lead to the question, where does the inductance in transmission line come from? Alternating current AC passing a conductor induces a reverse electromotive force (voltage). Therefore inductance can be defined as the ratio between the induced voltage and the rate of change of the current. There are two types of inductance in the transmission line, self-inductance and mutual inductance. Self-inductance is produced by flux due to a current passing through a conductor. When a magnetic field in one line induces voltage in adjacent line, that is defined as a mutual inductance. The amount of inductance depends on the configuration of the lines, transpositions, number of phases, earth resistivity, and tower configurations [40]. Figure 3.2 shows self-inductance and mutual inductance.

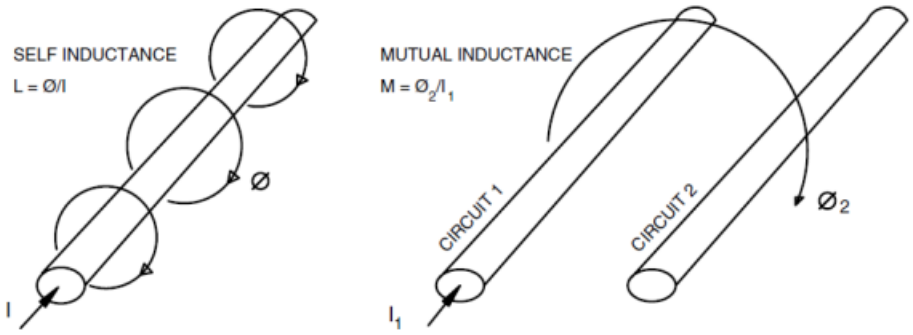

Figure 3.2: Self and mutual inductance
[40]

The relation between the flux linkages and the inductance is given in equation (3.5).

$$\begin{bmatrix} \lambda_A \\ \lambda_B \\ \lambda_C \end{bmatrix} = \begin{bmatrix} L_{AA} & L_{AB} & L_{AC} \\ L_{BA} & L_{BB} & L_{BC} \\ L_{CA} & L_{CB} & L_{CC} \end{bmatrix} \begin{bmatrix} I_A \\ I_B \\ I_C \end{bmatrix} \tag{3.5}$$

Where $\lambda_A, \lambda_B, \lambda_C$ are the total flux linkages of conductors A, B, and C. L_{AA}, L_{BB}, L_{cc} are the self-inductances of conductors A, B, and C, and I_A, I_B, I_C are the line currents. $L_{AB}, L_{BC}, L_{CA}, L_{BA}, L_{CB}, L_{AC}$ are the mutual inductance between conductors [41].
A three-phase line without bundled conductors has nine different inductances. However, if the distance between the phases are equal ($D = D_{AB} = D_{BC} = D_{AC}$), and the geometric mean radii (GMR_{phase}) for the three conductors are equal, the equivalent inductance per phase is given in equation (3.6):

$$L_{phase} = \frac{\mu_0}{2\pi} \ln \left(\frac{D}{GMR_{phase}}\right)(H/m) \tag{3.6}$$

Where μ_0 is the permeability of free space.

3.3 Impact of inductance on maximum transfer power

One of the values that needs to be known for any line is the maximum real power the line can transfer between two stations with voltages V1 and V2 as shown in Figure 3.3.

The transferred power P depends on several factors as shown in equation (3.7). One of those factors is inductive reactance of the line between the two stations.

$$P = \frac{V_1.V_2}{X_L} sin(\delta_{12}) \tag{3.7}$$

Where δ_{12} is the phase difference between the two voltages $V1$ and $V2$, and X_L is the positive

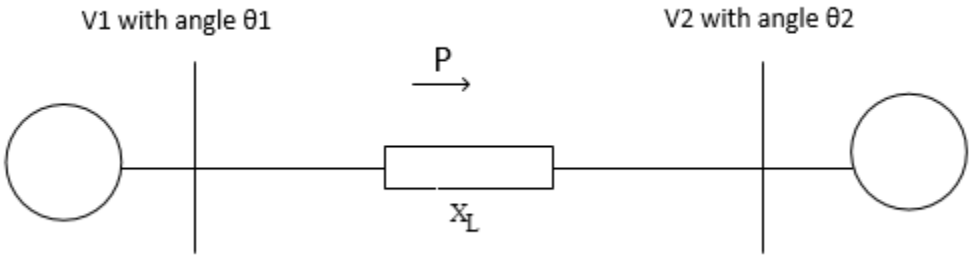

Figure 3.3: Real power transfer in transmission line.

sequence inductive reactance of the line [38]. Equation (3.7) is represented by the curve in Figure 3.4, which shows the relation between transmitted power (P) and the power angle δ_{12} considering constant values for the other elements of the equation.

The transferred power could be increased by a few methods:

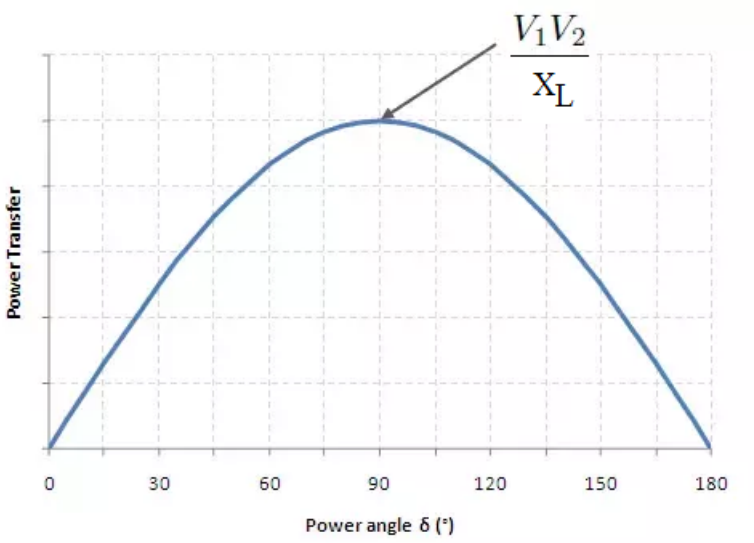

Figure 3.4: Power transfer versus power angle
[38]

1- Increasing the voltages.

2- Increasing the power angle toward 90°. Typically it is less than 25 deg for stability purposes [40]

3- Reducing the inductive reactance of the line, which could be done by installing a series

capacitor, a new parallel line which reduces X to half or by installing bundled conductors [40].

3.3.1 Impact of inductance on reactive power

Reactive power can be defined as the power taken from the generator in the first half of the voltage cycle and given to the generator in the second half. Even though the reactive power is not active power, it is very important for magnetic circuits in transformers and rotating machines. The amount and direction of the active power depend on the phase angle between the two stations [40]. On the other hand, the amount and direction of the reactive power depend on the voltage difference between the two stations. Increased inductance leads to a larger voltage drop across a line and then an increase to the amount of absorbed reactive power, causing even more voltage drop which can lead to voltage collapse [40].

3.3.2 Capacitance

The potential difference between two conductors, or between conductor and earth, in the presence of the air as the surrounding medium, leads to storage of charge (Q) in that medium. The equation for Q is

$$Q = C \cdot V \tag{3.8}$$

From equation (3.8) voltage is proportional to charge for a given physical arrangement by a constant, and the constant is called capacitance (C). The capacitance depends on the distance between conductors and permittivity of the medium (ϵ_0) where ϵ_0 the permittivity of free space for air. The air has the least permittivity, so it stores less charges than other medium. Table 3.2 shows different media with their permittivity and dielectric strength [40].

3.4 Capacitance of a single-phase line with two wires

Starting from two conductors ,A and B, which have the same radius r as shown in Figure 3.5. They are separated by distance D, and the conductor A has a charge $q+$. The

Table 3.2: estimation results for untransposed line with high ($\frac{X}{R}$) ratio

Material	Dielectric Constant (or Relative Permittivity) (Dimensionless)	Strength, E (V/m)
Barium	1200	$7.5 * 10^6$
Water (sea)	80	-
Water (distilled)	8.1	-
Nylon	8	-
Paper	7	$12 * 10^6$
Glass	5-10	$35 * 10^6$
Mica	6	$70 * 10^6$
Porcelain	6	-
Bakelite	5	$20 * 10^6$
Quartz (fused)	5	$30 * 10^6$
Rubber (hard)	3.1	$25 * 10^6$
Wood	2.5-8.0	-
Polystyrene	2.55	-
Polypropylene	2.25	-
Paraffin	2.2	$30 * 10^6$
Petroleum	2.1	$12 * 10^6$
Air (1 atm)	1	$3 * 10^6$

conductor B has a charge $q-$ as shown in equation (3.9) [41].

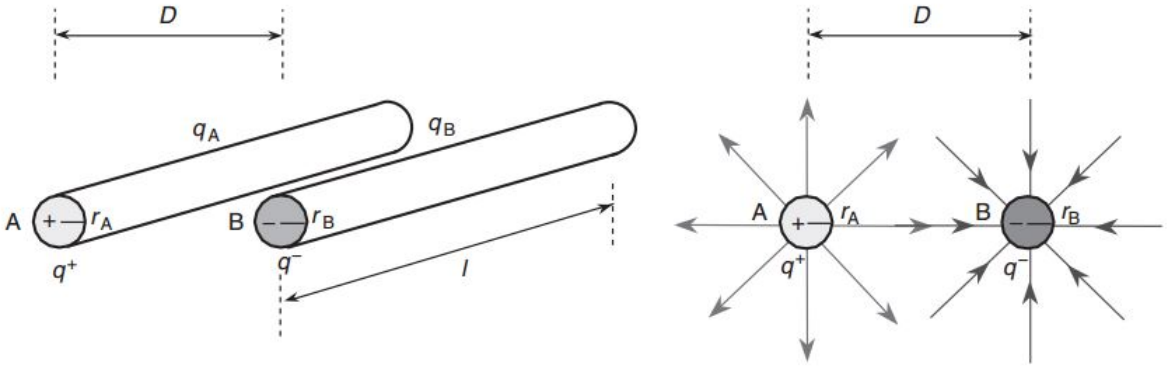

Figure 3.5: Electric field produced from a two-wire single-phase system [41]

Figure 3.6 shows the capacitance between line and ground for a single phase line with two conductors.

$$C_{AB} = \frac{\pi\epsilon_0}{ln(\frac{D}{r})}(F/m) \tag{3.9}$$

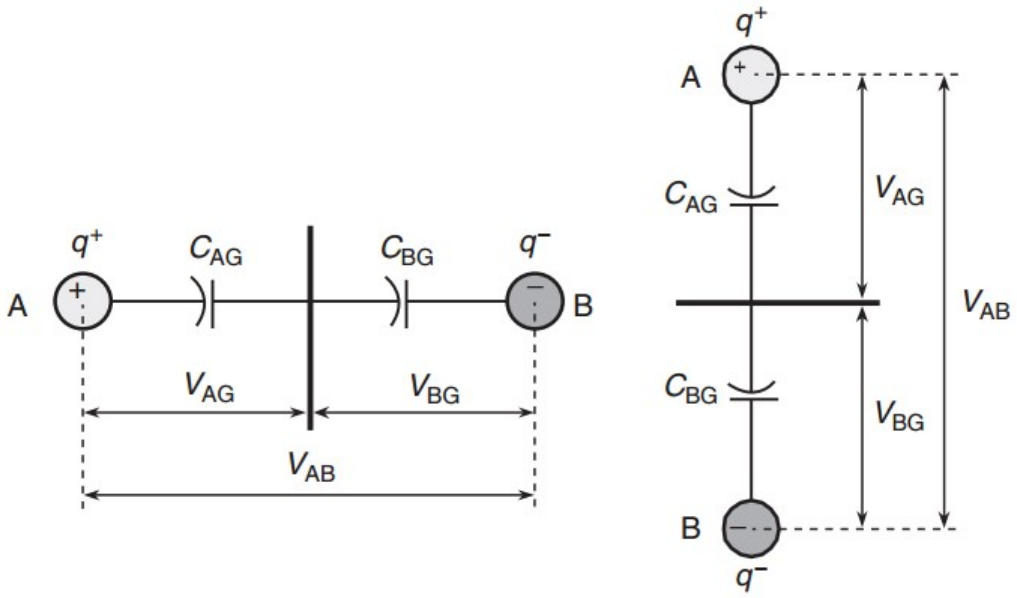

Figure 3.6: Capacitance between line to ground in two-wire single-phase line. [41]

The voltage between phase and ground is one-half the voltage between the two conductors, so the capacitance between the line and ground is [41]:

$$C_{AG} = \frac{q}{V_{AG}} = \frac{2\pi\epsilon_0}{ln(\frac{D}{r})}(F/m) \tag{3.10}$$

3.5 Shunt Capacitance of a Three-Phase Line

Three phase conductors with the same radius and equilateral spacing are shown in Figure 3.7. The capacitance for each conductor can be calculated from equation (3.11), where q_a is the charge of a conductor a, V_{an} is the phase voltage, and r is the radius.

$$C_n = \frac{q_a}{V_{an}} = \frac{2\pi.k}{ln(\frac{D}{r})}(F/m) \tag{3.11}$$

In the case of unsymmetrical spacing between the phases as shown in Figure 3.8, the positive sequence per phase capacitance can be calculated using equation (3.12).

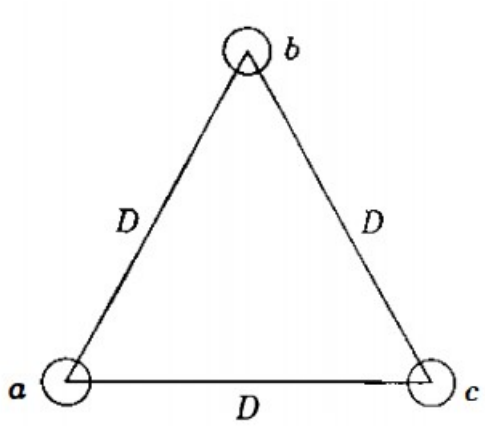

Figure 3.7: Cross section of a three-phase line with equilateral spacing. [38]

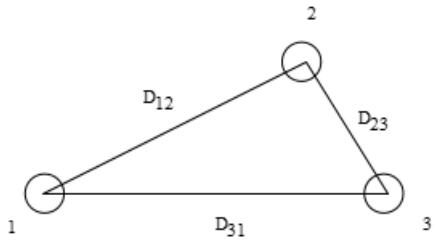

Figure 3.8: Cross section of a three-phase line with unsymmetrical spacing. [38]

$$C_n = \frac{q_a}{V_{an}} = \frac{2\pi.k}{ln(\frac{D_{eq}}{r})}(F/m) \tag{3.12}$$

where:

$$D_{eq} = \sqrt[3]{D_{12}.D_{23}.D_{31}}$$

3.6 Series Impedance of a Line

Figure 3.9 shows the three-phase line model with the shunt admittance neglected. The voltage drop across each phase can be calculated using equations (3.13), (3.14), and (3.15) [42].

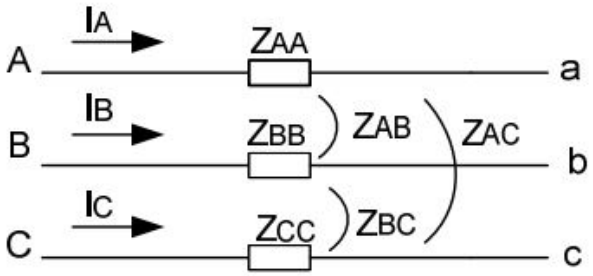

Figure 3.9: Three phase line model.

$$V_{AG} = Z_{AA}.I_A + Z_{AB}.I_B + Z_{AC}.I_C \tag{3.13}$$

$$V_{BG} = Z_{AB}.I_A + Z_{BB}.I_B + Z_{BC}.I_C \tag{3.14}$$

$$V_{CG} = Z_{AC}.I_A + Z_{BC}.I_B + Z_{cC}.I_C \tag{3.15}$$

Where:

Z_{XX}=line self-impedances.

Z_{XY}=line mutual coupled impedances.

V_{Aa}, V_{Bb}, V_{Cc}=voltage drops across each phase.

I_A, I_B, I_C=line currents.

From equations (3.13), (3.14), and (3.15) the impedance matrix, Z, can be formed

$$Z = \begin{bmatrix} Z_{AA} & Z_{AB} & Z_{AC} \\ Z_{AB} & Z_{BB} & Z_{BC} \\ Z_{AC} & Z_{BC} & Z_{CC} \end{bmatrix} \tag{3.16}$$

The sequence admittances and impedances for the line can be calculated by using the the symmetrical components transformation matrix A_{012} as shown in equation (3.17).

$$\mathbf{Z}_{012} = \mathbf{A}_{012}^{-1}\mathbf{Z}\mathbf{A}_{012};\ \mathbf{Y}_{012} = \mathbf{A}_{012}^{-1}\mathbf{Y}\mathbf{A}_{012} \tag{3.17}$$

The A_{012}, uses the operator $a = e^{j2\pi/3}$ and is defined as follows

$$\mathbf{A}_{012} = \begin{bmatrix} 1 & 1 & 1 \\ 1 & a^2 & a \\ 1 & a & a^2 \end{bmatrix} \tag{3.18}$$

$$Z_{012} = \begin{bmatrix} Z_0 & Z_{01} & Z_{02} \\ Z_{10} & Z_1 & Z_{12} \\ Z_{20} & Z_{21} & Z_2 \end{bmatrix} \tag{3.19}$$

Where:

Z_0=zero-sequence self-impedance.

Z_1=positive-sequence self-impedance.

Z_2=negative-sequence self-impedance.

Z_{01}= mutual coupling between the zero and positive sequences.

Z_{02}= mutual coupling between the zero and negative sequences.

Z_{21}= mutual coupling between the negative and positive sequences.

For fully transposed lines the self-impedances in the phase domain are all equal to each other and the mutual impedances in the phase domain all also equal to each other such that $Z_{AB} = Z_{BA}$, $Z_{BC} = Z_{CB}$, and $Z_{AC} = Z_{CA}$. As a results the sequence Z matrix is:

$$Z_{012}(transposed) = \begin{bmatrix} Z_0 & 0 & 0 \\ 0 & Z_1 & 0 \\ 0 & 0 & Z_2 \end{bmatrix} \tag{3.20}$$

Where Z_0, Z_1 and Z_2 are zero, positive, and negative sequences impedance of the line respectively [2], and there are no cross coupling terms between the sequence networks.

The shunt admittance matrix can be written as:

$$Y = \begin{bmatrix} Y_{AA} & Y_{AB} & Y_{AC} \\ Y_{AB} & Y_{BB} & Y_{BC} \\ Y_{AC} & Y_{BC} & Y_{CC} \end{bmatrix} \tag{3.21}$$

The sequence admittances can be calculated in the same fation as the sequence impedances.

3.7 Line Models

Steady-state transmission line models are classified into three different types depending on the length of the line. A short line model is used if the overhead line is less than 50 miles, the medium line model is between 50 miles long and 150 miles, and the long line model for lines longer than 150 miles. The parameters in short and medium line are a lumped representation of distributed parameters. The short line model neglects the shunt capacitance, and it approximates the line model using resistance and inductive as shown in the per phase equivalent Figure 3.10 [38].

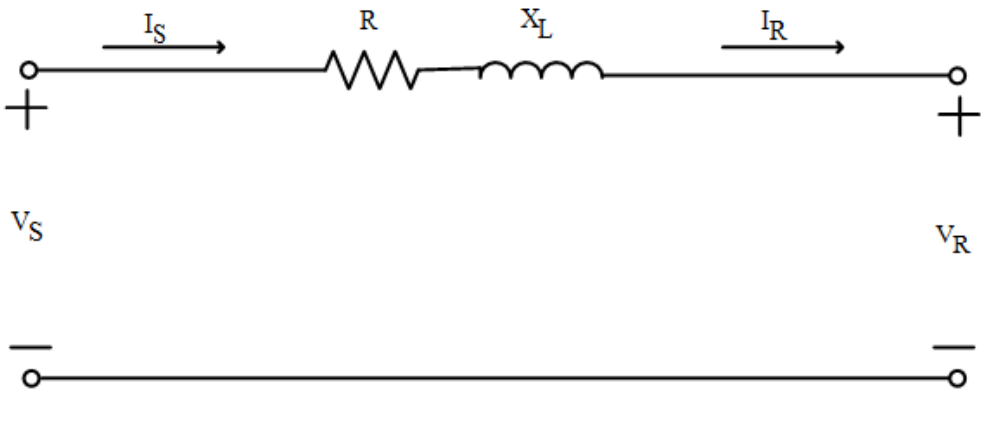

Figure 3.10: Short line model for steady-state analysis

In the medium length line, the total shunt admittance of the line is split in two, with half of the admittance at each terminal of the line. The model is also called a nominal PI as shown in Figure 3.11.

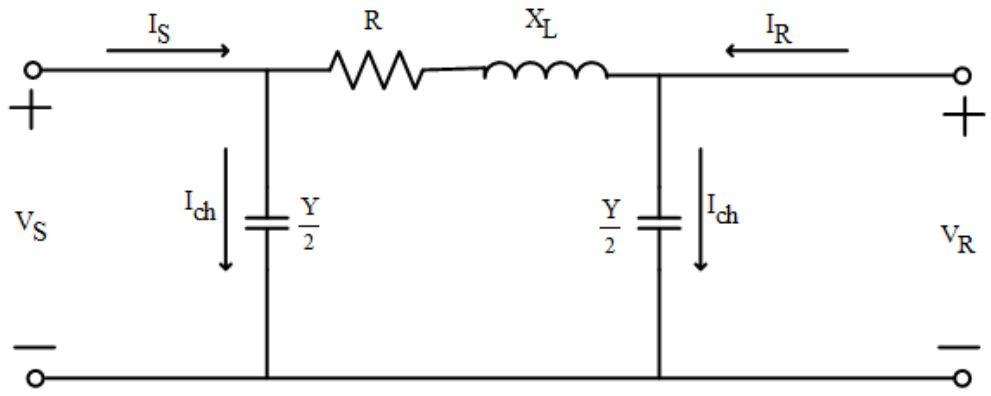

Figure 3.11: Nominal π model steady-state analysis

The line parameters are assumed to be distributed uniformly all along the line. Since the nominal PI model does not account for wave-line response, it is not accurate for long lines. A line model that has correction factors for distributed parameter effect is used for long length lines [38]. A true distributed parameter model is used for transient simulations.

Figure 3.12 shows the per phase distributed model. $Z_{\Delta X}$ is the series impedance of line per unit length (ΔX), similarly $Y_{\Delta X}$ is the shunt admittance per unit length of the line. The conductance is very small and can be neglected.

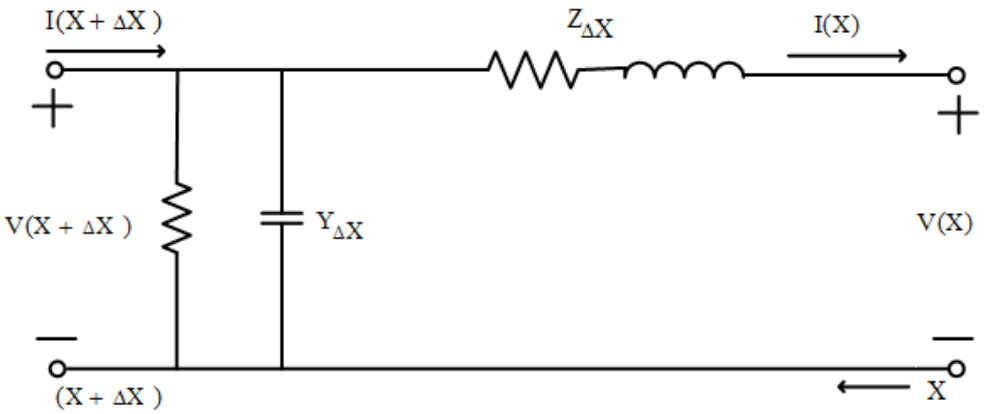

Figure 3.12: Distributed parameter model for length ΔX

3.8 Calculating Transposed Line Parameters

Typically, even for transposed lines the mutually coupled impedances are not entirely equal but to simplify the model they are treated as equal. Two methods are used in this work to calculate the transposed line parameters, one for producing a PI model and one for producing a distributed parameter line model.

3.8.1 Nominal Coupled PI Model of Transmission line

Figure .3.13 shows Three phase Nominal PI model of the transmission line. From the figure, the line currents in terms of sending currents can be written as:

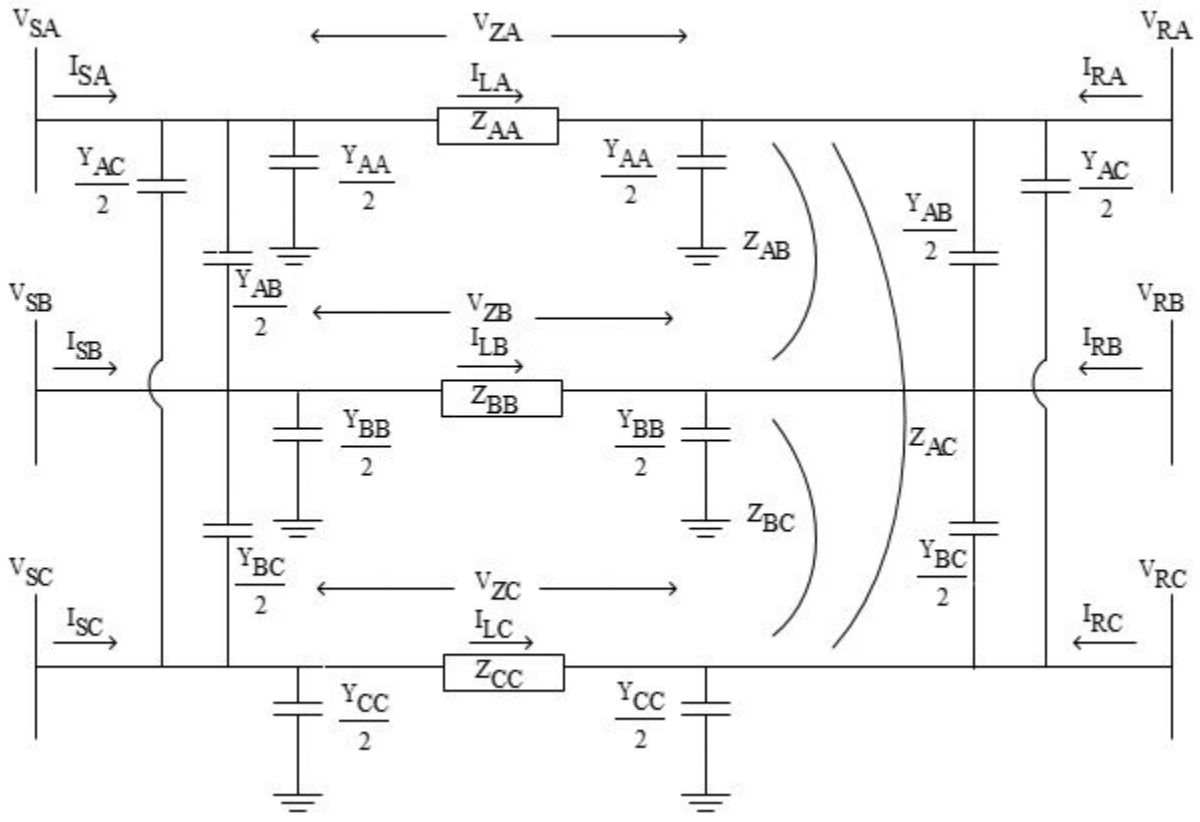

Figure 3.13: Three phase nominal π model of the transmission line [38]

$$I_{LA} = I_{SA} - (\frac{Y_{AA}}{2} \cdot V_{SA} + \frac{Y_{AB}}{2} \cdot V_{SB} + \frac{Y_{AA}}{2} \cdot V_{SC}) \tag{3.22}$$

$$I_{LB} = I_{SB} - (\frac{Y_{BA}}{2} \cdot V_{SA} + \frac{Y_{BB}}{2} \cdot V_{SB} + \frac{Y_{BC}}{2} \cdot V_{SC}) \tag{3.23}$$

$$I_{LC} = I_{SC} - (\frac{Y_{CA}}{2} \cdot V_{SA} + \frac{Y_{CB}}{2} \cdot V_{SB} + \frac{Y_{CC}}{2} \cdot V_{SC}) \tag{3.24}$$

Similarly, the line currents in terms of receiving currents can be written as:

$$I_{LA} = (\frac{Y_{AA}}{2} \cdot V_{RA} + \frac{Y_{AB}}{2} \cdot V_{RB} + \frac{Y_{AC}}{2} \cdot V_{RC}) - I_{RA} \tag{3.25}$$

$$I_{LB} = (\frac{Y_{BA}}{2} \cdot V_{RA} + \frac{Y_{BB}}{2} \cdot V_{RB} + \frac{Y_{BC}}{2} \cdot V_{RC}) - I_{RB} \tag{3.26}$$

$$I_{LC} = (\frac{Y_{CA}}{2} \cdot V_{RA} + \frac{Y_{CB}}{2} \cdot V_{RB} + \frac{Y_{CC}}{2} \cdot V_{RC}) - I_{RC} \tag{3.27}$$

The summations $(I_S + I_R)$ and $(V_S + V_R)$ are defined as:

$$I_M = I_{SM} + I_{RM} \tag{3.28}$$

$$V_M = V_{SM} + V_{RM} \tag{3.29}$$

Where M stands for phases A, B, and C. By rearranging the equations (3.22-3.29), the current equations can be written as:

$$IA = Y_{AA}.V_A + Y_{AB}.V_B + Y_{AC}.V_C \tag{3.30}$$

$$IB = Y_{BA}.V_A + Y_{BB}.V_B + Y_{BC}.V_C \tag{3.31}$$

$$IC = Y_{CA}.V_A + Y_{CB}.V_B + Y_{CC}.V_C \tag{3.32}$$

In case of fully transposed line, $Y_{AA} = Y_{BB} = Y_{CC}$ and $Y_{AB} = Y_{AC} = Y_{BC}$ Collect the shunt admittance terms in a vector of unknowns, Y_v, and rewrite the equations (3.30-3.32) in matrix format:

$$\begin{bmatrix} IA \\ IB \\ IC \end{bmatrix} = \begin{bmatrix} VA & VB & VC \\ VB & VA+VC & 0 \\ VC & VB & VA \end{bmatrix} \cdot \begin{bmatrix} Y_{AA} \\ Y_{AB} \\ Y_{AC} \end{bmatrix} \tag{3.33}$$

The shunt admittance Y_v term can be determined by solving equation (3.33).

To estimate the series impedance terms, Z, start by rewriting the line current equations (3.22), (3.23), and (3.24) in matrix form:

$$\begin{bmatrix} I_{LA} \\ I_{LB} \\ I_{LC} \end{bmatrix} = \begin{bmatrix} I_{SA} \\ I_{SB} \\ I_{SC} \end{bmatrix} - \begin{bmatrix} Y_{AA} & Y_{AB} & Y_{AB} \\ Y_{AB} & Y_{AA} & Y_{AB} \\ Y_{AB} & Y_{AB} & Y_{AA} \end{bmatrix} \cdot \begin{bmatrix} V_{SA} \\ V_{SB} \\ V_{SC} \end{bmatrix} \tag{3.34}$$

The voltages drop across the series impedance are defined as:

$$\begin{bmatrix} V_{SA} - V_{RA} \\ V_{SB} - V_{RB} \\ V_{SB} - V_{RB} \end{bmatrix} = \begin{bmatrix} Z_{AA} & Z_{AB} & Z_{AB} \\ Z_{AB} & Z_{AA} & Z_{AB} \\ Z_{AB} & Z_{AB} & Z_{AA} \end{bmatrix} \cdot \begin{bmatrix} I_{LA} \\ I_{LB} \\ I_{LC} \end{bmatrix} \tag{3.35}$$

Assuming voltages are known, define:

$$V_{ZA} = V_{SA} - V_{RA} \tag{3.36}$$

$$V_{ZB} = V_{SB} - V_{RB} \tag{3.37}$$

$$V_{ZC} = V_{SC} - V_{RC} \tag{3.38}$$

Substituting equations (3.36), (3.37), and (3.38) in equation (3.35) and rearranging the

terms to solve for the impedance Z parameters:

$$\begin{bmatrix} V_{ZA} \\ V_{ZB} \\ V_{ZC} \end{bmatrix} = \begin{bmatrix} I_{LA} & I_{LB} & I_{LC} \\ I_{LB} & I_{LA} + I_{LC} & 0 \\ I_{LC} & I_{LB} & I_{LA} \end{bmatrix} . \begin{bmatrix} Z_{AA} \\ Z_{AB} \\ Z_{AC} \end{bmatrix} \tag{3.39}$$

By employing the symmetrical components transformation, the sequence impedance parameters can be obtained from the shunt admittance matrix, $\mathbf{Y}$, and series impedance matrix $\mathbf{Z}$ as described below.

$$Z_{012} = A^{-1} \cdot Z \cdot A \tag{3.40}$$

$$Y_{012} = A^{-1} \cdot Y \cdot A \tag{3.41}$$

Where:

$a = e^{j120deg}$

$$A = \begin{bmatrix} 1 & 1 & 1 \\ 1 & a^2 & a \\ 1 & a & a^2 \end{bmatrix}$$

and

$$\mathbf{Z} = \begin{bmatrix} Z_{AA} & Z_{AB} & Z_{AB} \\ Z_{AB} & Z_{AA} & Z_{AB} \\ Z_{AB} & Z_{AB} & Z_{AA} \end{bmatrix}, \mathbf{Z} = \begin{bmatrix} Y_{AA} & Y_{AB} & Y_{AB} \\ Y_{AB} & Y_{AA} & Y_{AB} \\ Y_{AB} & Y_{AB} & Y_{AA} \end{bmatrix}$$

The sequence impedance parameters for the transposed line from the Z_{012} are shown in equation (3.42).

$$Z_{012} = \begin{bmatrix} Z_0 & 0 & 0 \\ 0 & Z_1 & 0 \\ 0 & 0 & Z_2 \end{bmatrix} \tag{3.42}$$

In order to solve $\mathbf{Z}$ and $\mathbf{Y}$ matrices to determine the parameters, the matrices have to be full rank, because each matrix has three unknowns. Since three equations can be obtained

from one unbalanced current state, one unbalanced state is sufficient for the estimation. The unbalanced currents can be generated by either single pole open conditions or by ground fault anywhere in the system, as long as it provides sufficient zero-sequence current at the measurement points. As will be seen later in the simulation results, a required condition for an unbalanced state is that the ratio of zero-sequence current to positive-sequence current ($\frac{I_0}{I_1}$) is between 10 and 20 percent.

3.9 Calculating Untransposed Line Parameters

Most transmission lines are untransposed, therefore estimating parameters for untransposed lines is essential. In this research, the model for untransposed lines limited to be nominal coupled π as a simplification.

3.9.1 Nominal Coupled π Model Calculations

Many transmission lines are untransposed, implying 6 unknowns to be determined in the line impedance matrix. These are three self impedances and three mutual impedances, as shown in equation (3.43). Similarly, the shunt admittances will have 6 unknowns.

$$\mathbf{Z}_{unt} = \begin{bmatrix} Z_{AA} & Z_{AB} & Z_{AC} \\ Z_{AB} & Z_{BB} & Z_{BC} \\ Z_{AC} & Z_{BC} & Z_{CC} \end{bmatrix}, \mathbf{Y_{unt}} = \begin{bmatrix} Y_{AA} & Y_{AB} & Y_{AC} \\ Y_{AB} & Y_{BB} & Y_{BC} \\ Y_{Ac} & Y_{BC} & Y_{CC} \end{bmatrix} \tag{3.43}$$

This means that at least three independent unbalanced states with unbalanced zero-sequence currents need to be recorded to estimate the unknown parameters. To determine the matrix of the shunt admittance parameters, the current and voltage measurements are applied in equation (3.44), where $\mathbf{Y}_{vec}$ is the shunt admittance parameters vector of the line, $\mathbf{B}_{unt}$ is a vector of the real and imaginary parts of I_A, I_B, and I_C.

$$\mathbf{B}_{unt} = \mathbf{A}_{unt}\mathbf{Y}_{vec} \tag{3.44}$$

The matrix $\mathbf{A}_{unt}$ contains the real and imaginary parts of V_A, V_B, and V_C. The elements of matrix $\mathbf{A}_{unt} \in \mathbb{R}^{6N\times 6}$, vector $\mathbf{B}_{unt} \in \mathbb{R}^{6N}$, and vector $\mathbf{Y}_{vec} \in \mathbb{R}^{6}$ are as follows:

$$\mathbf{B}_{unt} = \begin{bmatrix} \mathrm{Re}(I_{A1}) \\ \mathrm{Im}(I_{A1}) \\ \mathrm{Re}(I_{B1}) \\ \mathrm{Im}(I_{B1}) \\ \mathrm{Re}(I_{C1}) \\ \mathrm{Im}(I_{C1}) \\ \vdots \\ \mathrm{Re}(I_{AN}) \\ \mathrm{Im}(I_{AN}) \\ \mathrm{Re}(I_{BN}) \\ \mathrm{Im}(I_{BN}) \\ \mathrm{Re}(I_{CN}) \\ \mathrm{Im}(I_{CN}) \end{bmatrix} \tag{3.45}$$

Where N is the number of measurements.

$$\mathbf{Y_{vec}} = \begin{bmatrix} Y_{AA} \\ Y_{BB} \\ Y_{CC} \\ Y_{AB} \\ Y_{BC} \\ Y_{AC} \end{bmatrix} \tag{3.46}$$

$$\mathbf{A}_{unt} = \begin{bmatrix} -\mathrm{Im}(V_{A1}) & -\mathrm{Im}(V_{B1}) & -\mathrm{Im}(V_{C1}) & 0 & 0 & 0 \\ \mathrm{Re}(V_{A1}) & \mathrm{Re}(V_{B1}) & \mathrm{Re}(V_{C1}) & 0 & 0 & 0 \\ 0 & -\mathrm{Im}(V_{A1}) & 0 & -\mathrm{Im}(V_{B1}) & -\mathrm{Im}(V_{C1}) & 0 \\ 0 & \mathrm{Re}(V_{A1}) & 0 & \mathrm{Re}(V_{B1}) & \mathrm{Re}(V_{C1}) & 0 \\ 0 & 0 & -\mathrm{Im}(V_{A1}) & 0 & -\mathrm{Im}(V_{B1}) & -\mathrm{Im}(V_{C1}) \\ 0 & 0 & \mathrm{Re}(V_{A1}) & 0 & \mathrm{Re}(V_{B1}) & \mathrm{Re}(V_{C1}) \\ \vdots & \vdots & \vdots & \vdots & \vdots & \vdots \\ -\mathrm{Im}(V_{AN}) & -\mathrm{Im}(V_{BN}) & -\mathrm{Im}(V_{CN}) & 0 & 0 & 0 \\ \mathrm{Re}(V_{AN}) & \mathrm{Re}(V_{BN}) & \mathrm{Re}(V_{CN}) & 0 & 0 & 0 \\ 0 & -\mathrm{Im}(V_{AN}) & 0 & -\mathrm{Im}(V_{BN}) & -\mathrm{Im}(V_{CN}) & 0 \\ 0 & \mathrm{Re}(V_{AN}) & 0 & \mathrm{Re}(V_{BN}) & \mathrm{Re}(V_{CN}) & 0 \\ 0 & 0 & -\mathrm{Im}(V_{AN}) & 0 & -\mathrm{Im}(V_{BN}) & -\mathrm{Im}(V_{CN}) \\ 0 & 0 & \mathrm{Re}(V_{AN}) & 0 & \mathrm{Re}(V_{BN}) & \mathrm{Re}(V_{CN}) \end{bmatrix} \tag{3.47}$$

Once $\mathbf{Y}_{vec}$ is determined, the line currents can be calculated in equation (3.48)

$$\mathbf{I}_L = \mathbf{I}_S - (\mathbf{Y}_{diag}\mathbf{V}_S) \tag{3.48}$$

Where $\mathbf{Y}_{diag} \in \mathbb{R}^{6N\times 6N}$ is the block diagonal matrix containing N times the matrix $\mathbf{Y_{unt}}$ as shown in (3.49).

$$\mathbf{Y}_{diag} = \begin{bmatrix} \mathbf{Y_{unt}} & 0 & \dots & 0 \\ 0 & \mathbf{Y_{unt}} & \dots & 0 \\ \vdots & \vdots & \ddots & \vdots \\ 0 & 0 & \dots & \mathbf{Y_{unt}} \end{bmatrix} \tag{3.49}$$

$$\mathbf{I}_S = \begin{bmatrix} \mathrm{I}_{SA1} \\ \mathrm{I}_{SB1} \\ \mathrm{I}_{SC1} \\ \vdots \\ \mathrm{I}_{SAN} \\ \mathrm{I}_{SBN} \\ \mathrm{I}_{SCN} \end{bmatrix}, \mathbf{V}_S = \begin{bmatrix} \mathrm{V}_{SA1} \\ \mathrm{V}_{SB1} \\ \mathrm{V}_{SC1} \\ \vdots \\ \mathrm{V}_{SAN} \\ \mathrm{V}_{SBN} \\ \mathrm{V}_{SCN} \end{bmatrix} \tag{3.50}$$

The series impedance parameters are determined from the equation (3.51). The matrix $\mathbf{I}_{unt}$ contains the line current measurements and $\mathbf{V}_Z$ is a vector of voltage drops across the line impedance.

$$\mathbf{V}_Z = \mathbf{I}_{unt}\mathbf{Z}_{unt} \tag{3.51}$$

$$\mathbf{V}_Z = \begin{bmatrix} \mathrm{V}_{ZA1} \\ \mathrm{V}_{ZB1} \\ \mathrm{V}_{ZC1} \\ \vdots \\ \mathrm{V}_{ZAN} \\ \mathrm{V}_{ZBN} \\ \mathrm{V}_{ZCN} \end{bmatrix} = \begin{bmatrix} \mathrm{V}_{SA1} - \mathrm{V}_{RA1} \\ \mathrm{V}_{SB1} - \mathrm{V}_{RB1} \\ \mathrm{V}_{SC1} - \mathrm{V}_{RC1} \\ \vdots \\ \mathrm{V}_{SAN} - \mathrm{V}_{RAN} \\ \mathrm{V}_{SBN} - \mathrm{V}_{RBN} \\ \mathrm{V}_{SCN} - \mathrm{V}_{RCN} \end{bmatrix} \tag{3.52}$$

$$\mathbf{I}_{unt} = \begin{bmatrix} I_{LA1} & I_{LB1} & I_{LC1} & 0 & 0 & 0 \\ 0 & I_{LA1} & 0 & I_{LB1} & I_{LC1} & 0 \\ 0 & 0 & I_{LA1} & 0 & I_{LB1} & I_{LC1} \\ \vdots & \vdots & \vdots & \vdots & \vdots & \vdots \\ I_{LAN} & I_{LBN} & I_{LCN} & 0 & 0 & 0 \\ 0 & I_{LAN} & 0 & I_{LBN} & I_{LCN} & 0 \\ 0 & 0 & I_{LAN} & 0 & I_{LBN} & I_{LCN} \end{bmatrix} \tag{3.53}$$

Two calculation methods were performed for producing parameters for a nominal coupled PI model for transposed and untransposed lines. The two methods estimate the series impedance and the shunt impedance of the lines. One unbalanced current state was sufficient for the transposed line, and at least three unbalanced states were required for the untransposed line.

Chapter 4: Overview of Synchronized Phasor Measurements

4.1 Synchrophasors

The penetration of synchrophasor measurements technology in the power system has increased quickly in the last decade [5]. Most electric utilities started using synchrophasor technology in the 1980s [4]. A suitable communication of synchrophasors can provide dynamic information on the power system. A synchrophasor provides time-stamped magnitude and angle for current, voltage and power measurements from anywhere on the power system [30]. These measurements are time stamped with respect to a common time reference Global Positioning System GPS-clock signal which uses a reference sinusoidal wave as shown in Figure 4.1. Thus, all the data from the different location can be time aligned which allows the operators in the operating center to have a dynamic view for the whole grid [4].

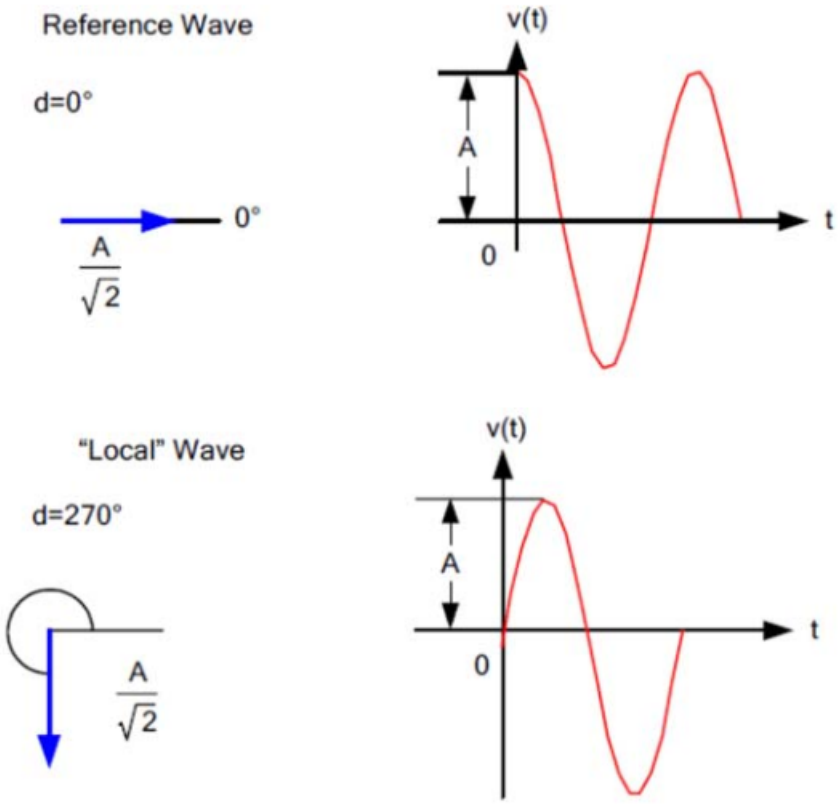

Figure 4.1: Reference wave and local wave with angular comparison [30]

The synchronized data is recoreded using phasor measurements units, PMUs, which provide data nearly in real-time, with minimal time delay. The time delay of phase angle data is potentially accurate to within ± 0.2 microsecond, and the update rate of the data is varying for 10, 30, to 60 samples per second [43]. The stages of the creation and transfer of a synchrophasor can be summarized in three steps which are: collecting, aligning, and archived data [44]. The deployment of PMUs and wide-area measurement systems (WAMS) can be used to provide synchronized measurements for parameter identification. The measurements include: precise voltage, current, power and phase angles measured at both ends of a line [45].

4.2 The PMUs Setup in a Hardware-in-the-Loop Simulation

The power system model has been implemented in a real digital simulation to validate the proposed LTS-based estimation method. The arrangement of structure set up is shown in Figure 4.2.

Two commercial protective relays with synchrophasor capabilities were set to transfer synchrophasor data at a reporting rate of 60 frames per second. The two actual relays were used as PMUs connected at the terminals of the series compensated line. The relays were connected to a GPS clock to add time stamps. Streaming of the real-time data was performed by using IEEE C37.118-2005 Standard for Synchrophasor Protocol [43]. The current transformer ratios (CTR) and the voltage transformer ratios (VTR) in the relays were set to match the (CTR) and (VTR) in the simulation as shown in Figure 4.3.

The settings for the PMUs in the relays are shown in Figure 4.4 and Figure 4.5. A TCP/IP network was used in the synchrophasor network data transmission. The 100 Mbps communications links are connected through a network switch shared with the real time digital simulator and other computers in the lab [30].

A Phasor Data Concentrator (PDC) was used to collect the data from the PMUs and time align them based on the information from the GPS clock. The data is then streamed to an application program. The PDC can receive data from 500 PMUs instantaneously

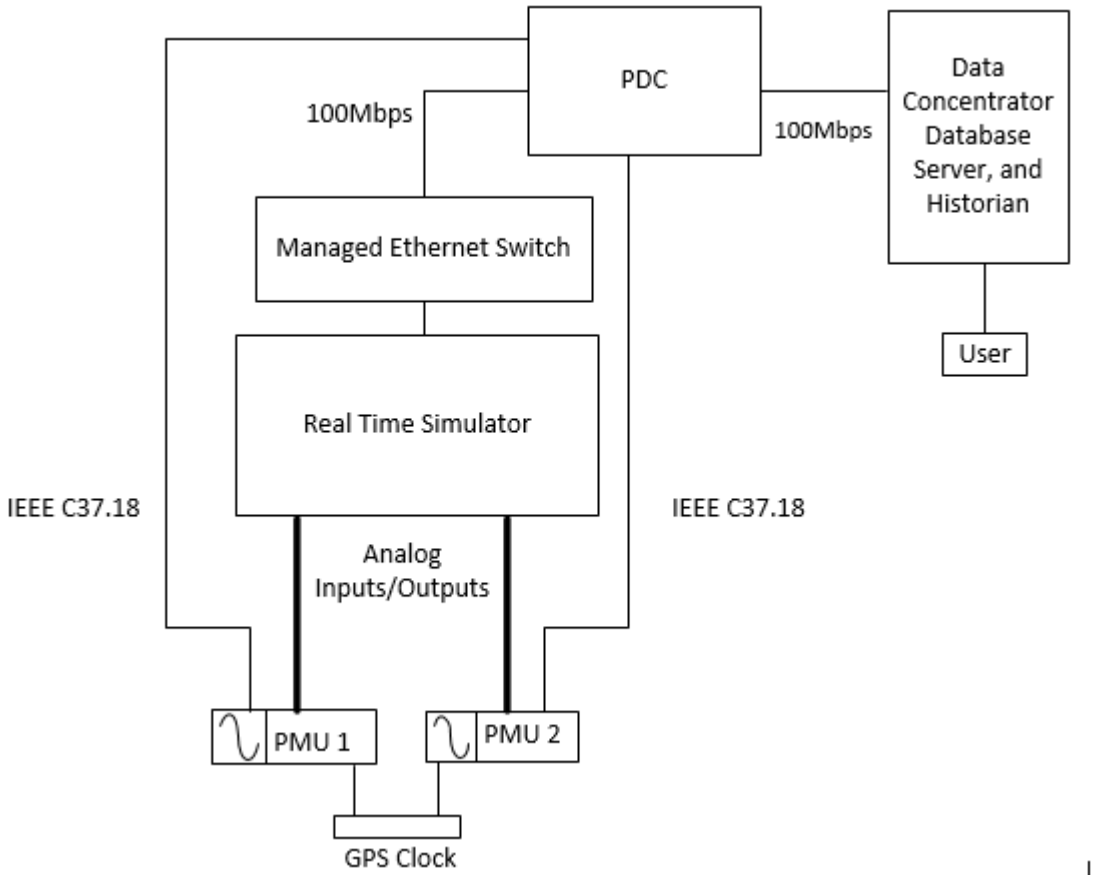

Figure 4.2: Real time simulation network set up.

with a rate of 240 message per second [46]. The synchrowave central administrator software was utilized to view and get the voltage and current measurements. The setting for the synchrowave central administrator software is shown in Figure 4.6.

The visualization of the current magnitude and the voltage magnitude are shown in Figure 4.7 and Figure 4.8 respectively using the synchrowave central software during a steady-state condition.

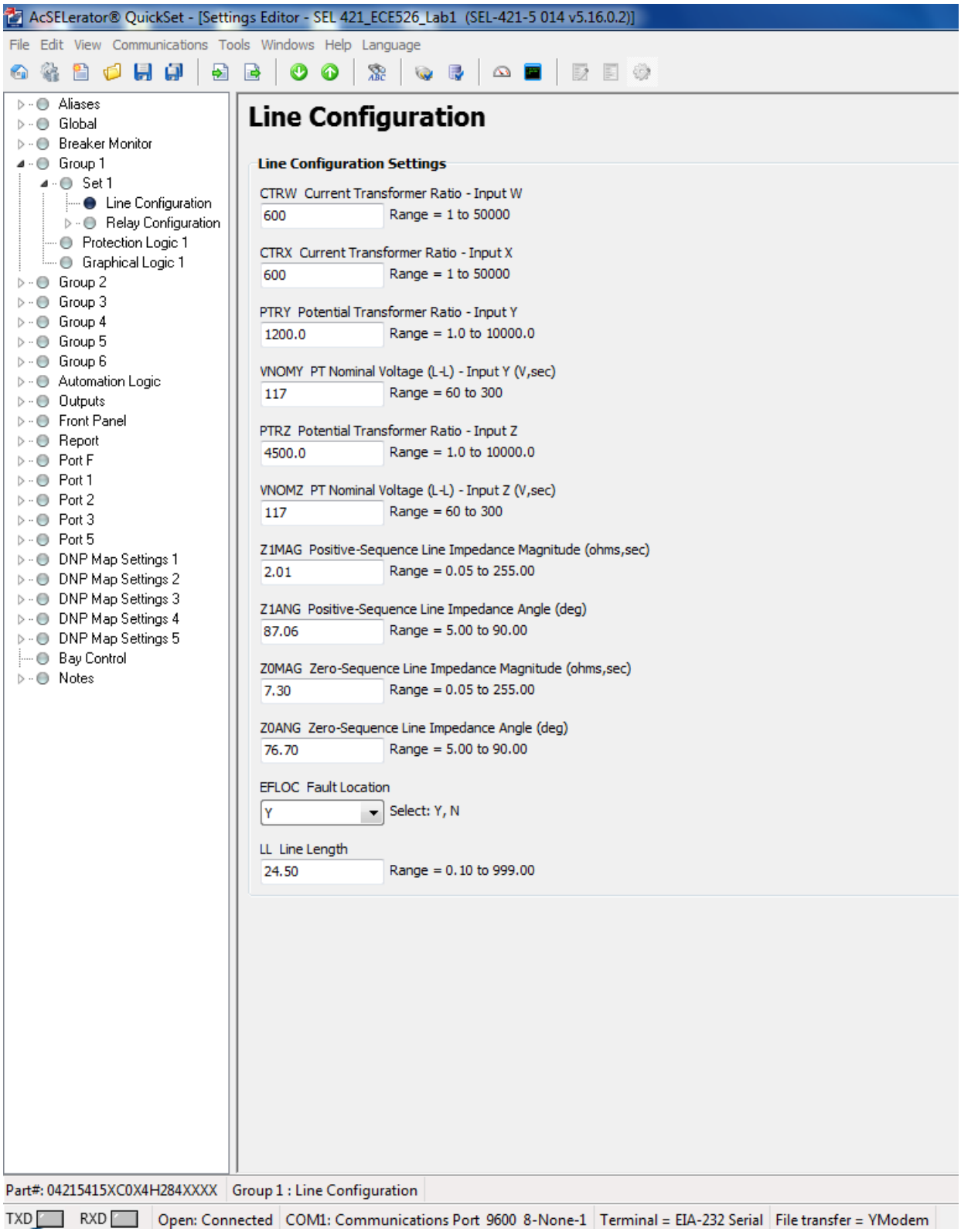

Figure 4.3: CT, VT, and line configuration setting.

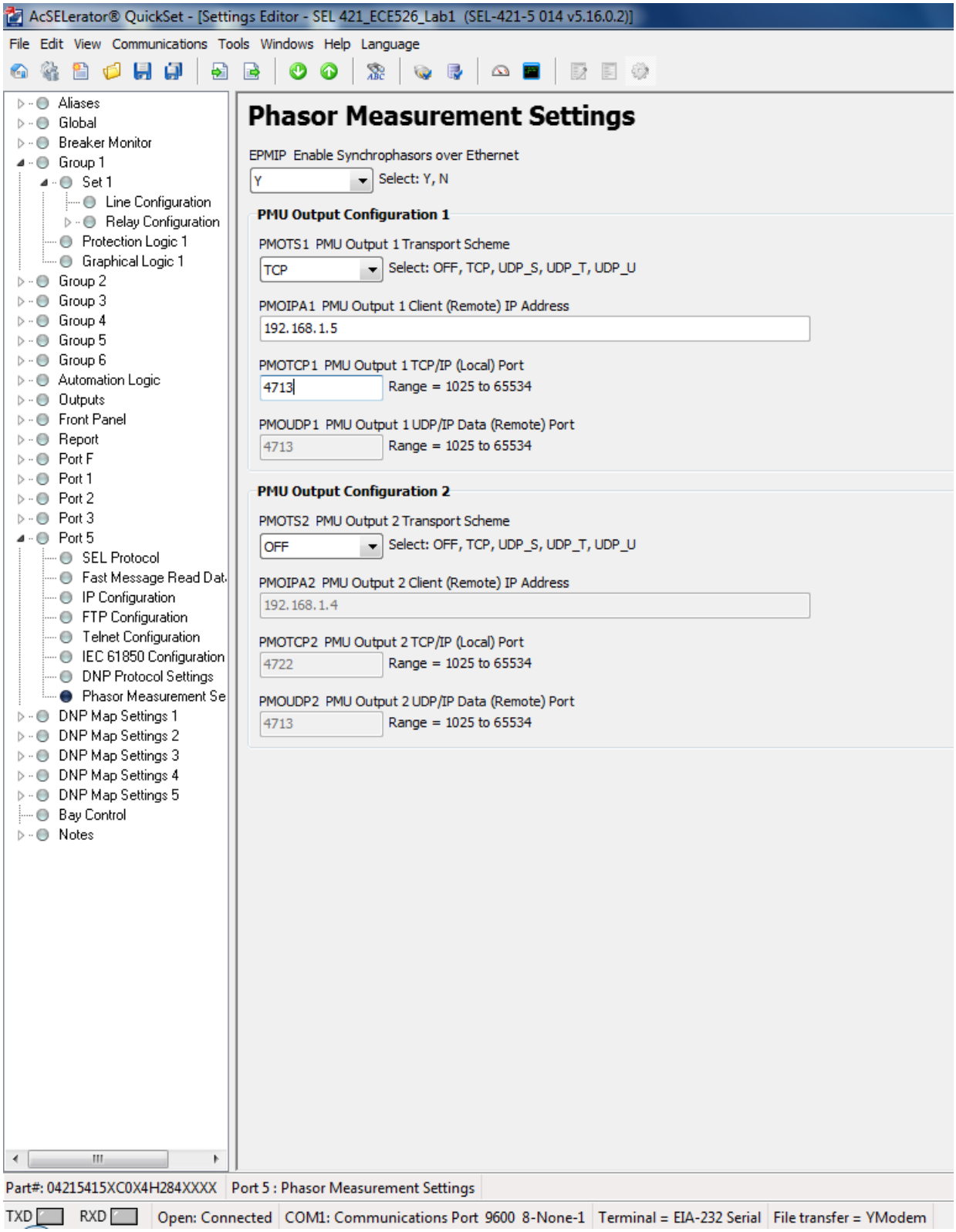

Figure 4.4: SEL 421 relay PMU setting screen.

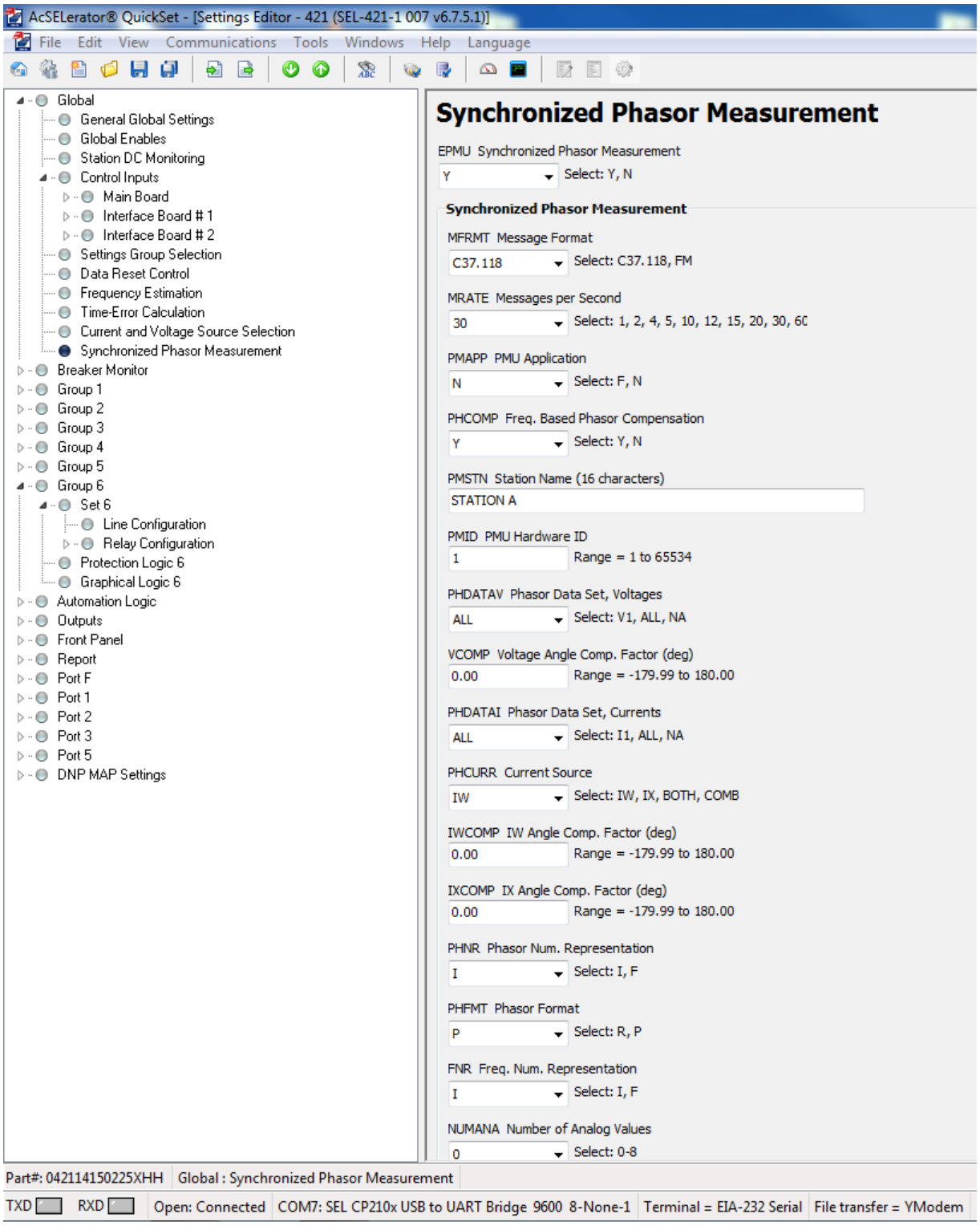

Figure 4.5: Additional PMU setting for SEL 421 relay screen.

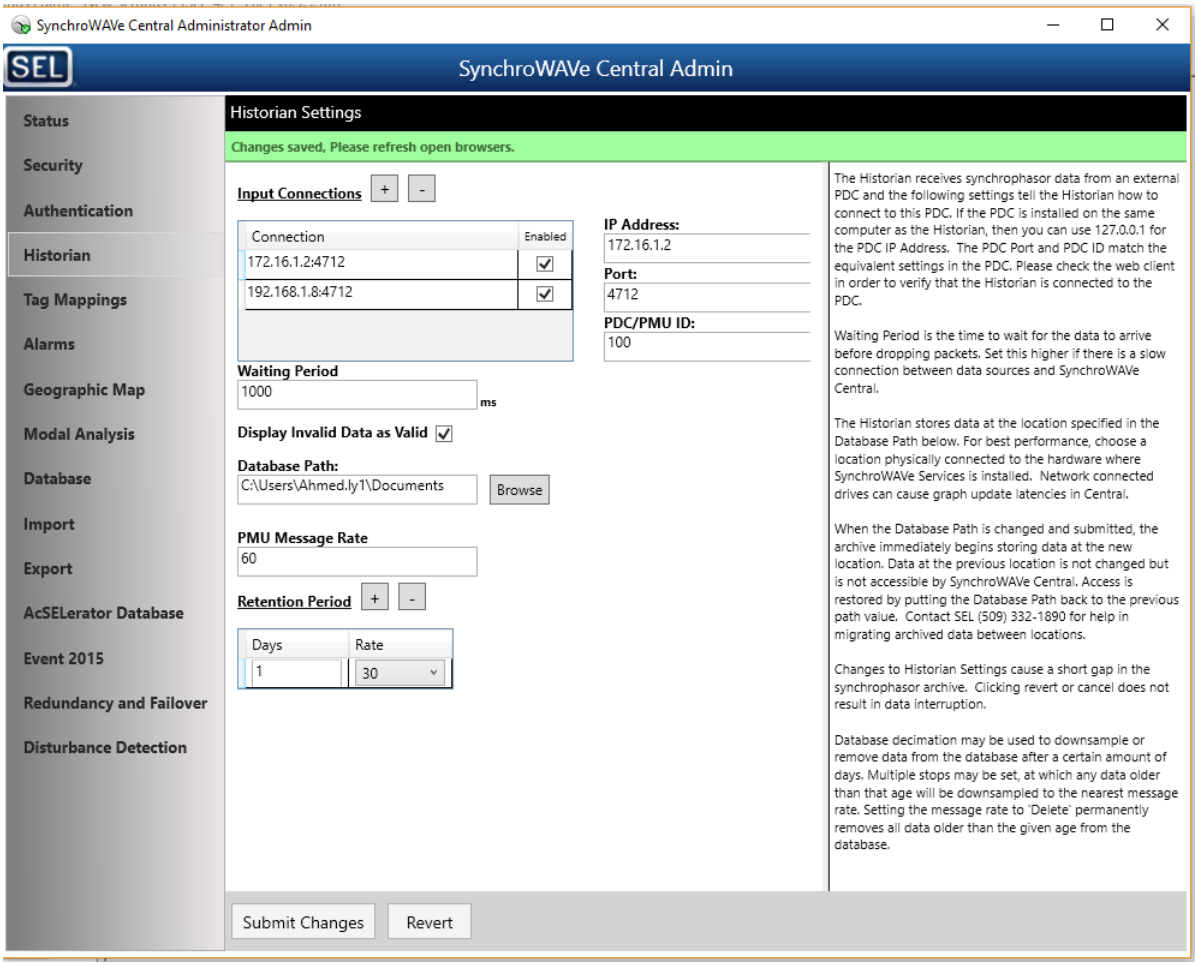

Figure 4.6: Synchrowave central administrator setting.

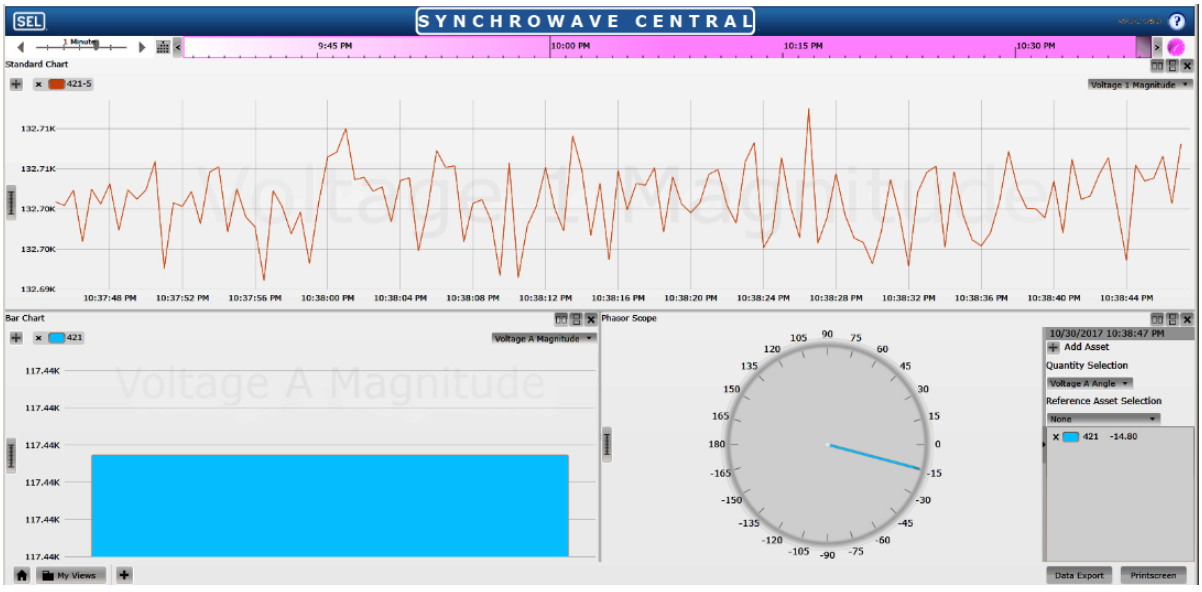

Figure 4.7: Visualization software output for current magnitude from PMU.

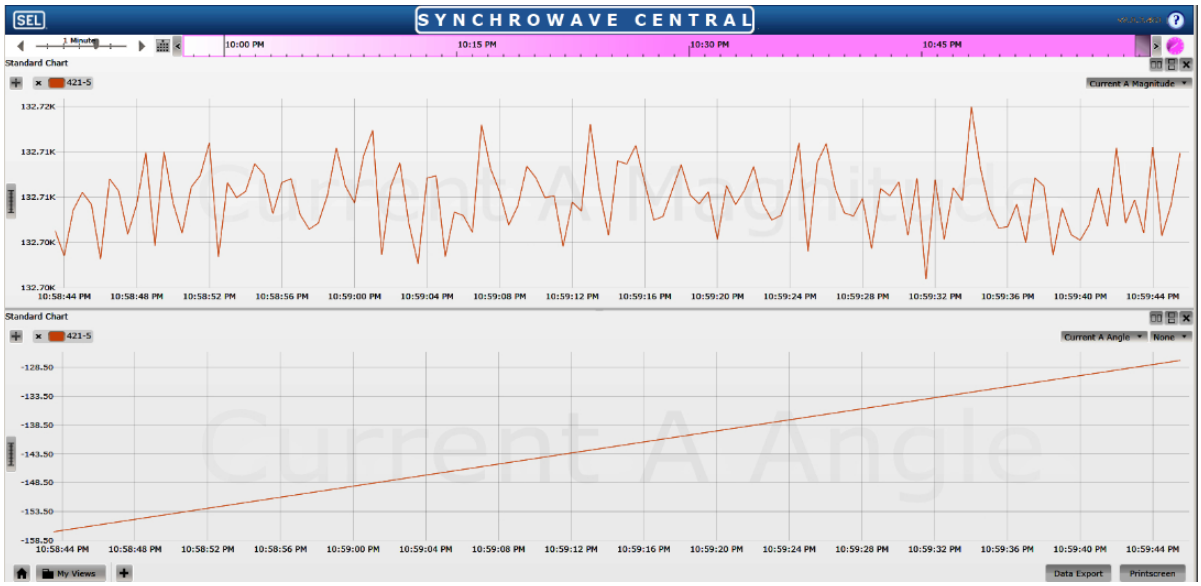

Figure 4.8: Visualization software output for voltage magnitude from PMU.

Chapter 5: Series Compensated Line Parameters Estimation Using Synchrophasor Measurements

This Chapter is a paper that was accepted in IEEE Transaction on Power Delivery and it will appear in 2019.

5.1 Abstract

This paper proposes a robust approach to accurately estimate parameters for compensated lines in the presence of low frequency oscillation (LFO) that arises in measurements during a fault close to the series capacitor. The estimation uses measurements available from phasor measurement units (PMUs) and considers both cases of transposed and untransposed lines. The robustness towards measurement errors or departures from the fundamental frequency model due to LFO present in PMU signals is introduced by exploiting the Least Trimmed Square (LTS) estimator. The least trimmed squares is a highly robust estimator that treats the bad effects of outliers. Mutual line parameters between the phases are calculated as well. Simulations were performed with the included sensor errors, and the results show the superiority of the LTS-based estimation compared to the classical estimation using the weighted least squares. The performance of the proposed approach was also assessed with a real time digital simulator.

5.2 Introduction

In this paper, a robust approach is proposed to estimate the zero- and the positive-sequence line parameters for both the transposed and untransposed lines. The series RLC circuit formed with the series capacitor produces a decaying low-frequency resonance in response to a fault which is superimposed to the 60 Hz component. The low-frequency envelope around the 60Hz response will impact the filtred V_{rms} and I_{rms} measurements. During the fault, there is a chance that the collected data contains LFO which impacts the

accuracy of the parameter estimation. The measurements affected by the LFO will be treated as bad data or outliers by the proposed approach. The proposed approach shows better performance than the classical Weighted Least Squares (WLS) estimator followed by a bad data detector (BDD). Indeed, in the presence of outliers or even a small deviation from the assumptions, the WLS degrades quickly. Outliers are measurements that do not follow the model of the majority of the data. In a regression context, outliers could be classified in two types: observation outliers and leverage points. Observation outliers are bad measurements impacting the observation vector, I (current measurements), and leverage points are outliers impacting the regressorâs matrix, V (voltage measurements). To handle observation outliers and leverage points, we use the Least Trimmed Squares (LTS) estimator that can resist both observation outliers and leverage points. The WLS plus BDD estimation is not robust against leverage points. The proposed method could be used for parameter estimation in general not only the compensated line. The contribution of this paper can be listed as:

1. A new method for parameter estimation, LTS, is used to detect and reject the bad data in both current and voltage measurements.

2. The estimation is performed for transposed and untransposed series compensated lines for a three phase model, so the mutual parameters are estimated. The LTS isolates the outliers in the measurements. These outliers caused by the LFO response of the series capacitor during the fault or other sources of measurements error.

The proposed method (LTS) is effective for line parameter estimation for non-compensated lines and cases with clean PMU data as well. Section 5.3 describes the line model and the estimation equations used for both transposed line and untransposed lines. Section 5.4 describes the principles of the proposed method LTS and reviews the classical WLS method for comparison. Section 5.5 shows the two methods results from an electromagnetic transients simulation. Section 5.6 shows a comparison between the two methods with a power system model implemented in a real time simulation environment with commercial PMUs

and Section 5.7 concludes the paper.

5.3 PMU-based parameter estimation in the presence of low frequency oscillation

5.3.1 Transposed line

The authors in [33] provided a set of three equations for evenly transposed line parameters estimation and since the transposed line has only two unknowns in the impedance Z matrix, one unbalanced state is enough for computing these parameters. To increase the estimation accuracy, the approach from [33] is extended to consider four unbalanced states. Figure 5.1 shows the three phase π model of the transmission line.

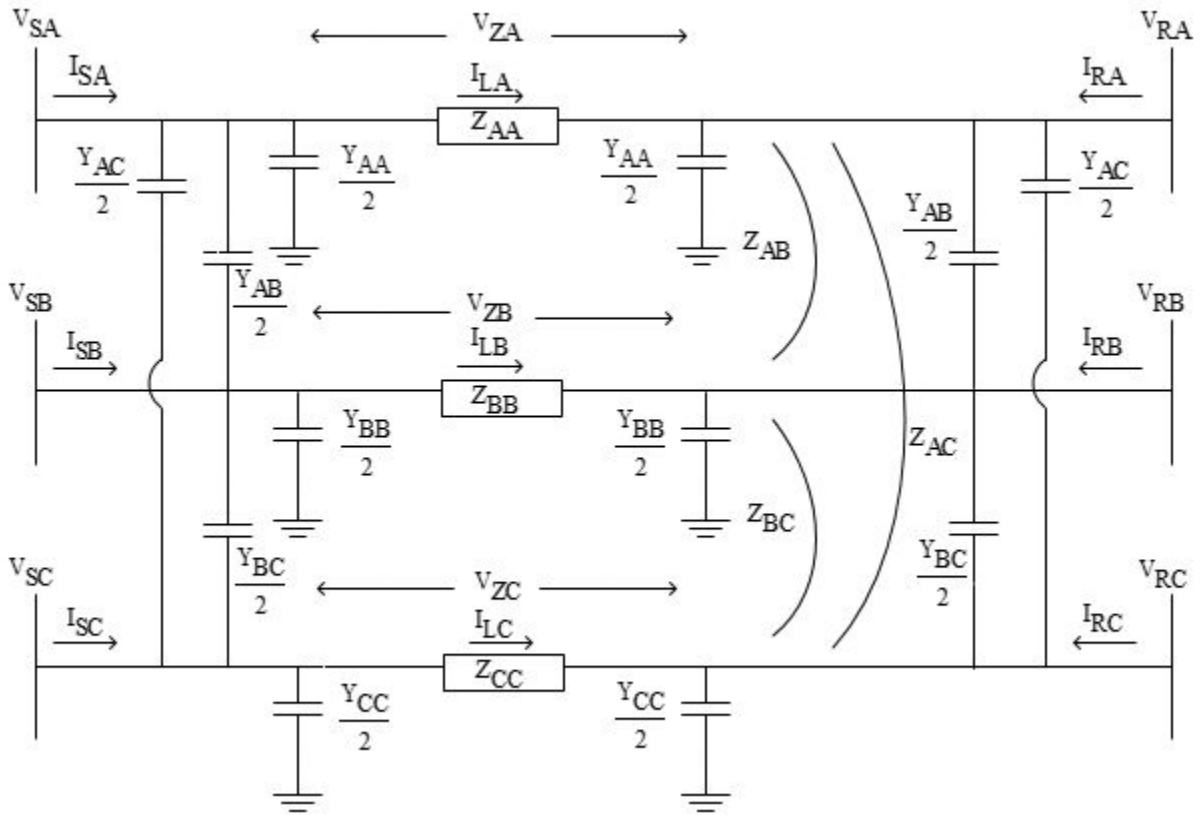

Figure 5.1: Three phase π model of the transmission line
[38]

A regression formulation can be considered:

$$\mathbf{B} = \mathbf{A}\mathbf{Y}_\mathbf{v} + \mathbf{e} \tag{5.1}$$

$\mathbf{Y_v}$ is an unknown vector containing of the parameters of the compensated line $\mathbf{Y}$ shunt admittances, where $\mathbf{Y_v} \in \mathbb{R}^2$. The error vector is denoted by $\mathbf{e}$ which is assumed Gaussian with a covariance matrix $\mathbf{R}$. The vector $\mathbf{B}$ contains the current phasors I_A, I_B, and I_C which are the phasor sum of sending and receiving currents for each phase, with polarities as shown in Fig. 3.13, measured by the PMUs as shown in equation (5.2), where $\mathbf{B} \in \mathbb{R}^{3N}$. The regressor matrix, $\mathbf{A} \in \mathbb{R}^{3N\times 2}$ is the voltage matrix. The V_A, V_B, and V_C are the phasor sums of sending and receiving voltages for each phase as measured by the PMUs as shown in equations (5.3) and (5.4). The PMUs are installed at both ends of the compensated line. The subscripts N represents the number of testing states which is equal to four in this case. The objective is to estimate $\mathbf{Y_v}$ from the measurements contained in the observation vector $\mathbf{B}$ and regressor matrix $\mathbf{A}$. The least trimmed squares will be used as explained in Section 5.4.2.

$$\mathbf{B} = \begin{bmatrix} \mathrm{I}_{A1} \\ \mathrm{I}_{B1} \\ \mathrm{I}_{C1} \\ \vdots \\ \mathrm{I}_{AN} \\ \mathrm{I}_{BN} \\ \mathrm{I}_{CN} \end{bmatrix} = \begin{bmatrix} \mathrm{I}_{SA1}+\mathrm{I}_{RA1} \\ \mathrm{I}_{SB1}+\mathrm{I}_{RB1} \\ \mathrm{I}_{SC1}+\mathrm{I}_{RC1} \\ \vdots \\ \mathrm{I}_{SAN}+\mathrm{I}_{RAN} \\ \mathrm{I}_{SBN}+\mathrm{I}_{RBN} \\ \mathrm{I}_{SCN}+\mathrm{I}_{RCN} \end{bmatrix} \tag{5.2}$$

$$\mathbf{A} = \begin{bmatrix} \mathrm{V}_{A1} & \mathrm{V}_{B1}+\mathrm{V}_{C1} \\ \mathrm{V}_{B1} & \mathrm{V}_{A1}+\mathrm{V}_{C1} \\ \mathrm{V}_{C1} & \mathrm{V}_{B1}+\mathrm{V}_{A1} \\ \vdots & \\ \mathrm{V}_{AN} & \mathrm{V}_{BN}+\mathrm{V}_{CN} \\ \mathrm{V}_{BN} & \mathrm{V}_{AN}+\mathrm{V}_{CN} \\ \mathrm{V}_{CN} & \mathrm{V}_{BN}+\mathrm{V}_{AN} \end{bmatrix} \tag{5.3}$$

Where V_A, V_B, andV_C are denoted as:

$$\begin{bmatrix} \mathrm{V}_{A1} \\ \mathrm{V}_{B1} \\ \mathrm{V}_{C1} \\ \vdots \\ \mathrm{V}_{AN} \\ \mathrm{V}_{BN} \\ \mathrm{V}_{CN} \end{bmatrix} = \begin{bmatrix} \mathrm{V}_{SA1}+\mathrm{V}_{RA1} \\ \mathrm{V}_{SB1}+\mathrm{V}_{RB1} \\ \mathrm{V}_{SC1}+\mathrm{V}_{RC1} \\ \vdots \\ \mathrm{V}_{SAN}+\mathrm{V}_{RAN} \\ \mathrm{V}_{SBN}+\mathrm{V}_{RBN} \\ \mathrm{V}_{SCN}+\mathrm{V}_{RCN} \end{bmatrix} \tag{5.4}$$

By solving the regression problem (5.1) using the LTS estimator, the $\mathbf{Y}$ matrix of the transposed lines can be determined from the estimated vector $\hat{\mathbf{Y}}_V = \left(\hat{Y}_{AA}, \hat{Y}_{AB}\right)^T$, i.e,

$$\mathbf{Y} = \begin{bmatrix} Y_{AA} & Y_{AB} & Y_{AB} \\ Y_{AB} & Y_{AA} & Y_{AB} \\ Y_{AB} & Y_{AB} & Y_{AA} \end{bmatrix} \tag{5.5}$$

Once $\mathbf{Y}$ is estimated, the vector of line currents $\mathbf{I}_L$ can be calculated from the following equation

$$\mathbf{I}_L = \mathbf{I}_S - (\mathbf{Y}_{Blk}\mathbf{V}_S) \tag{5.6}$$

Where $\mathbf{Y}_{Blk} \in \mathbb{R}^{3N\times 3N}$ is the block diagonal matrix containing N times the matrix $\mathbf{Y}$ as

shown in (5.7). $\mathbf{I}_S \in \mathbb{R}^{3N}$ is a vector with the sending end currents and $\mathbf{V}_S \in \mathbb{R}^{3N}$ is a vector with the sending end voltages.

$$\mathbf{I}_S = \begin{bmatrix} \mathrm{I}_{SA1} \\ \mathrm{I}_{SB1} \\ \mathrm{I}_{SC1} \\ \vdots \\ \mathrm{I}_{SAN} \\ \mathrm{I}_{SBN} \\ \mathrm{I}_{SCN} \end{bmatrix}, \mathbf{V}_S = \begin{bmatrix} \mathrm{V}_{SA1} \\ \mathrm{V}_{SB1} \\ \mathrm{V}_{SC1} \\ \vdots \\ \mathrm{V}_{SAN} \\ \mathrm{V}_{SBN} \\ \mathrm{V}_{SCN} \end{bmatrix}, \mathbf{Y}_{blk} = \begin{bmatrix} \mathbf{Y} & 0 & \dots & 0 \\ 0 & \mathbf{Y} & \dots & 0 \\ \vdots & \vdots & \ddots & \vdots \\ 0 & 0 & \dots & \mathbf{Y} \end{bmatrix} \tag{5.7}$$

The regression problem (5.8) is then solved using the LTS which determines the series impedance parameters of the transposed line.

$$\mathbf{V}_Z = \mathbf{I}\mathbf{Z}_v + \mathbf{e}, \tag{5.8}$$

where $\mathbf{Z}_v = \left(Z_{AA}, Z_{AB}\right)^T$

The observation vector, $\mathbf{V}_Z$, contains the measured voltage drops and $\mathbf{I}$ is the line current matrix.

$$\mathbf{I} = \begin{bmatrix} \mathrm{I}_{LA1} & \mathrm{I}_{LB1}+\mathrm{I}_{LC1} \\ \mathrm{I}_{LB1} & \mathrm{I}_{LA1}+\mathrm{I}_{LC1} \\ \mathrm{I}_{LC1} & \mathrm{I}_{LB1}+\mathrm{I}_{LC1} \\ \vdots & \\ \mathrm{I}_{LAN} & \mathrm{I}_{LBN}+\mathrm{I}_{LCN} \\ \mathrm{I}_{LBN} & \mathrm{I}_{LAN}+\mathrm{I}_{LCN} \\ \mathrm{I}_{LCN} & \mathrm{I}_{LBN}+\mathrm{I}_{LAN} \end{bmatrix} \tag{5.9}$$

$$\mathbf{V}_Z = \begin{bmatrix} \mathrm{V}_{ZA1} \\ \mathrm{V}_{ZB1} \\ \mathrm{V}_{ZC1} \\ \vdots \\ \mathrm{V}_{ZAN} \\ \mathrm{V}_{ZBN} \\ \mathrm{V}_{ZCN} \end{bmatrix} = \begin{bmatrix} \mathrm{V}_{SA1} - \mathrm{V}_{RA1} \\ \mathrm{V}_{SB1} - \mathrm{V}_{RB1} \\ \mathrm{V}_{SC1} - \mathrm{V}_{RC1} \\ \vdots \\ \mathrm{V}_{SAN} - \mathrm{V}_{RAN} \\ \mathrm{V}_{SBN} - \mathrm{V}_{RBN} \\ \mathrm{V}_{SCN} - \mathrm{V}_{RCN} \end{bmatrix} \tag{5.10}$$

The impedance matrix is given by

$$\mathbf{Z} = \begin{bmatrix} Z_{AA} & Z_{AB} & Z_{AB} \\ Z_{AB} & Z_{AA} & Z_{AB} \\ Z_{AB} & Z_{AB} & Z_{AA} \end{bmatrix} \tag{5.11}$$

The zero- and positive-sequence admittances and impedances of the line can be calculated by using the A_{012} matrix as shown in equation (5.12).

$$\mathbf{Z}_{012} = \mathbf{A}_{012}^{-1}\mathbf{Z}\mathbf{A}_{012};\ \mathbf{Y}_{012} = \mathbf{A}_{012}^{-1}\mathbf{Y}\mathbf{A}_{012} \tag{5.12}$$

The symmetrical components transformation matrix, A_{012}, uses the operator $a = e^{j2\pi/3}$ and is defined as follows

$$\mathbf{A}_{012} = \begin{bmatrix} 1 & 1 & 1 \\ 1 & a^2 & a \\ 1 & a & a^2 \end{bmatrix} \tag{5.13}$$

5.3.2 Untransposed line parameter estimation

Many transmission lines are untransposed, implying 6 unknowns in the line impedance matrix to be determined. These are three self impedances and three mutual impedances as shown

in equation (5.14). Similarly, the shunt admittances will have 6 unknowns.

$$\mathbf{Z}_{unt} = \begin{bmatrix} Z_{AA} & Z_{AB} & Z_{AC} \\ Z_{AB} & Z_{BB} & Z_{BC} \\ Z_{AC} & Z_{BC} & Z_{CC} \end{bmatrix}, \mathbf{Y_{unt}} = \begin{bmatrix} Y_{AA} & Y_{AB} & Y_{AC} \\ Y_{AB} & Y_{BB} & Y_{BC} \\ Y_{Ac} & Y_{BC} & Y_{CC} \end{bmatrix} \tag{5.14}$$

This means that at least three independent unbalanced states with unbalanced zero-sequence currents need to be recorded to estimate the unknown parameters. To determine the matrix of the shunt admittance parameters, the current and voltage measurements are used in the regression (5.15), where $\mathbf{Y}_{vec}$ is the shunt admittance parameters vector of the line, $\mathbf{B}_{unt}$ is a vector of the real and imaginary parts of I_A, I_B, and I_C. The matrix $\mathbf{A}_{unt}$ contains the real and imaginary parts of V_A, V_B, and V_C. The detailed elements of matrix $\mathbf{A}_{unt} \in \mathbb{R}^{6N\times 6}$, vector $\mathbf{B}_{unt} \in \mathbb{R}^{6N}$, and vector $\mathbf{Y}_{vec} \in \mathbb{R}^{6}$ are presented in Appendix A

$$\mathbf{B}_{unt} = \mathbf{A}_{unt}\mathbf{Y}_{vec} + \mathbf{e} \tag{5.15}$$

Once $\mathbf{Y}_{vec}$ is determined, the line currents can be calculated in equation (5.16)

$$\mathbf{I}_L = \mathbf{I}_S - (\mathbf{Y}_{diag}\mathbf{V}_S) \tag{5.16}$$

Where $\mathbf{Y}_{diag} \in \mathbb{R}^{6N\times 6N}$ is the block diagonal matrix containing N times the matrix $\mathbf{Y_{unt}}$ as shown in (5.17).

$$\mathbf{Y}_{diag} = \begin{bmatrix} \mathbf{Y_{unt}} & 0 & \dots & 0 \\ 0 & \mathbf{Y_{unt}} & \dots & 0 \\ \vdots & \vdots & \ddots & \vdots \\ 0 & 0 & \dots & \mathbf{Y_{unt}} \end{bmatrix} \tag{5.17}$$

The series impedance parameters are determined from the regression (5.18), where the LTS is executed using N measurements. The matrix $\mathbf{I}_{unt}$ contains the line current measurements

and $\mathbf{V}_Z$ is a vector of voltage drops across the line impedance.

$$\mathbf{V}_Z = \mathbf{I}_{unt}\mathbf{Z}_{unt} + \mathbf{e}, \tag{5.18}$$

$$\mathbf{I}_{unt} = \begin{bmatrix} I_{LA1} & I_{LB1} & I_{LC1} & 0 & 0 & 0 \\ 0 & I_{LA1} & 0 & I_{LB1} & I_{LC1} & 0 \\ 0 & 0 & I_{LA1} & 0 & I_{LB1} & I_{LC1} \\ \vdots & \vdots & \vdots & \vdots & \vdots & \vdots \\ I_{LAN} & I_{LBN} & I_{LCN} & 0 & 0 & 0 \\ 0 & I_{LAN} & 0 & I_{LBN} & I_{LCN} & 0 \\ 0 & 0 & I_{LAN} & 0 & I_{LBN} & I_{LCN} \end{bmatrix}$$

5.4 Robust PMU-based parameter estimation

In this section, the estimation of the line parameters in the presence of bad measurements or departures from the normal model due to LFO present in PMU signals is developed. Outliers could be present in both the observation vector or the regressors matrix, known as leverage points which create a more challenging case for the estimation. First, we will briefly introduce the classical WLS which will be used for comparison with the proposed LTS estimator.

5.4.1 WLS-based estimation of line parameters

The estimation problem follows a linear regression model expressed as

$$\mathbf{B} = \mathbf{A}\mathbf{Y}_v + \mathbf{e}. \tag{5.19}$$

The objective is to estimate the vector $\mathbf{Y}_v \in \mathbb{R}^n$ which is unknown and contains the shunt parameters of the line. The vector $\mathbf{B} \in \mathbb{R}^m$ contains current measurements collected from

PMUs. The regressor matrix $\mathbf{A} \in \mathbb{R}^{m \times n}$ is sparse and contains voltage measurements. The error is assumed Gaussian with a null average and a covariance diagonal matrix $\mathrm{Cov}(\mathbf{e}) = R$.

The estimation is conducted using the Weighted Least Squares estimator (WLS) which is a maximum likelihood estimator, i.e., an asymptotically consistent and unbiased estimator that reaches the Cramer-Rao lower bound when the error is Gaussian. The WLS estimate is obtained from

$$\hat{\mathbf{Y}} = \mathbf{G}^{-1}\mathbf{A}^T\mathbf{W}\mathbf{B} \tag{5.20}$$

where $\mathbf{G} = \left(\mathbf{A}^T\mathbf{W}\mathbf{A}\right)$ is known as the gain matrix, the matrix $\mathbf{A}^T$ is the transpose of $\mathbf{A}$ and $\mathbf{W}$ is the weight matrix corresponding to $\mathbf{R^{-1}}$ the inverse of the covariance matrix, $\mathbf{R}$, of the error.

In order to detect the bad data, the residuals could be analyzed. The estimated error or vector of residuals, $\mathbf{r}$, is calculated from (5.21).

$$\begin{aligned} \mathbf{r} &= \mathbf{B} - \hat{\mathbf{B}} = \mathbf{B} - \mathbf{A}\hat{\mathbf{Y}} \\ &= (\mathbf{I} - \mathbf{A}\mathbf{G}^{-1}\mathbf{A}^T\mathbf{W})\mathbf{B} \\ &= (\mathbf{I} - \mathbf{Q})\mathbf{B} \end{aligned} \tag{5.21}$$

The matrix $(\mathbf{I} - \mathbf{Q})$ relates the residuals to the measurement vector $\mathbf{B}$. The quantity F is the sum of weighted residuals is

$$F = \sum_{j=1}^{m} \boldsymbol{r}_j^2 \boldsymbol{W_{jj}} \tag{5.22}$$

where $\boldsymbol{W_{jj}}$ is the jth diagonal element of $\mathbf{W}$. If $F \geq \chi^2_{m-n,\alpha}$, the data contains at least one bad measurement. The quantity $\chi^2_{m-n,\alpha}$ is the α-quantile of the χ^2 distribution. The largest magnitude E_r of the standardized estimation error calculated from (5.23) is the bad

measurement.

$$E_r = \frac{\mid \boldsymbol{r}_j \mid}{\sqrt{\frac{\left(1-\text{diag}(Q)_{jj}\right)}{W_{jj}}}}. \tag{5.23}$$

While this approach is useful for detecting errors or outliers in the observation vector (i.e., vector $\mathbf{B}$), it could fail to detect bad measurements in the regressors or the rows of the matrix $\mathbf{A}$. Outliers in the regressors matrix are known as leverage points. The WLS is badly biased by leverage points and the residuals are not reliable enough to detect such outliers [47].

In the presence of leverage points, more sophisticated estimators than WLS must be implemented and their residuals analyzed for detecting this type of outliers [48, 49]. In this paper, we will use the least trimmed squares (LTS) which minimizes a trimmed percentage of the regression squared residuals [50]. The LTS has been recently implemented to robustly estimate the static power states in [49, 51, 52]. We outline the LTS in the following.

5.4.2 LTS-based estimation of line parameters

Denote $r_{(1)}, r_{(2)}, \ldots, r_{(m)}$ the residuals sorted from the smallest to the largest in their magnitudes as

$$r^2_{(1)} \leq r^2_{(2)} \leq \ldots \leq r^2_{(m)}.$$

Let the parameter $\gamma \in [0, 1)$ be the trimming fraction. The LTS finds the estimate $\hat{\mathbf{Y}}_v$ of the true state $\mathbf{Y}_v$ by discarding γ portion of the measurements that make the residuals large. More specifically, it minimizes the cost function

$$J(\hat{\mathbf{Y}}_v) = \sum_{i=1}^{\lfloor(1-\gamma)m\rfloor+1} r^2_{(i)}(\hat{\mathbf{Y}}_v), \tag{5.24}$$

where $\lfloor\cdot\rfloor$ is the floor function.

Another robust approach similar to the LTS in nature is the least median of squares (LMS). The LMS minimizes the sample median of squared residuals but suffers from a

lack of accuracy when the data is clean. The LTS can be resistant against outliers in the observation vector $\mathbf{B}$ and the regressor matrix $\mathbf{A}$ as long as the number of outliers is smaller than its γ portion, which will be discarded. This equivalently means that the limitation of the LTS is that if there are more outliers than the percentage specified by γ, then it will be affected similarly as the WLS. This is known as the breakdown point in robust statistics [50] which is the maximum fraction and estimator can handle before breaking down and giving unreliable estimates.

It is also important to ensure the best possible tradeoff between robustness and efficiency. The robustness represents the resistance of the estimator towards outliers while the efficiency reflects the accuracy of the estimator under the assumed assumptions, i.e., absence of outliers. The robustness could be measured by the breakdown point and the efficiency is evaluated by the mean square error (MSE) of the estimator. The MSE accounts for the bias and asymptotic variance of the estimator. Increasing γ to 0.5, for example, implies that the estimator can converge with up to 50% of outliers present in the data set. However, this will reduce the number of measurements considered in the estimation to half of the available data. Loosing clean data in the estimation implies degraded accuracy of the estimation. In order to ensure the best tradeoff of robustness vs. efficiency, the residuals of the LTS are analyzed. The residuals that are not Gaussian are rejected and the estimation is re-run with a WLS in a final step.

Since the matrix $\mathbf{A}$ is sparse, the breakdown point is not exactly equal to the rejected percentage γ. In fact, sparsity raises the question of observability, this means that the LTS should reject bad measurements but keep enough data to ensure that the matrix $\mathbf{A}$ has full rank. An unknown state in $\mathbf{Y}$, for example, is not linked to all measurements collected in $\mathbf{B}$. This has been studied theoretically in the context of logistic regression [53] where γ is bounded and the breakdown point is obtained. A fast algorithm for the LTS is provided in [54]. We adapted the program to handle sparse regressor matrices.

5.5 Offline Simulation results

5.5.1 LTS-based parameter estimation of a transposed Line

Fig. 5.3 shows a one line diagram for a four bus system used to test the estimation approach. The considered line is a 231kV line between bus S and Bus R and the nominal frequency is 60Hz. It is a 100 km long line with a series capacitor of 100 μF representing 16% degree of compensations respectively. The current transformers CTs are modeled as C-class C200 CTs with a burden of 2Ω [34] and the current transformer ratio (CTR) is 200 : 1. The voltage transformer is a Coupling Capacitor Voltage Transformer (CCVT) and the transformer ratio (VTR) is 345 kV : 115 V. The current transformers and the voltage transformers in the offline simulation were modeled as ideal and the current and voltage measurements were ideally synchronized. A separate program was used to create COMTRADE files for the measurements. In that analyzer, a low pass anti-aliasing filter with cutoff frequency of 480Hz was used to resample the voltages and currents measurements to 960 sample per second. A digital filter modeled in Mathcad implemented digital cosine filter (16 samples/cycles) and sine filter (cosine filter output delayed by a quarter of a cycle) have been used to represent the PMUs. Equation (5.25) shows the parameters of the compensated line.

$$\mathbf{Z} = \begin{bmatrix} 11 + 67.35i & 8.25 + 29.908i & 8.25 + 29.908i \\ 8.25 + 29.908i & 11 + 67.35i & 8.25 + 29.908i \\ 8.25 + 29.908i & 8.25 + 29.908i & 11 + 67.35i \end{bmatrix} \Omega \tag{5.25}$$

Four different states ($N = 4$) were created to produce unbalanced conditions to perform the estimation:

1. Single pole opening for phase A in switch 2
2. Two different unbalanced load conditions.
3. Single line to ground fault at the end of the compensated line.

The single line to ground fault induced a low frequency oscillation in current measurements as shown in Figure 5.2.

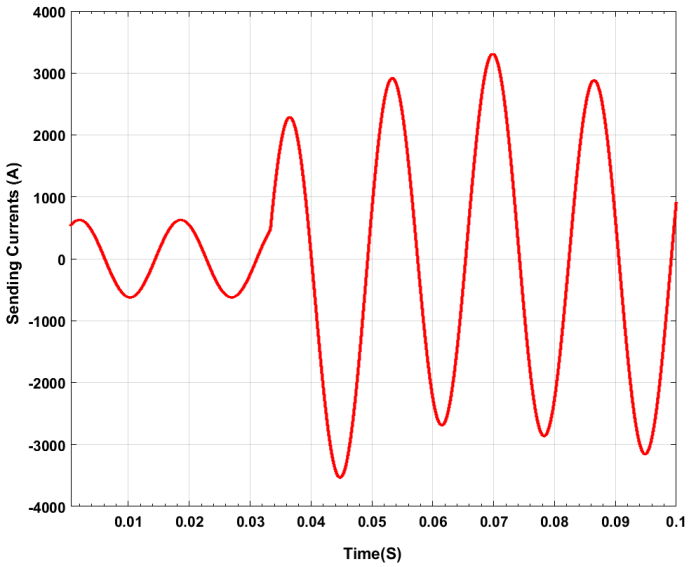

Figure 5.2: Phase A sending end current during a SLG fault with LFO.

We executed an estimation on the regression given in (5.1) with $m = 3N = 12$ and $n = 2$ to get the shunt admittance and then solved the second regression given in (5.8) to get the two impedance parameters with $m = 12$ as well. The data includes bad current measurements as a result of LFO which are observation outliers. In addition, the synchrophasor measurement units may contain some noise and errors. The bad data can be in either a current or a voltage measurement. Based on that, an intended incorrect voltage measurement was induced with an error in one of the sending voltages V_{SA} by increasing its value by 7%. Notice that a pre-check could detect certain large voltage values. The estimation method is automatic and could treat the 7% error without pre-treatment. The 7% error could, for example, be masked if the voltages are initially low and the errors raise these values. This issue could happen when the voltage is high and decreased by the error as well. The proposed method will however detect these cases using the sophisticated regression models and the LTS estimator.

The voltages and currents were passed through a low pass anti-aliasing filter to eliminate the high frequency components in the measurements. The data were sampled at 500 samples

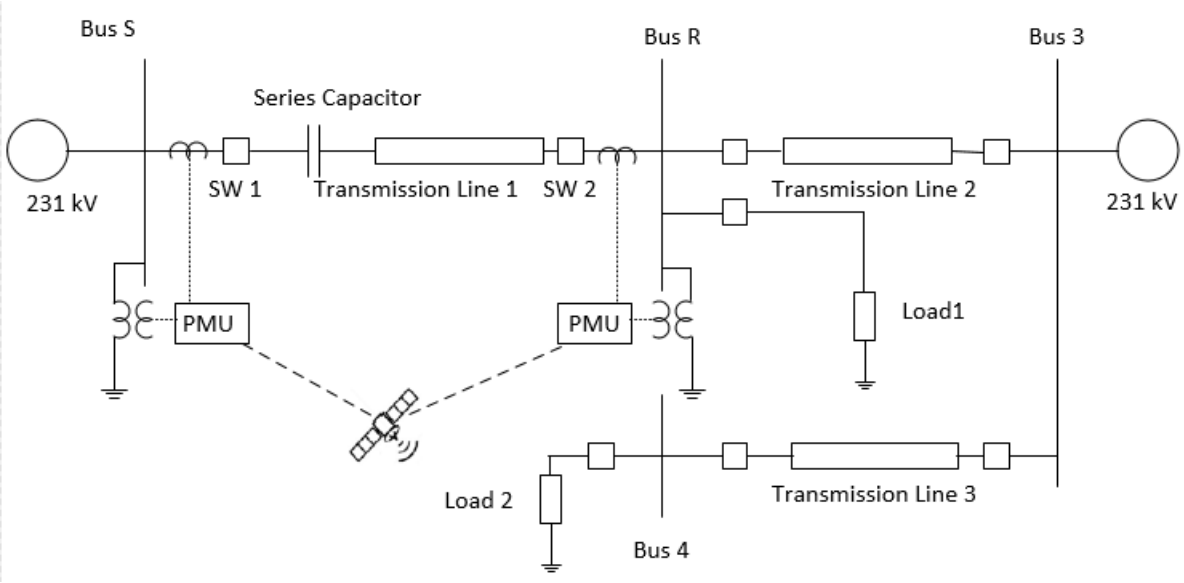

Figure 5.3: Test system model.

per cycle by using a cosine digital filter over the first two cycles to reduce the negative effect of LFO on the fundamental frequency. The program available from [55] was adapted and executed in MATLAB. The LTS detects the outliers caused by the LFO and removes those measurements automatically. Table 5.1 confirms that the LTS was able to detect and reject the bad data for both cases and all the errors were below 5% which is an acceptable percentage.

On the other hand the WLS was executed on the same test model. In this case, the threshold is set to the quantile $\chi^2_{m-n,\alpha} = \chi^2_{12-2,0.01} = 23.21$. The quantity computed from (5.22) was superior to the threshold. The measurement corresponding to the largest residual calculated in (5.23) was rejected and the WLS was re-executed. This step was repeated until no bad measurements were detected. The estimation was started with m=12 and the chi-square test detected 3 outliers.

Table 5.2 shows that the WLS gave an accurate estimation when the bad measurement was the current one. The error percentage was acceptable in this case because the chi-square rejected the bad data current caused by the LFO. This was not the case when the voltage was contaminated since the WLS was highly biased by this leverage point which made the

Table 5.1: LTS estimation results for transposed line

Calculation Method	Positive Seq. Mag.	Positive Seq. Angle	Zero Seq. Mag.	Zero Seq. Angle	Shunt C
Simulation Values	37.54 (Ω)	85.79 (deg)	130.1 (Ω)	77.79 (deg)	0.856 (μF)
LTS Results with 16% degree of compensation	38.11 (Ω)	85.16 (deg)	130.83 (Ω)	77.89 (deg)	0.848 (μF)
Error of LTS with 16% degree of compensation	1.5%	0.63 (deg)	0.55%	0.1 (deg)	0.9%
Error of WLS	1.5%	0.66 (deg)	0.56%	0.11 (deg)	2.1%

chi-square test applied to the residuals unreliable.

5.5.2 LTS-based parameter estimation of an untransposed Line

The same model was used for an untransposed line for which the impedance matrix is given in equation (5.26). In order to create a zero-sequence current, a single line to ground fault has been simulated in different locations in the system. The study starts with a fault close to the series compensated line and moves away from the bus to find the best unbalance ratio for the estimation. The unbalance ratio is the zero-sequence current to the positive-sequence current (I_0/I_1). The optimal estimates are obtained when the ratio of the unbalance is between 20 to 40 percent. Estimating the line parameters based on the faults is not a practical approach, some lines rarely experience faults. However, it has also been included in this study to consider the effect of LFO on the estimation. This case considering six ($N = 6$) states:

1. Internal single line to ground close to the series capacitor

2. External single line to ground fault at line 2

Table 5.2: WLS estimation results for transposed line

Calculation Method	Positive Seq. Mag.	Positive Seq. Angle	Zero Seq. Mag.	Zero Seq Angle	Shunt C
Simulation Values	37.54 (Ω)	85.79 (deg)	130.10 (Ω)	77.79 (deg)	0.856 (μF)
WLS Estimation Results Before Excluding the Bad Data	41.09 (Ω)	72.22 (deg)	144.8 (Ω)	73.21 (deg)	1.088 (μF)
Error	9.4%	13.57 (deg)	11.2%	4.58 (deg)	27.1%
WLS Estimation Results with Bad Current Measurements	38.133 (Ω)	85.14 (deg)	130.846 (Ω)	77.912 (deg)	0.838 (μF)
Error	1.5%	0.65 (deg)	0.56%	0.12 (deg)	2.1%
WLS Estimation Results with Bad Voltage Measurements	42.73 (Ω)	76.49 (deg)	150.7 (Ω)	71.32 (deg)	0.301 (μF)
Error	14.6%	9.3 (deg)	11.8%	6.47 (deg)	20%

3. External single line to ground fault at line 3

4. Three different single pole open conditions to generate unbalanced currents in the three phases created by opening switch 2

5. Two unbalanced load cases.

The first state has three scenarios of different fault locations. In the estimation in (5.15), $m = 6N = 36$ and $n = 6$. An additional incorrect voltage measurement was introduced to check the

ability of LTS to identify and detect bad measurements in currents and voltages as well.

$$\mathbf{Z} = \begin{bmatrix} 9.03 + 69.127i & 5.644 + 33.712i & 5.482 + 28.651i \\ 5.644 + 33.712i & 9.03 + 69.127i & 5.644 + 33.712i \\ 5.482 + 28.651i & 5.644 + 33.712i & 9.03 + 69.127i \end{bmatrix} \Omega \tag{5.26}$$

All currents and voltages phasor measurements were collected from both ends of the line using PMUs. The faults last for 5 cycles and the current and voltage measurements are passed through a low pass anti-aliasing filter and then through a digital cosine filter to represent the PMUs in the simulation. The LTS was applied to the regression (5.15) and (5.18) to estimate the line parameters. The results are shown in Table 5.3. The bad data was detected and excluded in the scenario of the presence of outliers in both current and voltage measurements. The performance of the LTS is good and the results are accurate.

The WLS with chi-square bad data detection was also implemented for comparison purpose. It was applied on bad current and voltage measurements. In addition the first and second cycle window of the measurements was taken for 16 and 500 samples per cycle in the digital cosine filter. The current measurements were taken from the first cycle and the second cycle after the fault and two WLS estimators were executed respectively as shown in Table 5.4. The WLS was only able to detect the bad current measurements but not the bad voltage measurements.

The error covariance matrix $\mathbf{R}$ is chosen to be diagonal containing the variances of the measured currents in the first regression (5.1). The variances of the sending and receiving current errors were added together. The errors in the voltages were added to the regressor matrix ($\mathbf{A}$) and matrix ($\mathbf{A_{unt}}$) which are random matrices. The error is changed for the case of the second regression (5.8) to voltage errors. In this case, R is evaluated from the variance of the voltage. If the covariance $\mathbf{R}$ is erroneous then the performance of both the WLS and LTS would be degraded. The LTS, however, could remove up to $\gamma\%$ of erroneous points if they do not agree with the majority. The majority should have correct weights in this case. The error could be due to the addition of uncertainties

Table 5.3: LTS estimation results for untransposed line

Calculation Method	Positive Seq. Mag.	Positive Seq. Angle	Zero Seq. Mag. (Ω)	Zero Seq. Angle (deg)	Shunt C
ATP Simulation Values	37.26 (Ω)	84.7 (deg)	134.7 (Ω)	81.37 (deg)	0.752 (μF)
LTS Results with bad current measurements	37.98 (Ω)	84.95 (deg)	134.93 (Ω)	81.48 (deg)	0.762 (μF)
Error	1.93%	0.25 (deg)	0.17%	0.11 (deg)	1.27%
LTS Results with bad voltage measurements	37.98 (Ω)	84.95 (deg)	134.94 (Ω)	81.48 (deg)	0.762 (μF)
Error	1.93%	0.25 (deg)	0.17%	0.11 (deg)	1.27%

from instrument transformers, and the interface such as the cables but these two components could be compensated by the calibration of the PMU as discussed in the literature [56]. The errors in the Analog/Digital converters create uncertainty in the PMU measurement. The authors in [57] proposed methods to evaluate the standard uncertainty for PMU measurements.

A Monte-Carlo simulation was conducted to confirm the performance of the LTS-based estimation approach. The simulation generated 100 replications where the error or noise of the PMUs was

Table 5.4: WLS estimation results for untransposed line

Calculation Method	Positive Seq. Mag.	Positive Seq. Angle	Zero Seq. Mag.	Zero Seq Angle	Shunt C
Simulation Values	37.543 (Ω)	85.799 (deg)	130.10 (Ω)	77.798 (deg)	0.856 (μF)
16 Samples 1^{st} cycle without WLS	32.453 (Ω)	72.273 (deg)	92.916 (Ω)	70.441 (deg)	0.792 (μF)
16 Samples 2^{nd} cycle without WLS	40.908 (Ω)	78.197 (deg)	101.203 (Ω)	75.488 (deg)	0929 (μF)
500 Samples 1^{st} cycle without WLS	33.915 (Ω)	77.214 (deg)	106.903 (Ω)	79.132 (deg)	0.891 (μF)
500 Samples 2^{nd} cycle without WLS	38.72 (Ω)	80.495 (deg)	153.608 (Ω)	80.724 (deg)	0.621 (μF)
WLS	38.0784 (Ω)	84.9406 (deg)	134.949 (Ω)	81.476 (deg)	0.775 (μF)
Error 16 Samples 1^{st} cycle	12.9%	13.5 (deg)	31%	7.3 (deg)	29.2%
Error 16 Samples 2^{nd} cycle	9.7%	7.6 (deg)	24.8%	2.3 (deg)	23.5%
Error 500 Samples 1^{st} cycle	9%	8.5 (deg)	20.6%	1.3 (deg)	18.5%
Error 500 Samples 2^{nd} cycle	3.8%	5.3 (deg)	14%	2.9 (deg)	17.3%
Error WLS without bad data	2.1%	0.85 (deg)	0.18%	3.6 (deg)	3%

considered Gaussian with a standard deviation of the phase angle equal to 0.006 degrees, 0.012% for the voltage magnitude, 0.017% for the current magnitude. These could also be obtained from meter characteristics provided by the manufacturer. The covariance **R** was evaluated from these errors of magnitudes and phase angles. The average and the standard deviation of the estimates is illustrated in Table 5.5. The first simulation consists of 24 clean measurements collected from 3 single pole open conditions and one unbalanced load case. The second simulation contains 30 measurements including 3 outliers due to the LFO generated from a single line to ground fault. The trimming percentage of the LTS was fixed to 0.19 which means that it could resist up to three outliers. The Monte-Carlo simulation confirms the good behaviour of the LTS based approach in both cases where the data is clean or has error.

Table 5.5: Monte-Carlo estimation results for the LTS-based estimation

Calculation method	Positive seq. mag.	Positive seq. angle	Zero seq. mag.	Zero seq. angle
ATP simulation values	37.26 (Ω)	84.7 (deg)	134.7 (Ω)	81.37 (deg)
LTS results with clean data	38.7±1.2 (Ω)	84.9±1.4 (deg)	135.5±4.4 (Ω)	81.4±2.17 (deg)
Error	3.8 %	0.2 (deg)	0.6 %	0.03 (deg)
LTS results with bad current data	39±1.9 (Ω)	84.9±2 (deg)	136.2±4.5 (Ω)	81.7±2.3 (deg)
Error	4.6 %	0.2 (deg)	1.1 %	0.33 (deg)

5.6 Hardware-in-the-Loop Simulation results

The power system model was implemented in a real-time digital simulation for testing the proposed LTS-based estimation with commercial PMUs. The compensated line was 100 km with 200 μF series capacitor which implies that the degree of compensation is 16%. A detailed 400 C-class CT model and detailed CCVT model with an active ferroresonance filter were used in the hardware-in-the-loop simulation. Commercial relays were used as PMUs at both ends of the compensated line with a GPS clock to synchronize the data and a data concentrator for time alignment. The CTR was $(400:1)$, and the VTR was $(345\ kV:115\ V)$. A distributed parameter transmission line model was used to represent the transmission lines in the system. A central admin software was exploited to view and get the voltage and current measurements. A Phasor Data Concentrator (PDC) collected PMUs with a reporting rate of 60 frames per second. The arrangement of the structure set up is shown in Figure 5.4. Five cases of unbalanced zero-sequence currents were applied. Three cases

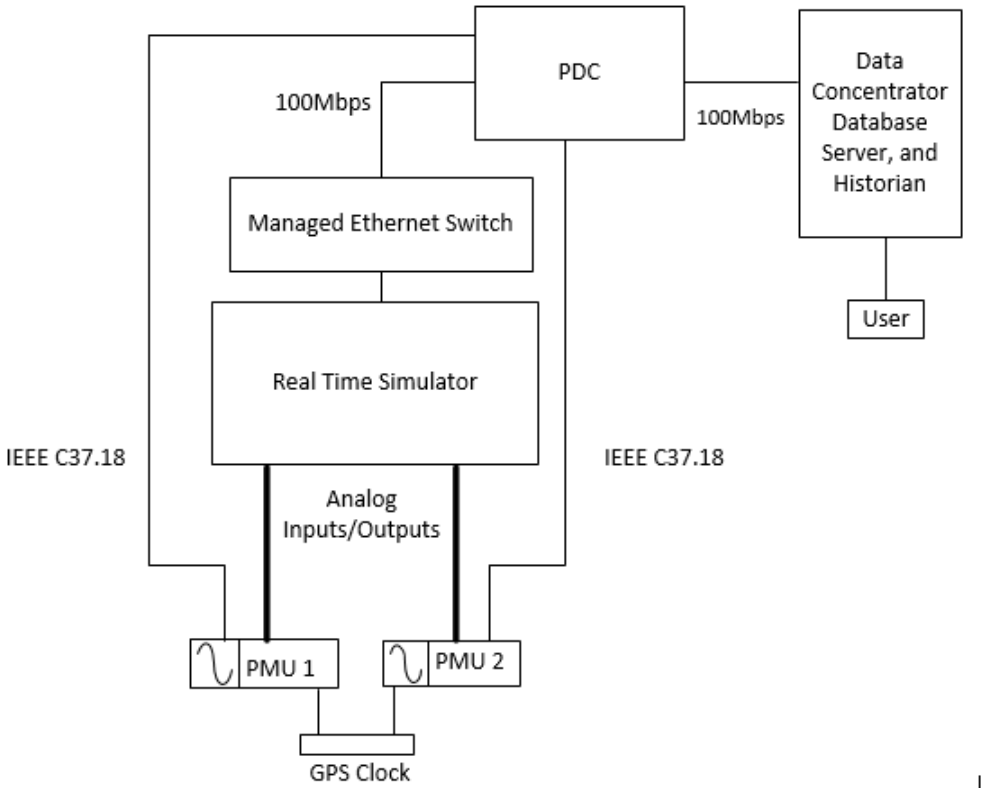

Figure 5.4: Network setup for real time simulation.

of single pole opening were applied in switch 2 and two cases of a single line to ground fault in line 1 and line 2 were generated respectively. The proposed LTS-based estimation and the classical WLS with bad data detection were applied for the transposed and untransposed line. Table 5.6 and Table 5.7 show the results for the transposed and the untransposed line respectively. From the two tables, the LTS-based approach was able to detect and reject the bad current and voltage measurements. The results show that even an external remote fault from the compensated line induced a sufficient unbalance for the LTS to perform an accurate estimation. The WLS with

Table 5.6: WLS and LTS results for transposed line

Calculation Method	Positive Seq. Mag.	Positive Seq. Angle	Zero Seq Mag.	Zero Seq Angle	Shunt C
ATP Simulation Values	37.54 (Ω)	85.80 (deg)	130.1 (Ω)	77.80 (deg)	0.856
LTS Results with bad current measurements	38.21 (Ω)	85.2 (deg)	130.4 (Ω)	77.81 (deg)	0.886 (μF)
Error	1.7%	0.52 (deg)	0.25%	0.01 (deg)	3.5%
WLS Results with bad current measurements	37.738 (Ω)	84.285 (deg)	128.4 (Ω)	78.8 (deg)	0.885 (μF)
Error	0.51%	1.5 (deg)	1.3%	1 (deg)	3.4%
LTS Results with bad voltage measurements	38.21 (Ω)	85.286 (deg)	130.4 (Ω)	77.81 (deg)	0.886 (μF)
Error	1.7%	0.52 (deg)	0.25%	0.01 (deg)	3.5%
WLS Results with bad voltage measurements	40.973 (Ω)	81.04 (deg)	95.783 (Ω)	88.24 (deg)	0.667 (μF)
Error	9.1%	4.76 (deg)	26.3%	10.4 (deg)	22.1%

chi-square test detected only the bad current data but was unable to detect the bad voltage data. The positive-sequence and zero-sequence parameters are estimated for both the transposed and untransposed cases.

Table 5.7: WLS and LTS results for untransposed line

Calculation Method	Positive Seq. Mag.	Positive Seq. Angle	Zero Seq. Mag.	Zero Seq. Angle	Shunt C
ATP Simulation Values	37.26 (Ω)	84.70 (deg)	134.70 (Ω)	81.37 (deg)	0.75 (μF)
LTS Results with bad current measurements	38.6 (Ω)	83.9 (deg)	133.3 (Ω)	83.06 (deg)	0.72 (μF)
Error	4.5%	0.72 (deg)	0.99%	1.69 (deg)	3.6%
WLS Results with bad current measurements	38.7 (Ω)	83.4 (deg)	136 (Ω)	83.4 (deg)	0.72 (μF)
Error	3.9%	1.3 (deg)	0.99%	2 (deg)	3.6%
LTS Results with bad voltage measurements	38.6 (Ω)	83.9 (deg)	133.3 (Ω)	83 (deg)	0.72 (μF)
Error	4.5%	0.8 (deg)	0.99%	1.63 (deg)	3.6%
WLS Results with bad voltage measurements	42.9 (Ω)	78.4 (deg)	108.7 (Ω)	72.6 (deg)	0.47 (μF)
Error	15.2%	6.3 (deg)	19.2%	8.77 (deg)	37.5%

5.7 Conclusion

A least trimmed squares estimation method was proposed to estimate the positive, negative and zero-sequence parameters of series compensated line. The LTS-based method is advocated to use in the presence of outliers due to low frequency oscillation that could happen in the series compen-

sated line. The proposed algorithm is also accurate when outliers are present in the current and voltage measurements obtained from PMUs. Simulation results showed the superior performance of the LTS-based algorithm with respect to the classical WLS with chi-square test. The simulation considered both the transposed and untransposed line parameter estimation. Emulation with a real time digital simulator confirmed the performance as well.

Chapter 6: Mutually Coupled Lines

6.1 Introduction

This chapter presents a new method to estimate the parameters for two mutually coupled lines. The two lines are parallel for part of a distance and are magnetically and capacitively coupled but not electrically coupled. Two cases were considered; the first one is when the two lines are transposed, and in the second case, both lines are untransposed. A transient simulation software tool was used to perform simulation and validate the proposed method for different power system configurations.

6.2 Coupling Between Two Lines That are Each Transposed

When the two lines are fully transposed, the mutual coupling between the lines will be eliminated for positive- and negative-sequence but not for zero-sequence [58]. The zero-sequence mutual coupling will exist whether the lines are transposed or not transposed. In the case of a parallel line with different voltages, the induced zero current on the lower level voltage will be bigger than the one on the higher voltage line, which will affect the accuracy of the estimation of a targeted line. Figure 6.1 shows two transposed lines that are mutually coupled. The relationship between sequence currents and sequence voltages can be written as shown in equation 6.1 [26]:

$$\begin{bmatrix} \Delta V0_{L1} \\ \Delta V1_{L1} \\ \Delta V2_{L1} \\ \Delta V0_{L2} \\ \Delta V1_{L2} \\ \Delta V2_{L2} \end{bmatrix} = \begin{bmatrix} \mathrm{Z0}_{L1} & 0 & 0 & \mathrm{Z0}_{m} & 0 & 0 \\ 0 & \mathrm{Z1}_{L1} & 0 & 0 & 0 & 0 \\ 0 & 0 & \mathrm{Z2}_{L1} & 0 & 0 & 0 \\ \mathrm{Z0}_{m} & 0 & 0 & \mathrm{Z0}_{L2} & 0 & 0 \\ 0 & 0 & 0 & 0 & \mathrm{Z1}_{L2} & 0 \\ 0 & 0 & 0 & 0 & 0 & \mathrm{Z2}_{L2} \end{bmatrix} . \begin{bmatrix} \mathrm{I0}_{L1} \\ \mathrm{I1}_{L1} \\ \mathrm{I2}_{L1} \\ \mathrm{I0}_{L2} \\ \mathrm{I1}_{L2} \\ \mathrm{I2}_{L2} \end{bmatrix} \tag{6.1}$$

where ΔV represents the difference between the sending and receiving sequence voltages. I_0, I_1, and I_2 are the sequence currents for the two lines, and $\mathrm{Z0}_m$ is the zero sequence mutual impedance.

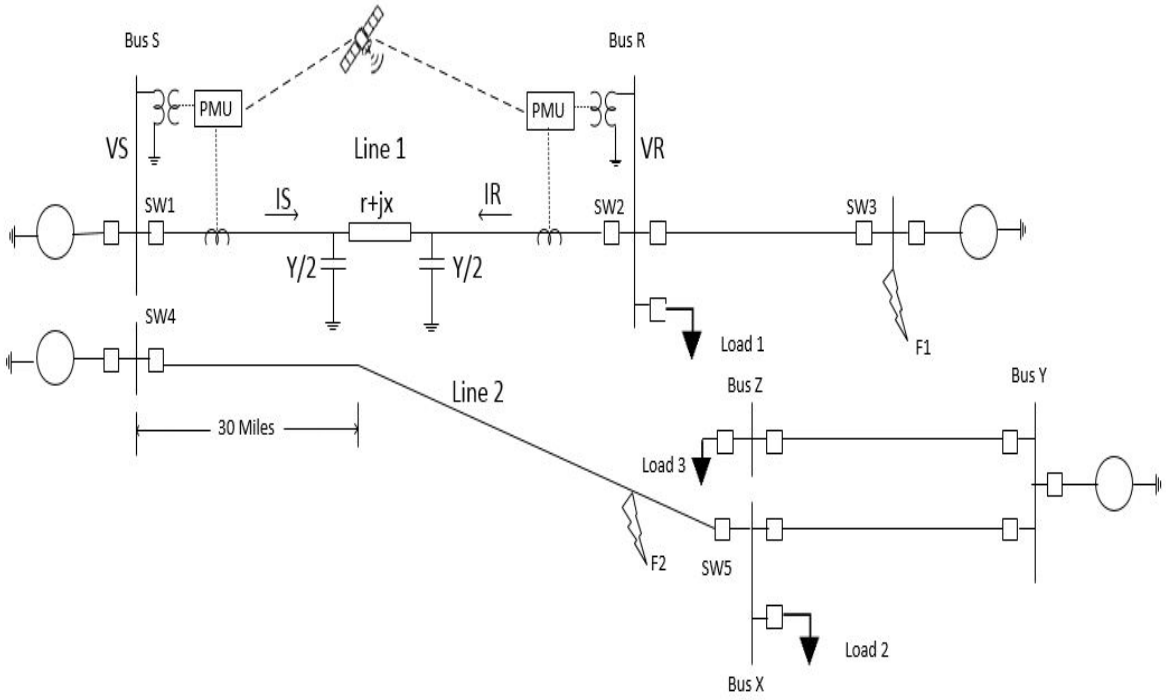

Figure 6.1: Two parallel transposed lines

The proposed method for parameter estimation is based on disconnecting one of the lines at both ends and inducing an unbalance in the other line. In this case all the current in the disconnected line will be zero, and the equation for the voltages and currents will be as follows:

$$\begin{bmatrix} \Delta V0_{L1} \\ \Delta V1_{L1} \\ \Delta V2_{L1} \\ \Delta V0_{L2} \\ \Delta V1_{L2} \\ \Delta V2_{L2} \end{bmatrix} = \begin{bmatrix} \mathrm{Z0}_{L1} & 0 & 0 & \mathrm{Z0}_m & 0 & 0 \\ 0 & \mathrm{Z1}_{L1} & 0 & 0 & 0 & 0 \\ 0 & 0 & \mathrm{Z2}_{L1} & 0 & 0 & 0 \\ \mathrm{Z0}_m & 0 & 0 & \mathrm{Z0}_{L2} & 0 & 0 \\ 0 & 0 & 0 & 0 & \mathrm{Z1}_{L2} & 0 \\ 0 & 0 & 0 & 0 & 0 & \mathrm{Z2}_{L2} \end{bmatrix} . \begin{bmatrix} \mathrm{I0}_{L1} \\ \mathrm{I1}_{L1} \\ \mathrm{I2}_{L1} \\ 0 \\ 0 \\ 0 \end{bmatrix} \tag{6.2}$$

The unbalanced conditions could be single pole open or unbalanced load or ground fault anywhere in the system as long as they provide sufficient zero sequence current unbalance in the line. The ratio of zero-sequence current to positive-sequence current (I0/I1) is used to measure the unbalance in the system. The zero sequence mutual impedance $Z0_m$ can be determined as follows:

$$Z0_m = \frac{\Delta V0_{L2}}{I0_{L1}} \tag{6.3}$$

This method does not consider the shunt capacitance of the line, but the approach is very accurate for determining the mutual zero-sequence impedance, as will be shown in the results. But this approach can not be used to determine the line series self impedance and the shunt capacitance accurately. Another method is proposed to estimate the series impedance and the shunt parameters. The authors of [59] provides a set of three equations for estimating positive parameters of a line. In this research the approach will be extended to consider both zero- and positive-sequence parameters for mutual coupled lines as shown in equations (6.4) and (6.5) respectively. B0 and B1 represent the real and imaginary sending and receiving currents as shown in equation (6.6). A0 and A1 are the real and imaginary parts of sending and receiving currents for zero- and positive-sequence as shown in equations (6.7) and (6.8) respectively. X0 and X1 represent the zero-sequence and positive-sequence parameters respectively as shown in equation (6.9).

$$\mathbf{B_0} = \mathbf{A_0 X_0} \tag{6.4}$$

$$\mathbf{B_1} = \mathbf{A_1 X_1} \tag{6.5}$$

$$\mathbf{B_0} = \begin{bmatrix} \mathrm{Re}(IS_0) \\ \mathrm{Im}(IS_0) \\ \mathrm{Re}(IR_0) \\ \mathrm{Im}(IR_0) \end{bmatrix}, \mathbf{B_1} = \begin{bmatrix} \mathrm{Re}(IS_1) \\ \mathrm{Im}(IS_1) \\ \mathrm{Re}(IR_1 \\ \mathrm{Im}(IR_1) \end{bmatrix} \tag{6.6}$$

$$\mathbf{A_0} = \begin{bmatrix} \mathrm{Re}(VS_0) - \mathrm{Re}(VR_0) & -(\mathrm{Im}(VS_0) - \mathrm{Im}(VR_0)) & -\mathrm{Im}(VS_0) \\ \mathrm{Im}(VS_0) - \mathrm{Im}(VR_0) & \mathrm{Re}(VS_0) - \mathrm{Re}(VR_0) & \mathrm{Re}(VS_0) \\ \mathrm{Re}(VR_0) - \mathrm{Re}(VS_0) & -(\mathrm{Im}(VR_0) - \mathrm{Im}(VS_0)) & -\mathrm{Im}(VR_0) \\ \mathrm{Im}(VR_0) - \mathrm{Im}(VS_0) & \mathrm{Re}(VR_0) - \mathrm{Re}(VS_0) & \mathrm{Re}(VR_0) \end{bmatrix} \tag{6.7}$$

$$\mathbf{A_1} = \begin{bmatrix} \mathrm{Re}(VS_1) - \mathrm{Re}(VR_1)_1 & -(\mathrm{Im}(VS_1) - \mathrm{Im}(VR_1)) & -\mathrm{Im}(VS_1) \\ \mathrm{Im}(VS_1) - \mathrm{Im}(VR_1) & \mathrm{Re}(VS_1) - \mathrm{Re}(VR_1) & \mathrm{Re}(VS_1) \\ \mathrm{Re}(VR_1) - \mathrm{Re}(VS_1) & -(\mathrm{Im}(VR_1) - \mathrm{Im}(VS_1)) & -\mathrm{Im}(VR_1) \\ \mathrm{Im}(VR_1) - \mathrm{Im}(VS_1) & \mathrm{Re}(VR_1) - \mathrm{Re}(VS_1) & \mathrm{Re}(VR_1) \end{bmatrix} \tag{6.8}$$

Where the subscripts 0, and 1 stand for zero-sequence and positive-sequence respectively.

$$\mathbf{X_0} = \begin{bmatrix} g_0 \\ b_0 \\ \frac{Y_0}{2} \end{bmatrix}, \mathbf{X_1} = \begin{bmatrix} g_1 \\ b_1 \\ \frac{Y_1}{2} \end{bmatrix} \tag{6.9}$$

Once equations (6.4) and (6.5) are solved, the positive- and zero-sequence impedances of the line can be determined from equations (6.10) and (6.11) respectively.

$$Z_0 = \frac{1}{g_0 + jb_0} \tag{6.10}$$

$$Z_1 = \frac{1}{g_1 + jb_1} \tag{6.11}$$

The sequence impedance and sequence shunt admittance can be written as follows:

$$\mathbf{Z}_{012} = \begin{bmatrix} Z_0 & 0 & 0 \\ 0 & Z_1 & 0 \\ 0 & 0 & Z_2 \end{bmatrix}; \mathbf{Y}_{012} = \begin{bmatrix} Y_0 & 0 & 0 \\ 0 & Y_1 & 0 \\ 0 & 0 & Y_2 \end{bmatrix} \tag{6.12}$$

The phase domain impedance and the phase admittance of the line are calculated using equation (6.13).

$$\mathbf{Z}_{abc} = \mathbf{A}_{012}.\mathbf{Z_{012}}.\mathbf{A}_{012}^{-1}; \qquad \mathbf{Y}_{abc} = \mathbf{A}_{012}.\mathbf{Y_{012}}.\mathbf{A}_{012}^{-1} \tag{6.13}$$

6.2.1 Offline Simulation Results for Two Mutually Coupled Transposed Lines

Figure 6.1 shows a seven bus system that was used in the simulation to test the proposed method. The considered line for parameter estimation is line 1, which is rated 120kV and is 90 miles long. Line 2 is 230 kV and 120 miles long. The two lines are mutually coupled for 30 miles long at the start of the test, and then the length of the mutually coupled section will be increased for comparison purposes. Both lines are fully transposed, and equation (6.7) shows that each unbalanced state provides four equations. Since there are three unknowns, g_0, b_0, $\frac{Y_0}{2}$, one unbalanced condition is sufficient. However, three unbalanced states have been induced to increase the accuracy of the results. The first state created with a single pole open condition by opening phase (A) in switch 2. The second state was done with an unbalanced load 1 condition. A single line to ground fault was induced in location (F1) for state 3.

To consider the effect of changing the length of the mutually coupled section on the parameter estimation, three cases with different section lengths were considered. The length of the mutually coupled sections were 30 miles, 60 miles, and 75 miles which represent 33%, 66%, and 88% of the line length respectively. To estimate the zero sequence mutual coupling impedance, $Z0_m$, line 2 is taken out of service by opening switch 4 and switch 5. Equation (6.3) is used to determine $Z0_m$. Equations (6.4) and (6.5) are used to calculate $Z0_{L1}$ and $Z1_{L1}$ respectively. Notice from Table 6.1 that the errors in calculating magnitude and angle are below 5 % and the angles below 2.7 degrees in all cases, which confirms the accuracy of the proposed method. Changing the length of the coupled section does not affect the accuracy of the estimation results.

Table 6.1: Results for two parallel transposed line

Calculation Method	Positive Seq. Mag.	Positive Seq. Angle	Zero Seq. Mag.	Zero Seq. Angle	Shunt C	mutual zero seq. Mag	mutual zero seq. Angle
Simulation Values	43.49 (Ω)	71.91 (deg)	182.27 (Ω)	77.86 (deg)	1.064 (μF)	35.78 (Ω)	76.67 (deg)
Case 1 (33% mutual coupling)	43.04 (Ω)	71.76 (deg)	178.76 (Ω)	77.35 (deg)	1.02 (μF)	35.59 (Ω)	78 (deg)
Error	1.03%	0.15 (deg)	1.92%	0.51 (deg)	3.77%	0.51%	1.3 (deg)
Case 2 (66% mutual coupling)	42.9 (Ω)	71.53 (deg)	190.7 (Ω)	78.1 (deg)	1.027 (μF)	71.56 (Ω)	78.06 (deg)
Error	1.36%	0.38 (deg)	4.62%	0.24 (deg)	3.11%	1.65%	1.3 (deg)
Case 3 (88% mutual coupling)	42.2 (Ω)	74 (deg)	189.2 (Ω)	80.5 (deg)	1.021 (μF)	89.28 (Ω)	78.13 (deg)
Error	2.98%	2 (deg)	3.8%	2.64 (deg)	3.67%	0.18%	1.4 (deg)

6.3 Coupling Between Two Lines That are Each Untransposed

When a line is untransposed the sequence mutual impedances will not be zero [58]. Therefore in the case of two parallel untransposed lines, the sequence mutual impedances terms on the individual lines can not be considered zero. On the other hand the sequence mutual impedances between the two lines are still very small and can be neglected. In this case, the sequence voltage drop across each line can be written as follows.

$$\begin{bmatrix} \Delta V0L1 \\ \Delta V1L1 \\ \Delta V2L1 \\ \Delta V0L2 \\ \Delta V1L2 \\ \Delta V2L2 \end{bmatrix} = \begin{bmatrix} \mathrm{Z00}_{L1} & \mathrm{Z01}_{L1} & \mathrm{Z02}_{L1} & \mathrm{Z0}_{m} & 0 & 0 \\ \mathrm{Z10}_{L1} & \mathrm{Z11}_{L1} & \mathrm{Z12}_{L1} & 0 & 0 & 0 \\ \mathrm{Z20}_{L1} & \mathrm{Z21}_{L1} & \mathrm{Z22}_{L1} & 0 & 0 & 0 \\ \mathrm{Z0}_{m} & 0 & 0 & \mathrm{Z00}_{L2} & \mathrm{Z01}_{L2} & \mathrm{Z02}_{L2} \\ 0 & 0 & 0 & \mathrm{Z10}_{L2} & \mathrm{Z11}_{L2} & \mathrm{Z12}_{L2} \\ 0 & 0 & 0 & \mathrm{Z20}_{L2} & \mathrm{Z21}_{L2} & \mathrm{Z22}_{L2} \end{bmatrix} . \begin{bmatrix} \mathrm{I0}_{L1} \\ \mathrm{I1}_{L1} \\ \mathrm{I2}_{L1} \\ \mathrm{I0}_{L2} \\ \mathrm{I1}_{L2} \\ \mathrm{I2}_{L2} \end{bmatrix} \tag{6.14}$$

Equation (6.14) can be rearranged to solve for the sequence impedances based on N different cases of current and voltage measurements. The matrix $\mathbf{F}$ contains the sequence current phasors

$$F = \begin{bmatrix} I0\mathrm{L1}_1 & I1\mathrm{L1}_1 & I2\mathrm{L1}_1 & 0 & 0 & 0 & 0 & 0 & I0\mathrm{L2}_1 & 0 & 0 & 0 & 0 & 0 & 0 & 0 & 0 \\ 0 & 0 & 0 & I0\mathrm{L1}_1 & I1\mathrm{L1}_1 & I2\mathrm{L1}_1 & 0 & 0 & 0 & 0 & 0 & 0 & 0 & 0 & 0 & 0 & 0 \\ 0 & 0 & 0 & 0 & I2\mathrm{L1}_1 & 0 & I0\mathrm{L1}_1 & I1\mathrm{L1}_1 & 0 & 0 & 0 & 0 & 0 & 0 & 0 & 0 & 0 \\ 0 & 0 & 0 & 0 & 0 & 0 & 0 & 0 & I0\mathrm{L1}_1 & I0\mathrm{L2}_1 & I1\mathrm{L2}_1 & I2\mathrm{L2}_1 & 0 & 0 & 0 & 0 & 0 \\ 0 & 0 & 0 & 0 & 0 & 0 & 0 & 0 & 0 & 0 & 0 & 0 & I0\mathrm{L2}_1 & I1\mathrm{L2}_1 & I2\mathrm{L2}_1 & 0 & 0 \\ 0 & 0 & 0 & 0 & 0 & 0 & 0 & 0 & 0 & 0 & 0 & 0 & 0 & I2\mathrm{L2}_1 & 0 & I0\mathrm{L2}_1 & I0\mathrm{L2}_1 \\ \vdots & \vdots & \vdots & \vdots & \vdots & \vdots & \vdots & \vdots & \vdots & \vdots & \vdots & \vdots & \vdots & \vdots & \vdots & \vdots & \vdots \\ I0\mathrm{L1}_N & I1\mathrm{L1}_N & I2\mathrm{L1}_N & 0 & 0 & 0 & 0 & 0 & I0\mathrm{L2}_N & 0 & 0 & 0 & 0 & 0 & 0 & 0 & 0 \\ 0 & 0 & 0 & I0\mathrm{L1}_N & I1\mathrm{L1}_N & I2\mathrm{L1}_N & 0 & 0 & 0 & 0 & 0 & 0 & 0 & 0 & 0 & 0 & 0 \\ 0 & 0 & 0 & 0 & I2\mathrm{L1}_N & 0 & I0\mathrm{L1}_N & I1\mathrm{L1}_N & 0 & 0 & 0 & 0 & 0 & 0 & 0 & 0 & 0 \\ 0 & 0 & 0 & 0 & 0 & 0 & 0 & 0 & I0\mathrm{L1}_N & I0\mathrm{L2}_N & I1\mathrm{L2}_N & I2\mathrm{L2}_N & 0 & 0 & 0 & 0 & 0 \\ 0 & 0 & 0 & 0 & 0 & 0 & 0 & 0 & 0 & 0 & 0 & 0 & I0\mathrm{L2}_N & I1\mathrm{L2}_N & I2\mathrm{L2}_N & 0 & 0 \\ 0 & 0 & 0 & 0 & 0 & 0 & 0 & 0 & 0 & 0 & 0 & 0 & 0 & I2\mathrm{L2}_N & 0 & I0\mathrm{L2}_N & I1\mathrm{L2}_N \end{bmatrix}$$

(6.15)

I0, I1, and I2 for both lines, where $\mathbf{F} \in \mathbb{R}^{17\times 6N}$. The subscripts 1 and N represent the different unbalance states. $\mathbf{Z_{seq}}$ is an unknown vector containing of the sequence impedances of the two lines and the zero sequence mutual impedance, where $\mathbf{Z_{seq}} \in \mathbb{R}^{1}6$. The vector $\mathbf{G}$ contains the the sequence voltage drop across each line. $L1$ and $L2$ stand for line 1 and line 2 respectively.

$$\mathbf{G} = \begin{bmatrix} \\ \Delta V0L1_1 \\ \Delta V1L1_1 \\ \Delta V2L1_1 \\ \Delta V0L2_1 \\ \Delta V1L2_1 \\ \Delta V2L2_1 \\ \vdots \\ \Delta V0L1_N \\ \Delta V1L1_N \\ \Delta V2L1_N \\ \Delta V0L2_N \\ \Delta V1L2_N \\ \Delta V2L2_N \end{bmatrix}, \mathbf{Z_{seq}} = \begin{bmatrix} \\ \mathrm{Z00}_{L1} \\ \mathrm{Z01}_{L1} \\ \mathrm{Z02}_{L1} \\ \mathrm{Z11}_{L1} \\ \mathrm{Z12}_{L1} \\ \mathrm{Z20}_{L1} \\ \mathrm{Z21}_{L1} \\ \mathrm{Z0}_{m} \\ \mathrm{Z00}_{L2} \\ \mathrm{Z01}_{L2} \\ \mathrm{Z02}_{L2} \\ \mathrm{Z10}_{L2} \\ \mathrm{Z11}_{L2} \\ \mathrm{Z12}_{L2} \\ \mathrm{Z20}_{L2} \\ \mathrm{Z21}_{L2} \end{bmatrix} \tag{6.16}$$

The shunt capacitance is small and can be neglected for simplification. It can be seen from equation (6.14) that are 16 unknowns and 6 equations. At least more 10 equations need to be added

to solve for the unknown parameters. Since each unbalance states can provide set of 6 independent equations, at least 3 unbalance states need to be performed to execute the estimation. To estimate the impedance parameters, the least singular value of the multiplication of $(F \cdot F')$ has to be greater than 10^{-5}, and the ratio of maximum to minimum singular value has to be less than 10^4 [25]. Then the least squares approach is utilized to estimate the line parameters. Once the sequence impedance for each line is determined, the phase impedance can be calculated by using:

$$\mathbf{Z}_{abc} = \mathbf{A}_{012}.\mathbf{Z_{012}}.\mathbf{A}_{012}^{-1} \tag{6.17}$$

6.3.1 Offline Simulation Results for Two Mutually Coupled Untransposed Lines

The same model applied for transposed lines was used for untransposed lines. The phase impedance matrices for line 1 and line 2 are given in equation (6.18) and equation (6.19) respectively.

$$\mathbf{Z}_{L1} = \begin{bmatrix} 9.141 + 82.37i & 5.596 + 33.856i & 5.593 + 28.631i \\ 5.596 + 33.856i & 9.141 + 82.37i & 5.596 + 33.856i \\ 5.593 + 28.631i & 5.596 + 33.856i & 9.141 + 82.37i \end{bmatrix} \tag{6.18}$$

$$\mathbf{Z}_{L2} = \begin{bmatrix} 15.982 + 144.011i & 9.782 + 56.791i & 9.775 + 47.656i \\ 9.782 + 56.791i & 15.982 + 144.011i & 9.782 + 56.791i \\ 9.775 + 47.656i & 9.782 + 56.791i & 15.982 + 144.011i \end{bmatrix} \tag{6.19}$$

The lengths of line 1 and line 2 were 100 miles and 175 miles respectively. The estimation was executed for two cases of mutual coupling, the mutually coupled part was 30 mile in case 1, which represents 30% of the total length of line 1. In the second case, the mutually coupled length was been changed to 80 miles, which represents 80% of the total length of line 1. In order to create a

zero-sequence current, four different unbalance states are induced as follows:

1. Single pole open in phase A in switch 2
2. Single pole open in phase B in switch 2
3. Single pole open in phase C in switch 5
4. Single line to ground fault at location $F2$

All currents and voltages phasor measurements were collected from both ends of the line using PMUs.

To make sure there is an acceptable solution for the estimation, a singularity check has been performed for the current matrix using Matlab software.

Table 6.2: Results for parallel untransposed line

Calculation Method	Positive seq. Mag.	Positive Seq. Angle	Zero Seq. Mag.	Zero Seq. Angle	Mutual zero seq. Mag	Mutual zero seq. Angle
Simulation Values (Case 1)	50.38 (Ω)	85.96 (deg)	148 (Ω)	82.1 (deg)	22.63 (Ω)	77.17 (deg)
Case 1 (30% mutual coupling)	52.1 (Ω)	82.8 (deg)	142.2 (Ω)	84.9 (deg)	21.6 (Ω)	75.3 (deg)
Error	3.4%	3.1 (deg)	3.9%	2.8 (deg)	4.5%	1.8 (deg)
Simulation Values (Case 2)	50.38 (Ω)	85.96 (deg)	148 (Ω)	82.1 (deg)	60.35 (Ω)	77.17 (deg)
Case 2 (80% mutual coupling)	51 (Ω)	83.3 (deg)	141 (Ω)	86.1 (deg)	63.3 (Ω)	80.1 (deg)
Error	1.2%	2.6 (deg)	4.7%	4 (deg)	4.8%	2.9 (deg)

Table 6.2 shows the estimation results for two untransposed mutually coupled lines for the two cases. In case 1, all the magnitude percentage errors are under 5% and all angle errors are less than

5 degrees which can be acceptable. Including the shunt capacitance in the estimation equations will reduce the error.

6.4 Summary

Two methods are proposed to estimate parameters for two mutually coupled lines. The two lines are parallel for part of a distance and are magnetically and capacitively coupled but not electrically coupled. Two cases were considered; the first one is when the two lines are transposed, and in the second case, both lines are untransposed. In the first case, the proposed method was based on disconnecting one of the lines, and performed the Least Squares estimator to estimate the line parameters. In the second case, 3 unbalanced conditions were induced in the system to determine the line parameters. A least singular value and the ratio of maximum to minimum singular value were applied to check if there is a solution for the equations or not. The simulation results for all cases were under 5 % error for the parameter magnitudes and less than 5 degrees for parameter angles.

Chapter 7: Parameters Estimation for a Short Line Length Using the Least Trimmed Squares (LTS)

This is a paper that presented in IEEE Innovative Smart Grid Technologies (ISGT) conference in Washington, DC from February 17-20, 2019 and will appear in the proceeding of 2019.

7.1 Abstract

This paper introduces a novel method to estimate positive and zero-sequence transmission line parameters for short length lines. The current and voltage measurements are taken from synchronized phasor measurements (PMUs) located at both terminals of the line. Current transformer saturation was induced by the close in three-phase fault to consider its effect on the estimation accuracy. The method was applied for untransposed line with two different ratios of inductive reactive to resistance (X/R). The Least Trimmed Square (LTS) estimator was used to detect and reject the incorrect data. Two different simulation tools have used for simulating and validating the proposed method.

7.2 Introduction

The operation and response of many protection devices depend on line parameters settings. The accuracy of line parameters are essential for zone settings for distance relays and differential relays [60]. Also, inaccurate parameter estimation can affect the system simulation applications like system stability, fault location, and load flow study [57]. The sensitivity of current transformer (CT) errors in the very short line presents a challenge for estimating line parameters [30]. The author of [18] applied four different methods to estimate short line parameters. The least squares method and Jacobian based method have been used in the estimation to reduce the measurement noise. The authors in [5, 15, 61, 62] have used different methods to calculate the transmission line parameters utilizing the PMU data. In [33] the parameters for both transposed and untransposed are determined for longer lines. The previous methods were applied for either long lines or medium lines but they did not consider a short line which is less than 50 miles long.

Phasor measurements units (PMUs) provides accurate synchronized voltage, current, and power

measurements from anywhere on the system, and can be used to perform the parameters estimation [5]. CT saturation is expected as transient response to close-in shunt faults and can lead to a significant error in the current measurements coming from PMUs which negatively impact the accuracy of line parameter estimation, especially in cases when the fault is cleared before the CTs pull out of saturation caused by a decaying dc offset [37]. An untransposed line has 6 unknowns parameters to determine as will be seen later, multiple independent unbalanced operating states are required for estimating line parameters accurately. These different states could be single pole open conditions, unbalanced loading and unbalanced shunt faults. The condition needs to have an unbalanced ratio (I0/I1) between 3 to 5 percentage [33].

A new method to estimate short line parameters has been developed in this paper. Both the zero- and the positive-sequence line parameters are determined in this paper. The method utilizes PMU measurements at both ends of the line. The effect of CT saturation on the measurement accuracy impacting parameter determination is considered. The sensor error is detected and eliminated from the estimation by the LTS. Two different simulation software tools are used to simulate the system to test the approach and validate the results. The method was applied for untransposed lines with different $(\frac{X}{R})$ ratios. Section II gives a general review of CT saturation. Section II provides the estimation equations for an untransposed line. The principle of LTS is described in Section IV. The simulation results and analysis will be provided in Section V and the conclusions are presented in Section VI.

7.3 CT Saturation

The basic objective of a measurement CT is to step down the current for metering purpose and provide isolation. The C-class CTs are designed to have good dynamic response for protection applications. The error for protection CT is going to be about 3 % under normal operating conditions and the maximum error during fault condition is 10 % if the current is 20 times the nominal current with standard burden. The characteristic curve for metering class CTs is almost straight line for small range, so it is very accurate under normal operating conditions, which is a fractions of percent error, but the error is going to large during fault conditions.

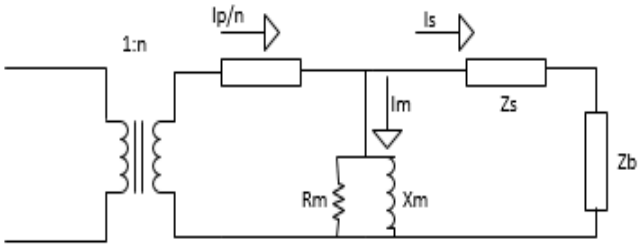

Figure 7.1: CT model with impedance referred to secondary side

Figure 7.1 shows a CT equivalent circuit model. Ideally, all of the secondary current should go through the relay. The magnetizing branch will start to saturate because of the changing in the permeability due to an increase in flux due to increase in voltage. Increasing flux decreases the permeability of the CT core decreasing the inductance of the magnetizing branch so more of the secondary current goes through it instead of to the relay. Equation (7.1) shows the relation between the permeability and the inductance of the magnetizing branch.

$$L_m = {N_s}^2.(\frac{\mu.A}{l}) \tag{7.1}$$

Where L_m is the inductivity of the magnetizing branch, A is the cross section area of the CT, l is the length of the CT, and μ is the permeability.

If the fault happens near the voltage minimum, the DC offset could be significant and the CT is more likely to saturate [37].

7.4 Untransposed Line Parameter Calculation for Short Line

The total shunt capacitance in the short line is very small so it can be ignored in steady state models. A regression calculation can be used.

$$\mathbf{V} = \mathbf{IZ} + \mathbf{e} \tag{7.2}$$

Where $\mathbf{V}$ is a observation vector with the difference between sending and receiving end voltages, which is the mesured voltage drops across the line impedance. The matrix $\mathbf{I}$ represents the line

currents and in the case of short line, it is nearly equal to the measured sending end currents.

$$\mathbf{V} = \begin{bmatrix} V_{ZA1} \\ V_{ZB1} \\ V_{ZC1} \\ \vdots \\ V_{ZAN} \\ V_{ZBN} \\ V_{ZCN} \end{bmatrix} \tag{7.3}$$

$$\mathbf{I} = \begin{bmatrix} I_{LA1} & I_{LB1} & I_{LC1} & 0 & 0 & 0 \\ 0 & I_{LA1} & 0 & I_{LB1} & I_{LC1} & 0 \\ 0 & 0 & I_{LA1} & 0 & I_{LB1} & I_{LC1} \\ \vdots & \vdots & \vdots & \vdots & \vdots & \vdots \\ I_{LAN} & I_{LBN} & I_{LCN} & 0 & 0 & 0 \\ 0 & I_{LAN} & 0 & I_{LBN} & I_{LCN} & 0 \\ 0 & 0 & I_{LAN} & 0 & I_{LBN} & I_{LCN} \end{bmatrix} \tag{7.4}$$

Where N is the number of measurements states. The impedance vector is:

$$\mathbf{Z} = \begin{bmatrix} Z_{AA} \\ Z_{BB} \\ Z_{CC} \\ Z_{AB} \\ Z_{BC} \\ Z_{AC} \end{bmatrix} \tag{7.5}$$

The **Z** vector contains six unknowns which need a full rank matrix to solve. To get a full rank set of equations, at least three independent measurements states are needed to solve equations (7.2). Single pole open (SPO) conditions for each phase can be used anywhere in the system to provide three different states with sufficient unbalance for the estimation. The ratio of positive-sequence current to the zero-sequence current (I0/I1) is used to measure the unbalance in the system. The results show that the best unbalance ratio for the parameter estimation is between 3 and 5. The data from internal faults can be used as well for the estimation. However, since some lines may go years without experiences faults, relying on internal line faults to provide unbalance conditions is not a practical approach. Therefore in this method, single pole open conditions can be used for estimation complemented with external faults. The faults could push the CT to saturate and leads to incorrect data measured by the PMUs, which effects the accuracy of the estimation. Five different cases have been applied for the estimation. To test the method, cases with varied degrees of saturation are considered later in the paper.

Once **Z** determined, the zero- and positive-sequence impedances of the line can be calculated by using the A_{012} matrix as shown in equation (7.6).

$$\mathbf{Z}_{012} = \mathbf{A}_{012}^{-1}\mathbf{Z}\mathbf{A}_{012};\ \mathbf{Y}_{012} = \mathbf{A}_{012}^{-1}\mathbf{Y}\mathbf{A}_{012} \tag{7.6}$$

The symmetrical components transformation matrix, A_{012}, uses the operator $a = e^{j2\pi/3}$ and is defined as follows:

$$\mathbf{A}_{012} = \begin{bmatrix} 1 & 1 & 1 \\ 1 & a^2 & a \\ 1 & a & a^2 \end{bmatrix} \tag{7.7}$$

7.5 Robust least trimmed squares estimator

The regression estimation problem defined in (7.2) could be solved using the weighted least squares (WLS) estimator. The WLS estimator minimizes the sum of the squared residuals, which are estimates of the errors. WLS is the best linear unbiased estimator (BLUE) under the assumption that the noise is really Gaussian. In this case, the WLS is the optimal estimator. The WLS estimate $\hat{\mathbf{Z}}$ satisfies

$$\hat{\mathbf{Z}} = \arg\min_{\mathbf{Z}} \sum_{i=1}^{m} r_i^2 = \arg\min_{\mathbf{Z}} \boldsymbol{r}^T \boldsymbol{r} \tag{7.8}$$

However, in the presence of outliers or even a small deviation from the assumption, the WLS degrades quickly. Outliers are observations or measurements that do not follow the model followed by the majority of the data. The WLS is heavily impacted by the presence of these deviations. Even a single outlier could create a large bias and an inflated variance in the WLS estimates. This implies that the estimation quality is degraded and unreliable [47]. In a regression context, outliers could be classified in two types: observation outliers and leverage points. Observation outliers are bad measurements impacting the observation vector, $\mathbf{V}$, and leverage points are outliers impacting the regressors' matrix, i.e, $\mathbf{I}$. To handle observation outliers, robust estimators have been proposed in the literature such as the Huber M-estimator [50]. In this paper, we use the so-called least trimmed squares (LTS) estimator than can resist both observation outliers and leverage points [50]. The

LTS minimizes the sum of the smallest squared residuals which implies that

$$\hat{\mathbf{Z}} = \arg\min_{\mathbf{Z}} \sum_{i=1}^{\lfloor (1-\alpha)m \rfloor + 1} r^2_{(i)} \tag{7.9}$$

where $\alpha \in [0, 1)$ is the trimming fraction of the LTS and $\lfloor \cdot \rfloor$ is the floor function. The i^{th} order statistic is given by $r_{(i)}$ and the residuals are sorted as follows $r^2_{(1)} \leq r^2_{(2)} \leq \ldots \leq r^2_m$. The trimming fraction, α, impacts the breakdown point which is the percentage of bad measurements an estimator can resist while giving reliable estimates. The α is generally chosen smaller than 0.5 and the LTS can resist both observation outliers and leverage points. An accelerated algorithm is proposed to compute the LTS estimates [63]. The LTS has been applied in power state estimation to improve estimation and cyber-security [49, 52, 64, 65]

7.6 Simulation Results

A one line diagram for the test system model is shown in Figure 7.2.

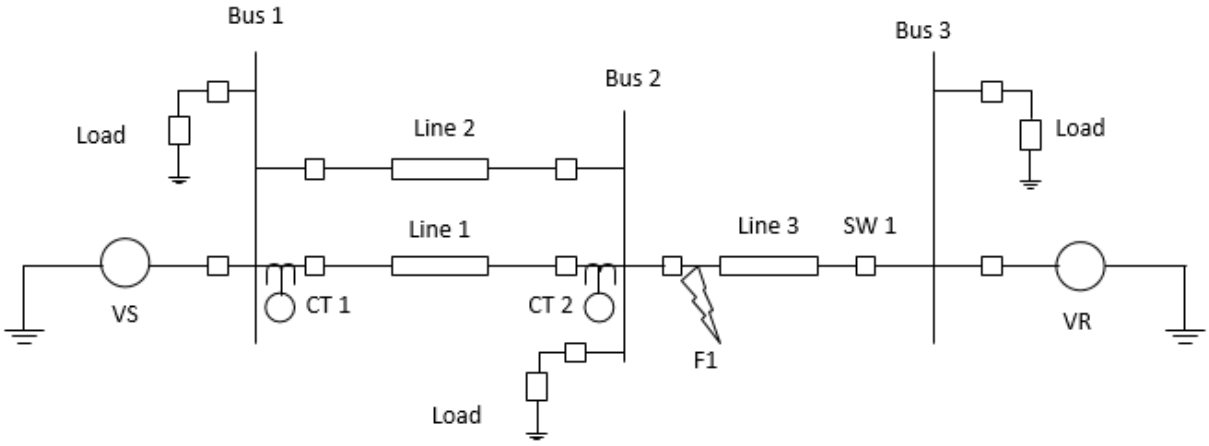

Figure 7.2: Test system model.

Line 1 between Bus1 and Bus 2 is considered for the parameter estimation. The line is 9 miles long and rated at 120 kV. The weighted least squares (WLS) method is used for the estimation in the first three cases. To consider the effect of CT saturation on the estimation a single line to ground fault in location F1 was placed on the system for 5 cycles and then cleared. A single pole open was

performed to increase the estimation accuracy. In addition to the (SPO), a measurements from the first, second, and third cycles of line current waveform were taken and used in the estimation in case 1, case 2, and case 3 respectively. In the fourth case, the data recorded from the previous first case is tested using the LTS approach. The estimation was performed for a line with a high ($\frac{X}{R}$) ratio (angle 84.5°) and low ($\frac{X}{R}$) ratio (angle 66.9°). The results of the estimation for the cases with high X over R ratio line are shown in Table 7.1.

Table 7.1: Estimation results for untransposed line with high ($\frac{X}{R}$) ratio

Calculation Method	Positive Seq. Mag.	Positive Seq. Angle	Zero Seq. Mag.	Zero Seq. Angle
Simulation Set Values	8.05 (Ω)	80.2 (deg)	21.95 (Ω)	79.89 (deg)
Error (Case 1) WLS Method	4.51%	4 (deg)	58.9%	5.3 (deg)
Error (Case 2) WLS Method	0.65%	2.7 (deg)	23.6%	5.5 (deg)
Error (Case 3) WLS Method	0.81%	0.7 (deg)	3.37%	1.5 (deg)
Error (Case 4) LTS Method	1.89%	0.7 (deg)	1.26%	2.6 (deg)

It can be noticed from Table 7.1 that creating three phase fault pushes the CTs to saturate. Including that data in the classical estimation method which is the weighted least square estimator leads to significant error in the results. Using the first cycle of the measured current waveform in the calculation of case 1 leads to inaccurate results. The error still exists in case 2 due to the CT saturation. As the CT saturation decayed in the third cycle of the current measurements, the results get more accurate and in the acceptable tolerance of a 5% error. Repeating the previous cases and using the proposed method LTS, the results are accurate and under 5% error even with CT saturation included as shown in case 4. LTS was able to detect and reject the bad data and perform the estimation correctly.

Table 7.2 shows the estimation results for low X over R ratio line. The good results are achieved in the second case instead of the third case because the CT saturation decayed quickly. However,

the LTS detected and rejected the incorrect measurements in the all cases and provided a precised results.

Table 7.2: Estimation results for untransposed line with Low ($\frac{X}{R}$) ratio

Calculation Method	Positive Seq. Mag.	Positive Seq. Angle	Zero Seq. Mag.	Zero Seq. Angle
Simulation Set Values	5.68 (Ω)	50.58 (deg)	22.8 (Ω)	74.4 (deg)
Error (Case 1) WLS Method	0.49%	3.4 (deg)	20.74%	6.9 (deg)
Error (Case 2) WLS Method	0.86%	1 (deg)	0.7%	2.1 (deg)
Error (Case 4) LTS Method	0.36%	0.16 (deg)	1.17%	1.6 (deg)

7.7 Conclusion

A new method to estimate the parameters of short line was introduced. The impact of CT saturation on the estimation accuracy was described for cases with a line with a low X over R ratio and with a shorter line with a high X over R ratio. The method depends on voltage and current measurements from PMUs at both terminals of the line. The advantage of using this method is that the required unbalance current condition for the estimation could be a fault anywhere in the system not just in the line of interest as long as it provides sufficient unbalance for the calculation. Four unbalance conditions were generated in the simulation to have a full rank matrices to solve the estimation equations. The positive-sequence and negative-sequence impedances were estimated accurately. The LTS estimator was able to detect and reject the sensor error measurements for all cases when a close in fault led to saturation.

Chapter 8: Summary, and Future Work

8.1 Summary

A least trimmed squares estimation method was proposed to estimate the positive, negative and zero-sequence transmission line parameters for a series compensated line. The LTS-based method is advocated for use in the presence of outliers due to low frequency oscillations in the transient response of a series compensated line to a fault. The proposed algorithm is also accurate when outliers are present in the current and voltage measurements obtained from PMUs. Simulation results showed the superior performance of the LTS-based algorithm with respect to the classical WLS with chi-squares test. The simulation considered both the transposed and untransposed line parameter estimation. Emulation with a real time digital simulator confirmed the performance as well.

A new method to estimate the parameters of short length line was also introduced. The impact of CT error on the estimation accuracy was described for cases with a short line with a low X over R ratio and with a short line with a high X over R ratio. The method depends on voltage and current measurements from PMUs at both terminals of the line. The advantage of using this method is that the required unbalance current condition for the estimation could be due to faults or disturbance anywhere in the system not just, in the line of interest as long as it provides sufficient unbalance for the calculation. Four unbalance conditions were generated in the simulation to have a full rank matrices to solve the estimation equations. The positive-sequence and negative-sequence impedances were estimated accurately. The LTS estimator was able to detect and reject the sensor error measurements due to CT saturation for all cases.

Two cases of mutually coupled lines are considered, two transposed parallel lines, and two untransposed parallel lines. The two lines are parallel for part of the length of the shorter line and magnetically and capacitively coupled but not electrically coupled. Two cases were considered; first one when the two lines were transposed, and in the second case both lines were untransposed. For the transposed case, the proposed method combined two algorithms, the first algorithm is based on disconnecting one of the lines and inducing an unbalance in the other line to determine the mutual zero-sequence impedance. This approach is mainly estimates the mutual zero-sequence impedance

Z_{0m}. A second algorithm was used to estimate the series impedance parameters.

The second algorithm is based on solving set of equations using Least Squares method to estimate the sequence parameters of the targeted line. In this case only using one unbalanced condition is sufficient. However, three unbalanced states have been induced to increase the accuracy of the results. For untransposed lines, the shunt capacitance is neglected for simplification. Four unbalanced states were used for the estimation. To make sure there is an acceptable solution for the estimation, a singularity check has been performed for the current matrix by using Matlab software. The length of the mutually coupled parts between lines were changed to validate the proposed method. A transient offline simulation (ATP) with different configurations for the lines was performed for cases with transposed and untransposed lines to simulate and validate the proposed method. The results showed that all the percentage errors are under 5%, which can be acceptable

8.2 Conclusion

This dissertation proposed a new method, LTS, to estimate parameters for series compensated lines in presence of low-frequency oscillations. The proposed method was able to detect and reject errors in both current and voltage measurements. Series impedance, mutual impedances, and shunt capacitance are estimated accurately for both transposed and untransposed lines. An ATP simulation was performed to apply the proposed approach, and RTDS simulation for validation. All the results confirmed the performance of LTS. This dissertation also developed a different algorithms for estimating parameters of two mutually coupled lines that are magnetically coupled but not electrically coupled weather they are each transposed or each untransposed.

The mutual zero-sequence impedance was determined by disconnecting one of the lines and inducing an unbalance in the other line. The sequence impedance matrices for each line were estimated by creating unbalanced current in one of the lines and then using the current and voltage measurements at ends of the line to solve set of equations. All the results from the offline simulation were under 5%, demonstrating that the objectives were achieved.

8.3 Future Work

- Additional investigation is needed for a series compensated lines with a tapped loads. Tapped loads present a challenge to estimate the line parameters accurately. Tapped load affects the current measurements at both end of the line, which impacts the quality of the data for the parameter estimation as an . A new method needs to be developed to estimate the parameters accurately.

- The proposed method for estimating parameter of series compensated line (LTS) was able to detect and eliminate the effect of errors of 7% in voltage measurements. Further work is needed to characterize the effect of voltage errors less than 7 % on the accuracy of estimation. If the effect is significant, then work is needed to develop a method to detect and eliminate voltage errors less than 7%.

- The proposed method for estimating parameter of mutually coupled lines were performed for two lines only. Often three lines or more could be in the same right of way, or transmission lines with under built distribution lines or light rail tracks. Future work is needed to estimate lines parameters for that case.

- Since the LTS in this research was used for series compensated lines and short length lines, an area of investigation is to apply the LTS method for estimating parameters of mutually coupled lines.

- The mutually coupled lines cases and short length line cases need to be validated using actual PMUs in the lab.

- Field data is needed to compare the results of synchrophasor-derived values to the actual values to validate methods developed.

Bibliography

[1] K. Dasgupta and S. A. Soman, "Line parameter estimation using phasor measurements by the total least squares approach," in *2013 IEEE Power Energy Society General Meeting*, July 2013, pp. 1–5.

[2] B. K. Johnson and S. Jadid, "Synchrophasors for Validation of Distance Relay Settings: Real Time Digital Simulation and Field Results," *International Conference on Power Systems Transients*, pp. 1–8, 2015.

[3] NERC, "COMPLIANCE OPERATIONS," pp. 1–5, 2013. [Online]. Available: https://www.nerc.com/pa/Stand/Project 201003 Modeling Data MOD B/MODB_MOD-032_MOD-033_Compliance_GuidanceCLEAN2013-102.pdf#search=MOD-032

[4] M. Devendra and K. Manjunathachari, "Synchrophasor Technology: PMU Applications in Smart Grids," *International Advanced Research Journal in Science, Engineering and Technology (IARJSET)*, vol. 2, no. 1, pp. 1–5, 2015.

[5] R. Rubesa, V. Kirincic, and S. Skok, "Transmission line positive sequence impedance estimation based on multiple scans of Phasor Measurements," *ENERGYCON 2014 - IEEE International Energy Conference*, pp. 644–651, 2014.

[6] A. M. Dan and D. Raisz, "Estimation of transmission line parameters using wide-area measurement method," *2011 IEEE Trondheim PowerTech*, pp. 1–6, 2011.

[7] S. G. Srivani and K. P. Vittal, "An integrated adaptive distance relaying scheme in series compensated transmission lines," *Journal of Electrical Engineering*, vol. 11, no. 1, p. 112, 2011.

[8] B. Vyas, R. P. Maheshwari, and B. Das, "Protection of series compensated transmission line: Issues and state of art," *Electric Power Systems Research*, vol. 107, pp. 93–108, 2014. [Online]. Available: http://dx.doi.org/10.1016/j.epsr.2013.09.017

[9] D. A. Tziouvaras, H. J. Altuve, and F. Calero, "Protecting mutually coupled transmission lines: Challenges and solutions," *2014 67th Annual Conference for Protective Relay Engineers, CPRE 2014*, pp. 30–49, 2014.

[10] A. ElMehdi, A. Momen, and B. K. Johnson, "Dynamic reactive compensation requirements at the rectifier end of an lcc hvdc link connected to a weak ac system," in *2014 North American Power Symposium (NAPS)*, Sep. 2014, pp. 1–6.

[11] A. Momen, Y. Chakhchoukh, and B. K. Johson, "Series Compensated Line Parameters Estimation Using Synchrophasor Measurements," *Accepted for IEEE Transactions on Powr Delivery*, 2019.

[12] A. Momen, B. K. Johnson, and Y. Chakhchoukh, "Parameters Estimation for Short Line Using the Least Trimmed Squares (LTS)," in *Proceeding of 2019 IEEE Innovative Smart Grid Technologies conference*, Washington, DC, pp. 1–5.

[13] T. Bi, J. Chen, J. Wu, and Q. Yang, "Synchronized Phasor based On-line Parameter Identification of Overhead Transmission Line," in *Third International Conference on Electric Utility Deregulation and Restructuring and Power Technologies*, no. April, 2008, pp. 1657–1662.

[14] H. K. Karegar and B. Alinejad, "On-line transmission line zero sequence impedance estimation using phasor measurement units," in *2012 22nd Australasian Universities Power Engineering Conference (AUPEC)*, Sept 2012, pp. 1–5.

[15] C. S. Indulkar and K. Ramalingam, "Estimation of transmission line parameters from measurements," *International Journal of Electrical Power and Energy Systems*, vol. 30, no. 5, pp. 337–342, 2008.

[16] P. Dawidowski, J. Izykowski, and A. Nayir, "Analytical synchronization of two-end measurements for transmission line parameters estimation and fault location," *Istanbul University - Journal of Electrical and Electronics Engineering*, vol. 13, no. 1, pp. 1569–1574, 2013.

[17] Y. Liao, "Algorithms for power system fault location and line parameter estimation," *Proceedings of the Annual Southeastern Symposium on System Theory*, pp. 189–193, 2007.

[18] D. Shi, D. J. Tylavsky, N. Logic, and K. M. Koellner, "Identification of short transmission-line parameters from synchrophasor measurements," *40th North American Power Symposium, NAPS2008*, pp. 1–8, 2008.

[19] D. Lan, B. I. Tianshu, and Z. Daonong, "Transmission Line Parameters Identification Based on Moving-Window TLS and PMU data," *The International Conference on Advanced Power System Automation and Protection*, pp. 2187–2191, 2011.

[20] X. Jiao and Y. Liao, "A linear estimator for transmission line parameters based on distributed parameter line model," *2017 IEEE Power and Energy Conference at Illinois, PECI 2017*, 2017.

[21] S. Gajare, A. K. Pradhan, and V. Terzija, "A Method for Accurate Parameter Estimation of Series Compensated Transmission Lines Using Synchronized Data," *IEEE Transactions on Power Systems*, vol. 32, no. 6, pp. 4843–4850, 2017.

[22] S. S. Mousavi-Seyedi, F. Aminifar, and S. Afsharnia, "Application of WAMS and SCADA Data to Online Modeling of Series-Compensated Transmission Lines," *IEEE Transactions on Smart Grid*, vol. 8, no. 4, pp. 1968–1976, 2017.

[23] Y. Liao, "Some algorithms for transmission line parameter estimation," *2009 IEEE International Symposium on Sustainable Systems and Technology, ISSST 2009*, pp. 127–132, 2009.

[24] Y. Du and Y. Liao, "Parameter estimation for series compensated transmission line," *International Journal of Emerging Electric Power Systems*, vol. 12, no. 3, 2011.

[25] I. D. Kim and R. K. Aggarwal, "A study on the on-line measurement of transmission line impedances for improved relaying protection," *International Journal of Electrical Power and Energy Systems*, vol. 28, no. 6, pp. 359–366, 2006.

[26] S. V. Unde and S. S. Dambhare, "Double circuit transmission line parameter estimation using PMU," *2016 IEEE 6th International Conference on Power Systems, ICPS 2016*, 2016.

[27] X. Zhiying and L. Zhirui, "An on-line measurement method of zero-sequence parameters of double-line on the same tower based on WAMS," *Asia-Pacific Power and Energy Engineering Conference, APPEEC*, pp. 1–4, 2009.

[28] N. Kang and Y. Liao, "Double-circuit transmission-line fault location with the availability of limited voltage measurements," *IEEE Transactions on Power Delivery*, vol. 27, no. 1, pp. 325–336, 2012.

[29] K. Dasgupta and S. A. Soman, "Estimation of zero sequence parameters of mutually coupled transmission lines from synchrophasor measurements," *IET Generation, Transmission & Distribution*, vol. 11, no. 14, pp. 3539–3547, 2017. [Online]. Available: http://digital-library.theiet.org/content/journals/10.1049/iet-gtd.2017.0057

[30] S. Jadid, "Application of Synchrophasors for Validation of Transmission Line Distance Relay Parameters," Ph.D. dissertation, University of Idaho, 2014.

[31] D. Shi, D. J. Tylavsky, K. M. Koellner, N. Logic, and D. E. Wheeler, "Transmission line parameter identification using PMU measurements," *European Transactions on Electrical Power*, vol. 21, no. 4, pp. 1574–1588, 2011.

[32] B. S. Lowe, J. D. L. Reelopez, and R. M. Gardner, "A New Method of Determining the Transmission Line Parameters of an Untransposed Line using Synchrophasor Measurements," Ph.D. dissertation, Virginia Polytechnic Institute and State University in, 2015.

[33] B. K. Johnson and S. Jadid, "Validation of Transmission Line Relay Parameters Using Synchrophasors Validation of Transmission Line Relay Parameters Using Synchrophasors," in *41st Annual Western Protective Relay Conference*, no. April, 2014.

[34] J. Blackburn and T. Domin, *Principles and Applications.* Taylor & Francis Group, LLC., 1995, vol. 2.

[35] F. Calero, "Mutual Impedance in Parallel Lines - Protective Relaying and Fault Location Considerations," in *34th Annual Western Protective Relay Conference*, no. November 2008, 2008, pp. 1–15.

[36] Z. H. Z. Huang, B. Kasztenny, V. Madani, K. Martin, S. Meliopoulos, D. Novosel, and J. Stenbakken, "Performance evaluation of phasor measurement systems," *2008 IEEE Power and Energy Society General Meeting - Conversion and Delivery of Electrical Energy in the 21st Century*, pp. 1–7, 2008.

[37] B. K. Johnson, N. Fischer, and Y. Xia, "Impacts of superconducting cables on the dynamic response of current transformers and protective relaying devices," *IEEE Transactions on Applied Superconductivity*, vol. 21, no. 3 PART 2, pp. 2149–2152, 2011.

[38] J. Grainger and W. Stevenson, *Power System Analysis*, 2nd ed. New York: McGraw-Hill, 1994.

[39] C. W. Taylor and D. C. Erickson, "Recording and analyzing the july 2 cascading outage [western usa power system]," *IEEE Computer Applications in Power*, vol. 10, no. 1, pp. 26–30, Jan 1997.

[40] M. Jelani, *Electric Power Engineering*, 1st ed. Cairo: Dar Alfjr, 2016.

[41] L. Leonard, *"Electric Power Generation, Transmission, and Distribution"*, 3rd ed. Boca Raton: Taylor & Francis Group, LLC., 2012.

[42] S. E. Zocholl, "Sequence Components and Untransposed Lines," *Schweitzer Engineering Laboratories, Inc.*, pp. 1–14. [Online]. Available: http://www.pacw.org/fileadmin/doc/Sequence-Components-Untransposed-Lines.pdf

[43] "IEEE Standard for Synchrophasor Measurements for Power Systems IEEE Power & Energy Society," Tech. Rep. December, 2012.

[44] A. Apostolov, "Synchrophasors - can we use them for protection?" *11th IET International Conference on Developments in Power Systems Protection (DPSP 2012)*, pp. 61–61, 2012. [Online]. Available: http://digital-library.theiet.org/content/conferences/10.1049/cp.2012.0024

[45] A. Phadke and J. Thorp, "Synchronized Phasor Measurements and Their Applications," 2008, [Accessed: 02-Feb-2018]. [Online]. Available: http://link.springer.com/10.1007/978-0-387-76537-2

[46] "SEL-5073 SYNCHRO WAVE Phasor Data Concentrator Instruction Manual," Pullman,WA, Tech. Rep., 2010.

[47] A. M. Zoubir, V. Koivunen, Y. Chakhchoukh, and M. Muma, "Robust estimation in signal processing: A tutorial-style treatment of fundamental concepts," *IEEE Signal Processing Magazine*, vol. 29, no. 4, pp. 61–80, July 2012.

[48] L. Mili, M. G. Cheniae, N. S. Vichare, and P. J. Rousseeuw, "Robust state estimation based on projection statistics [of power systems]," *IEEE Transactions on Power Systems*, vol. 11, no. 2, pp. 1118–1127, 1996.

[49] L. Mili, M. G. Cheniae, and P. J. Rousseeuw, "Robust state estimation of electric power systems," *IEEE Transactions on Circuits and Systems I: Fundamental Theory and Applications*, vol. 41, no. 5, pp. 349–358, 1994.

[50] R. A. Maronna, R. D. Martin, and V. J. Yohai, *Robust Statistics: Theory and Methods*, ser. Wiley Series in Probability and Statistics. Chichester: Wiley, 2006.

[51] Y. Weng, R. Negi, Q. Liu, and M. D. Ilic, "Robust state-estimation procedure using a least trimmed squares pre-processor," in *Proc. IEEE PES Innovative Smart Grid Technologies (ISGT)*, 2011, pp. 1–6.

[52] Y. Chakhchoukh and H. Ishii, "Coordinated cyber-attacks on the measurement function in hybrid state estimation," *IEEE Transactions on Power Systems*, vol. 30, no. 5, pp. 2487–2497, May 2015.

[53] L. Mili and C. W. Coakley, "Robust estimation in structured linear regression," *Ann. Statist.*, vol. 24, no. 6, pp. 2593–2607, 1996.

[54] J. Agullo, C. Croux, and S. Van Aelst, "The multivariate least-trimmed squares estimator," *Journal of Multivariate Analysis*, vol. 99, no. 3, pp. 311–338, 2008, program available at: http://www.econ.kuleuven.be/public/NDBAE06/programs/mlts/mlts.txt.

[55] A. Abur and A. Gomez-Exposito, *Power System State Estimation: Theory and Implementation*. New York: CRC Press, 2004.

[56] S. Chakrabarti and E. Kyriakides, "PMU Measurement Uncertainty Considerations in WLS State Estimation," vol. 24, no. 2, pp. 1062–1071, 2009.

[57] G. Sivanagaraju, S. Chakrabarti, and S. C. Srivastava, "Uncertainty in transmission line parameters: Estimation and impact on line current differential protection," *IEEE Transactions on Instrumentation and Measurement*, vol. 63, no. 6, pp. 1496–1504, 2014.

[58] M. Eden, R. Herrick, and G. F. Hoffnagle, *Analysis of Faulted Power Systems*, 1st ed. New York: Wiley-Interscience-IEEE, 1995.

[59] K. Dasgupta, , and S. A. Soman, "Line Parameter Estimation using Phasor Measurements by the Total Least Squares Approach," pp. 1–5, 2013.

[60] T. Bil, J. Chen, J. Wu, and Q. Yang, "Synchronized phasor based on-line parameter identification of overhead transmission line," in *2008 Third International Conference on Electric Utility Deregulation and Restructuring and Power Technologies*, April 2008, pp. 1657–1662.

[61] R. E. Wilson, Gary A. Zevenbergen, Dan, "Calculation of Transmission Line Parameters From Synchronized Measurements," *Electric Machines & Power Systems*, vol. 27, no. 12, pp. 1269–1278, 1999.

[62] Z. Hu and Y. Chen, "New method of live line measuring the inductance parameters of transmission lines based on GPS technology," *IEEE Transactions on Power Delivery*, vol. 23, no. 3, pp. 1288–1295, 2008.

[63] M. Salibian-Barrera and V. J. Yohai, "A fast algorithm for S-regression estimates," *J. Comput. Graph. Statist.*, vol. 15, no. 2, pp. 414–427, 2006.

[64] Y. Chakhchoukh and H. Ishii, "Enhancing Robustness to Cyber-Attacks in Power Systems Through Multiple Least Trimmed Squares State Estimations," *IEEE Transactions on Power Systems*, vol. 31, no. 6, pp. 4395–4405, 2016.

[65] Y. Chakhchoukh, V. Vittal, G. T. Heydt, and H. Ishii, "LTS-based robust hybrid SE integrating correlation," *IEEE Transactions on Power Systems*, vol. 32, no. 4, pp. 3127–3135, July 2017.

Appendix A: The regressor matrix for the untransposed line

The regressor matrix for the untransposed line is $\mathbf{A}_{unt}$.

$$
\mathrm{A}_{unt} = \begin{bmatrix}
-\mathrm{Im}(V_{A1}) & -\mathrm{Im}(V_{B1}) & -\mathrm{Im}(V_{C1}) & 0 & 0 & 0 \\
\mathrm{Re}(V_{A1}) & \mathrm{Re}(V_{B1}) & \mathrm{Re}(V_{C1}) & 0 & 0 & 0 \\
0 & -\mathrm{Im}(V_{A1}) & 0 & -\mathrm{Im}(V_{B1}) & -\mathrm{Im}(V_{C1}) & 0 \\
0 & \mathrm{Re}(V_{A1}) & 0 & \mathrm{Re}(V_{B1}) & \mathrm{Re}(V_{C1}) & 0 \\
0 & 0 & -\mathrm{Im}(V_{A1}) & 0 & -\mathrm{Im}(V_{B1}) & -\mathrm{Im}(V_{C1}) \\
0 & 0 & \mathrm{Re}(V_{A1}) & 0 & \mathrm{Re}(V_{B1}) & \mathrm{Re}(V_{C1}) \\
\vdots & \vdots & \vdots & \vdots & \vdots & \vdots \\
-\mathrm{Im}(V_{AN}) & -\mathrm{Im}(V_{BN}) & -\mathrm{Im}(V_{CN}) & 0 & 0 & 0 \\
\mathrm{Re}(V_{AN}) & \mathrm{Re}(V_{BN}) & \mathrm{Re}(V_{CN}) & 0 & 0 & 0 \\
0 & -\mathrm{Im}(V_{AN}) & 0 & -\mathrm{Im}(V_{BN}) & -\mathrm{Im}(V_{CN}) & 0 \\
0 & \mathrm{Re}(V_{AN}) & 0 & \mathrm{Re}(V_{BN}) & \mathrm{Re}(V_{CN}) & 0 \\
0 & 0 & -\mathrm{Im}(V_{AN}) & 0 & -\mathrm{Im}(V_{BN}) & -\mathrm{Im}(V_{CN}) \\
0 & 0 & \mathrm{Re}(V_{AN}) & 0 & \mathrm{Re}(V_{BN}) & \mathrm{Re}(V_{CN})
\end{bmatrix}
$$

Appendix B: LCC untransposed calculations in ATPDraw

The calculations to determine the series impedance matrix and the shunt admittance matrix for untransposed short line are illustrated in this appendix. The Bergeron transmission line model was used in this case and the details of the line is shown in Figure B.1.

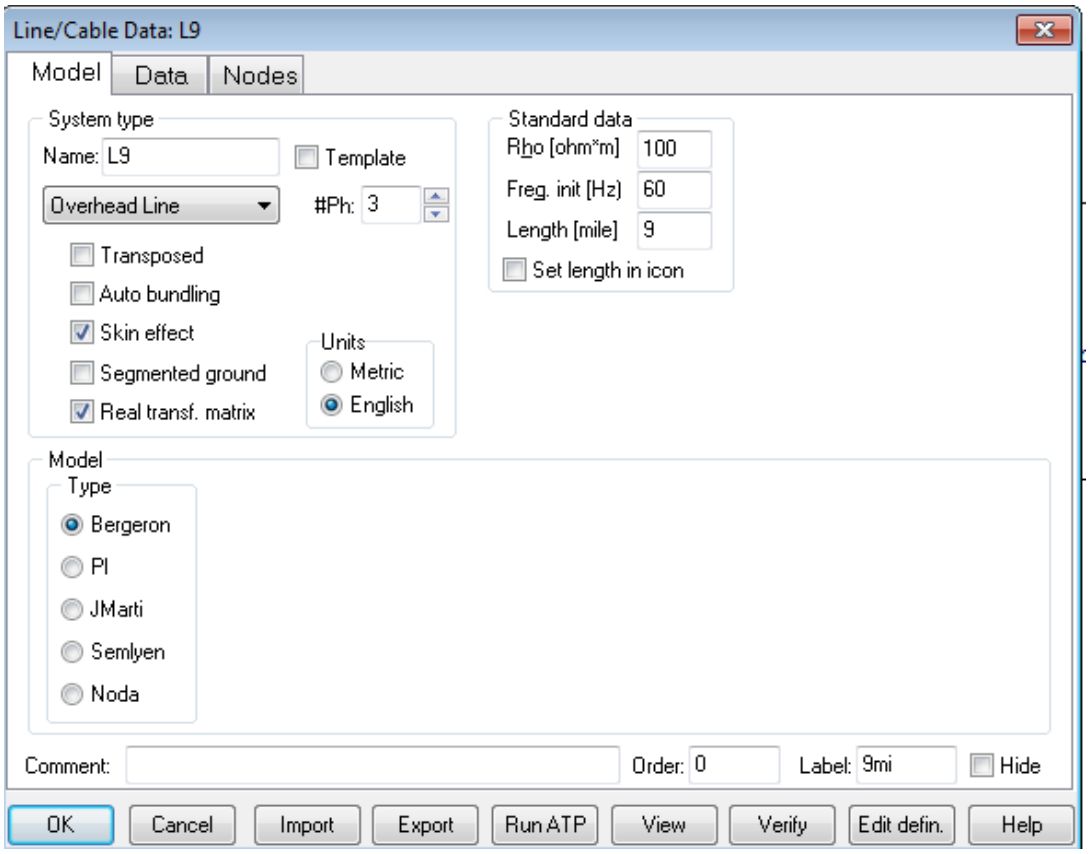

Figure B.1: Bergeron line details.

The L9.Lib file is shown in figure B.2

Text Editor: L9.lib

File Edit Character Help

```
KARD  3  3  4  4  5  5
KARG  1  4  2  5  3  6
KBEG  3  9  3  9  3  9
KEND  8 14  8 14  8 14
KTEX  1  1  1  1  1  1
/BRANCH
$VINTAGE, 1
-1IN___AOUT__A             4.27530E-01 8.22382E+02 1.29293E+05-9.00000E+00 1  3
-2IN___BOUT__B             1.52109E-01 4.49043E+02 1.80574E+05-9.00000E+00 1  3
-3IN___COUT__C             1.52038E-01 3.99772E+02 1.82673E+05-9.00000E+00 1  3
$VINTAGE, 0
  0.58976595 -0.70710678 -0.41131261
  0.00000000  0.00000000  0.00000000
  0.55168129  0.00000000  0.81341495
  0.00000000  0.00000000  0.00000000
  0.58976595  0.70710678 -0.41131261
  0.00000000  0.00000000  0.00000000
$EOF
ARG, IN___A, IN___B, IN___C, OUT__A, OUT__B, OUT__C
```

Figure B.2: Bergeron line model data

- The line modal parameters are in the lines starting "-1", "-2", etc

- The modal transformation matrix for the currents, "Ti" starts after the "VINTAGE, 0"

$R_{m0} = 4.27530 * 10^{-1} \frac{ohm}{mi}$ $R_{m1} = 1.52109 * 10^{-1} \frac{ohm}{mi}$ $R_{m2} = 1.52038 * 10^{-1} \frac{ohm}{mi}$

$Z_{m0} = 8.22382 * 10^{2} ohm$ $Z_{m1} = 4.49043 * 10^{2} ohm$ $Z_{m2} = 3.99772 * 10^{2} ohm$

$\nu_{m0} = 1.29293 * 10^{5} \frac{mi}{sec}$ $\nu_{m1} = 1.80574 * 10^{5} \frac{mi}{sec}$ $\nu_{m2} = 1.82673 * 10^{5} \frac{mi}{sec}$

The capacitance and inductance modal parameters can be calculated from equations (B.1) and (B.2)

$$Z_m = \sqrt{\frac{L_m}{C_m}} \tag{B.1}$$

$$\nu_m = \frac{1}{\sqrt{L_m.C_m}} \tag{B.2}$$

The model transformation matrix for current is:

$$\mathbf{T}_i = \begin{bmatrix} 0.58866938 & -0.70710678 & -0.41186567 \\ 0.55401871 & 0 & 0.81285506 \\ 0.58866938 & 0.70710678 & -0.41186567 \end{bmatrix}$$

$$\mathbf{I} = \begin{bmatrix} 1 & 0 & 0 \\ 0 & 1 & 0 \\ 0 & 0 & 1 \end{bmatrix} \Omega$$

$$\mathbf{T}_e = \mathbf{I}(\mathbf{T}_i^T)^{-1}$$

Table B.1: The modal parameters for the line under test

C_{m0}	$9.405\frac{nF}{mi}$	L_{m0}	$6.361\frac{mH}{mi}$
C_{m1}	$12.333\frac{nF}{mi}$	L_{m1}	$2.487\frac{mH}{mi}$
C_{m2}	$13.693\frac{nF}{mi}$	L_{m2}	$2.188\frac{mH}{mi}$

The modal transformation matrix for voltage is:

$$\mathbf{T}_e = \begin{bmatrix} 0.575119 & -0.707107 & -0.391985 \\ 0.582814 & 0 & 0.833002 \\ 0.575119 & 0.707107 & -0.391985 \end{bmatrix}$$

$\mathbf{R}^{'}$ per unit length is:

$$\mathbf{R}^{'} = \mathbf{T}_e \begin{bmatrix} R_{m0} & 0 & 0 \\ 0 & R_{m1} & 0 \\ 0 & 0 & R_{m2} \end{bmatrix} \mathbf{T}_i^{-1} = \begin{bmatrix} 0.2408 & 0.0937 & 0.0887 \\ 0.0937 & 0.2507 & 0.0937 \\ 0.0887 & 0.0937 & 0.2408 \end{bmatrix} \frac{ohm}{mi}$$

$\mathbf{L}^{'}$ per unit length is:

$$\mathbf{L}^{'} = \mathbf{T}_e \begin{bmatrix} L_{m0} & 0 & 0 \\ 0 & L_{m1} & 0 \\ 0 & 0 & L_{m2} \end{bmatrix} \mathbf{T}_i^{-1} = \begin{bmatrix} 3.6835 & 1.4174 & 1.1967 \\ 1.4174 & 3.6791 & 1.4174 \\ 1.1967 & 1.4174 & 3.6835 \end{bmatrix} \frac{mH}{mi}$$

$\mathbf{C}^{`}$ per unit length is:

$$\mathbf{C}^{`} = \mathbf{T}_e \begin{bmatrix} C_{m0} & 0 & 0 \\ 0 & C_{m1} & 0 \\ 0 & 0 & C_{m2} \end{bmatrix} .\mathbf{T}_i^{-1} = \begin{bmatrix} 11.7483 & -1.5172 & -0.5844 \\ -1.5172 & 11.9344 & -1.5172 \\ -0.5844 & -1.5172 & 11.7483 \end{bmatrix} \frac{nF}{mi}$$

$$a = e^{j2\pi/3}, \quad \mathbf{A}_{012} = \begin{bmatrix} 1 & 1 & 1 \\ 1 & a^2 & a \\ 1 & a & a^2 \end{bmatrix}$$

Length=9mi $\qquad \omega = 2.\pi.60Hz$

$$\mathbf{Z_{ABC}} = (\mathbf{R}^{`} + j.\omega.\mathbf{L}^{`}).Length$$

$$\mathbf{Z_{ABC}} = \begin{bmatrix} 2.167 + 12.498i & 0.843 + 4.809i & 0.798 + 4.06i \\ 0.843 + 4.809i & 2.256 + 12.483i & 0.843 + 4.809i \\ 0.798 + 4.06i & 0.843 + 4.809i & 2.167 + 12.498i \end{bmatrix} ohm$$

$$\mathbf{Z_{012}} = \mathbf{A}_{012}^{-1}\mathbf{Z_{ABC}}\mathbf{A}_{012}$$

$$\mathbf{Z_{012}} = \begin{bmatrix} 3.853 + 21.612i & 0.19 - 0.161i & -0.234 - 0.084i \\ -0.234 - 0.084i & 1.369 + 7.933i & -0.437 + 0.252i \\ 0.19 - 0.161i & 0.437 + 0.252i & 1.369 + 7.933i \end{bmatrix} ohm$$

Appendix C: Current transformer and capacitor voltage transformer detailed models

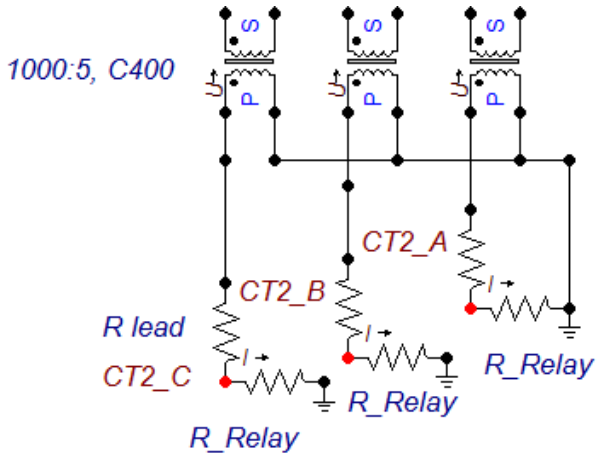

Figure C.1: Detailed CT model.

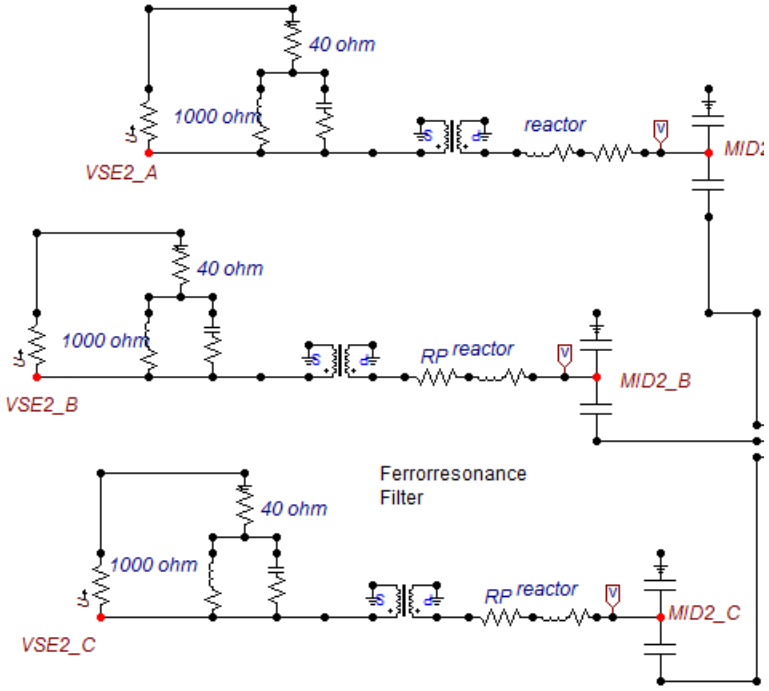

Figure C.2: Detailed CCVT model.

Appendix D: Matlab Code for Monte-Carlo Simulation

```
clear all;
a=exp(1i*2*pi/3);
A012=[1 1 1;1 a^2 a;1 a a^2];
%%%%%%%%%%%%%%%%%%%%%%%%%%%%%%%%%%%%%%%%%%%%%%%%%%%%%%%%%%%%%%%%%%%%%%%%%%%%
A = zeros(24,6);
A(1,:) =[-5.403e4   2.275e5 -2.02e5 0   0   0];
A(2,:) =[2.707e5    -8.541e4    -1.481e5    0   0   0];
A(3,:) =[0  -5.403e4    0   2.275e5 -2.02e5 0];
A(4,:) = [0 2.707e5 0   -8.541e4    -1.481e5    0];
A(5,:) =[0  0 -5.403e4  0   2.275e5 -2.02e5];
A(6,:) =[0  0   2.707e5 0   -8.541e4    -1.481e5];
A(7,:) =[-2.731e4   2.631e5 -1.887e5    0   0   0];
A(8,:) =[2.473e5    -9.039e4    -1.529e5    0   0   0];
A(9,:) =[0  -2.731e4    0   2.631e5 -1.887e5    0];
A(10,:) =[0 2.473e5 0   -9.039e4    -1.529e5    0];
A(11,:) =[0 0   -2.731e4    0   2.631e5 -1.887e5];
A(12,:) =[0 0   2.473e5 0   -9.039e4    -1.529e5];
A(13,:) =[-3.979e4  2.292e5 -2.118e5    0   0   0];
A(14,:) =[2.398e5   -1.009e5    -1.81e5 0   0   0];
A(15,:) =[0 -3.979e4    0   2.292e5 -2.118e5    0];
A(16,:) =[0 2.398e5 0   -1.009e5    -1.81e5 0];
A(17,:) =[0 0   -3.979e4    0   2.292e5 -2.118e5];
A(18,:) =[0 0   2.398e5 0   -1.009e5    -1.81e5];
A(19,:) =[-3.808e4  2.324e5 -1.991e5    0   0   0];
A(20,:) =[2.464e5   -9.228e4    -1.529e5    0   0   0];
A(21,:) =[0 -3.808e4    0   2.324e5 -1.991e5    0];
A(22,:) =[0 2.464e5 0   -9.228e4    -1.529e5    0];
A(23,:) =[0 0   -3.808e4    0   2.324e5 -1.991e5];
A(24,:) =[0 0   2.464e5 0   -9.228e4    -1.529e5];

VA1=A(2,1)-1i * A(1,1);
VB1=A(2,2)-1i * A(1,2);
VC1=A(2,3)-1i * A(1,3);

VA2=A(8,1)-1i * A(7,1);
VB2=A(8,2)-1i * A(7,2);
VC2=A(8,3)-1i * A(7,3);

VA3=A(14,1)-1i * A(13,1);
VB3=A(14,2)-1i * A(13,2);
VC3=A(14,3)-1i * A(13,3);

VA4=A(20,1)-1i * A(19,1);
VB4=A(20,2)-1i * A(19,2);
VC4=A(20,3)-1i * A(19,3);
stdang=0.006*2;
stdmag=0.012;

%%%%%%%%%%%%%%%%%%%%%% Z Vector Data %%%%%%%%%%%%%%%%%%%%%%%%%%%%%%
B=[-11.385
42.49
```

```
41.652
-16.709
-32.412
-23.796
-8.836
40.297
44.219
-15.659
-33.456
-23.205
-9.95
39.472
40.488
-12.596
-35.76
-25.981
-9.715
40.267
41.635
-16.71
-31.764
-23.876
];
stdmagc=0.017;

[VA1theta,VA1mag]=cart2pol(real(VA1), imag(VA1))
[VB1theta,VB1mag]=cart2pol(real(VB1), imag(VB1))
[VC1theta,VC1mag]=cart2pol(real(VC1), imag(VC1))
[VA2theta,VA2mag]=cart2pol(real(VA2), imag(VA2))
[VB2theta,VB2mag]=cart2pol(real(VB2), imag(VB2))
[VC2theta,VC2mag]=cart2pol(real(VC2), imag(VC2))
[VA3theta,VA3mag]=cart2pol(real(VA3), imag(VA3))
[VB3theta,VB3mag]=cart2pol(real(VB3), imag(VB3))
[VC3theta,VC3mag]=cart2pol(real(VC3), imag(VC3))
[VA4theta,VA4mag]=cart2pol(real(VA4), imag(VA4))
[VB4theta,VB4mag]=cart2pol(real(VB4), imag(VB4))
[VC4theta,VC4mag]=cart2pol(real(VC4), imag(VC4))

for jj=1:4
    [IAtheta(jj),IAmag(jj)]=cart2pol(B(6*(jj-1)+1),B(6*jj-4));
    [IBtheta(jj),IBmag(jj)]=cart2pol(B(6*(jj-1)+3),B(6*(jj)-2));
    [ICtheta(jj),ICmag(jj)]=cart2pol(B(6*(jj-1)+5),B(6*(jj)));
end
[stdreaA,stdimaA]=RcovAhmed(IAtheta,IAmag,stdang,stdmagc);
[stdreaB,stdimaB]=RcovAhmed(IBtheta,IBmag,stdang,stdmagc);
[stdreaC,stdimaC]=RcovAhmed(ICtheta,ICmag,stdang,stdmagc);
for jj=1:4
stdvec(6*(jj-1)+1)=stdreaA(jj);
stdvec(6*jj-4)=stdimaA(jj);
stdvec(6*(jj-1)+3)=stdreaB(jj);
stdvec(6*(jj)-2)=stdimaB(jj);
```

```
stdvec(6*(jj-1)+5)=stdreaC(jj);
stdvec(6*(jj))=stdimaC(jj);
end
Rcov=diag(stdvec.^2);

ISA4=(-11.385+42.49i);ISB4=(-385.966-205.222i);ISC4=(150.629+407.422i);
ISA5=(268.379-320.978i);ISB5=(44.219-15.659i);ISC5=(27.088+430.555i);
ISA6=(366.967-237.401i);ISB6=(-424.349-67.21i);ISC6=(-35.76-25.981i);
ISA8=(327.181-306.171i);ISB8=(-439.259-151.249i);ISC8=(90.923+468.197i);
%%
VSA4=(1.314*10^5+2.308i*10^4);VSB4=(-4.484*10^4-1.249i*10^5);VSC4=(-8.602*10^4+1.↙
013i*10^5);
VSA5=(1.308*10^5+2.379i*10^4);VSB5=(-4.57*10^4-1.253i*10^5);VSC5=(-8.577*10^4+1.↙
013i*10^5);
VSA6=(1.306*10^5+2.362i*10^4);VSB6=(-4.477*10^4-1.252i*10^5);VSC6=(-8.565*10^4+1.↙
022i*10^5);
VSA8=(1.307*10^5+2.376i*10^4);VSB8=(-4.474*10^4-1.25i*10^5);VSC8=(-8.59*10^4+1.↙
012i*10^5);
%%
VRA4=(1.393*10^5+3.095i*10^4);VRB4=-4.056*10^4-1.026i*10^5;VRC4=-6.212*10^4+1.006i*10^5;
VRA5=1.165*10^5+3.512i*10^3;VRB5=-4.469*10^4-1.378i*10^5;VRC5=-6.711*10^4+8.736i*10^4;
VRA6=1.092*10^5+1.617i*10^4;VRB6=-5.609*10^4-1.041i*10^5;VRC6=-9.533*10^4+1.095i*10^5;
VRA8=1.157*10^5+1.431i*10^4;VRB8=-4.754*10^4-1.074i*10^5;VRC8=-6.698*10^4+9.783i*10^4;
%%%%%%%%%%%%%%%%%%%%%%%%%%%%%%%%%%%%%%%%%%%%
VS= zeros(12,1);
VS=[VSA4
    VSB4
    VSC4
    VSA5
    VSB5
    VSC5
    VSA6
    VSB6
    VSC6
    VSA8
    VSB8
    VSC8
    ];

VR= zeros(12,1);
VR=[VRA4
    VRB4
    VRC4
    VRA5
    VRB5
    VRC5
    VRA6
    VRB6
    VRC6
    VRA8
    VRB8
```

```
    VRC8
    ];
%%%%%%%%%%%%%%%%%%%%%%%%%%%%%%%%%%%%%%%%%%%%%%%%%%%%%%%%%%%%%%%%%%%%%%%%%%%%%%%%
IS = zeros(12,1);
IS=[ISA4
    ISB4
    ISC4
    ISA5
    ISB5
    ISC5
    ISA6
    ISB6
    ISC6
    ISA8
    ISB8
    ISC8
    ];

[stdreaVS,stdimaVS]=RcovAhmedIs(VS,stdang,stdmag);
[stdreaVR,stdimaVR]=RcovAhmedIs(VR,stdang,stdmag);

for jj=1:length(IS)
stdvec2(jj)=stdreaVS(jj)+li*stdimaVS(jj);
stdvec3(jj)=stdreaVR(jj)+li*stdimaVR(jj);
end
Rcov2S=diag(abs(stdvec2).^2);
Rcov2R=diag(abs(stdvec3).^2);
Rcov2=Rcov2S+Rcov2R;
%Rcov2=eye(12);

mc=100;
zave=0;
stdn=0.001;
stdnm=0.001;

for ij=1:mc

    [VA1nreal,VA1nimag]=pol2cart(VA1theta+stdang*rand(1)*pi/180,VA1mag*(1+stdmag*randn↙
(1)))

    [VB1nreal,VB1nimag]=pol2cart(VB1theta+stdang*rand(1)*pi/180,VB1mag*(1+stdmag*randn↙
(1)))

    [VC1nreal,VC1nimag]=pol2cart(VC1theta+stdang*rand(1)*pi/180,VC1mag*(1+stdmag*randn↙
(1)))

    [VA2nreal,VA2nimag]=pol2cart(VA2theta+stdang*rand(1)*pi/180,VA2mag*(1+stdmag*randn↙
(1)))

    [VB2nreal,VB2nimag]=pol2cart(VB2theta+stdang*rand(1)*pi/180,VB2mag*(1+stdmag*randn↙
(1)))
```

```
    [VC2nreal,VC2nimag]=pol2cart(VC2theta+stdang*rand(1)*pi/180,VC2mag*(1+stdmag*randn↙
(1)))

    [VA3nreal,VA3nimag]=pol2cart(VA3theta+stdang*rand(1)*pi/180,VA3mag*(1+stdmag*randn↙
(1)))

    [VB3nreal,VB3nimag]=pol2cart(VB3theta+stdang*rand(1)*pi/180,VB3mag*(1+stdmag*randn↙
(1)))

    [VC3nreal,VC3nimag]=pol2cart(VC3theta+stdang*rand(1)*pi/180,VC3mag*(1+stdmag*randn↙
(1)))

    [VA4nreal,VA4nimag]=pol2cart(VA4theta+stdang*rand(1)*pi/180,VA4mag*(1+stdmag*randn↙
(1)))

    [VB4nreal,VB4nimag]=pol2cart(VB4theta+stdang*rand(1)*pi/180,VB4mag*(1+stdmag*randn↙
(1)))

    [VC4nreal,VC4nimag]=pol2cart(VC4theta+stdang*rand(1)*pi/180,VC4mag*(1+stdmag*randn↙
(1)))

An(1,:) =[-VA1nimag  -VB1nimag  -VC1nimag   0   0   0];
An(2,:) =[VA1nreal  VB1nreal    VC1nreal    0   0   0];
An(3,:) =[0        -VA1nimag    0    -VB1nimag  -VC1nimag   0];
An(4,:) = [0       VA1nreal     0   VB1nreal    VC1nreal    0];
An(5,:) =[0             0 -VA1nimag 0    -VB1nimag  -VC1nimag];
An(6,:) =[0     0   VA1nreal    0   VB1nreal    VC1nreal];

An(7,:) =[-VA2nimag  -VB2nimag  -VC2nimag   0   0   0];
An(8,:) =[VA2nreal  VB2nreal    VC2nreal    0   0   0];
An(9,:) =[0        -VA2nimag    0    -VB2nimag  -VC2nimag   0];
An(10,:) = [0      VA2nreal     0   VB2nreal    VC2nreal    0];
An(11,:) =[0                0 -VA2nimag 0    -VB2nimag  -VC2nimag];
An(12,:) =[0        0   VA2nreal    0   VB2nreal    VC2nreal];

An(13,:) =[-VA3nimag     -VB3nimag  -VC3nimag   0   0   0];
An(14,:) =[VA3nreal VB3nreal    VC3nreal    0   0   0];
An(15,:) =[0           -VA3nimag    0    -VB3nimag  -VC3nimag   0];
An(16,:) = [0      VA3nreal     0   VB3nreal    VC3nreal    0];
An(17,:) =[0          0   -VA3nimag 0    -VB3nimag  -VC3nimag];
An(18,:) =[0        0   VA3nreal    0   VB3nreal    VC3nreal];

An(19,:) =[-VA4nimag     -VB4nimag  -VC4nimag   0   0   0];
An(20,:) =[VA4nreal VB4nreal    VC4nreal    0   0   0];
An(21,:) =[0           -VA4nimag    0    -VB4nimag  -VC4nimag   0];
An(22,:) = [0      VA4nreal     0   VB4nreal    VC4nreal    0];
An(23,:) =[0        0  -VA4nimag    0    -VB4nimag  -VC4nimag];
An(24,:) =[0        0   VA4nreal    0   VB4nreal    VC4nreal];

for jj=1:4
```

```
[IAnreal(jj),IAnimag(jj)]=pol2cart(IAtheta(jj)+stdang*rand(1)*pi/180,IAmag(jj)*↙
(1+stdmagc*randn(1)));
%%
[IBnreal(jj),IBnimag(jj)]=pol2cart(IBtheta(jj)+stdang*rand(1)*pi/180,IBmag(jj)*↙
(1+stdmagc*randn(1)));
%%
[ICnreal(jj),ICnimag(jj)]=pol2cart(ICtheta(jj)+stdang*rand(1)*pi/180,ICmag(jj)*↙
(1+stdmagc*randn(1)));
%%
Bn(6*(jj-1)+1)=IAnreal(jj);
Bn(6*jj-4)=IAnimag(jj);
Bn(6*(jj-1)+3)=IBnreal(jj);
Bn(6*(jj)-2)=IBnimag(jj);
Bn(6*(jj-1)+5)=ICnreal(jj);
Bn(6*(jj))=ICnimag(jj);
end
Bn=reshape(Bn,length(Bn),1);
Berror=Bn;
Aerror=An;

CovR=Rcov;
Lcho=chol(CovR,'lower');
BerrorN=(Lcho)\Berror;
AerrorN=(Lcho)\Aerror;

results=mltsY3M(AerrorN,BerrorN,0.03,1);
beta(:,ij)=results.beta;

Y1=beta(1,ij);
Y2=beta(2,ij);
Y3=beta(3,ij);
Y4=beta(4,ij);
Y5=beta(5,ij);
Y6=beta(6,ij);

for ii=1:length(IS)
[ISr(ii),ISm(ii)]= coverty(real(IS(ii)),imag(IS(ii)),stdmagc)
IServer(ii)=ISr(ii)+1i*ISm(ii);
end
%VSerror=VS+stdn.*VS.*randn(length(VS),1);
for ii=1:length(VS)
[VSr(ii),VSm(ii)]= coverty(real(VS(ii)),imag(VS(ii)),stdmag);
VSerror(ii)=VSr(ii)+1i*VSm(ii);
end
%%%%%%%%%%%%%%%%%%%%%%%%%%%%%%%%%%%%%%%%%%%%%%%
Y= zeros(12,12);
Y(1,:) =[Y1 Y2 Y3 0 0 0 0 0 0 0 0 0 ];
Y(2,:) =[Y2 Y4 Y5 0 0 0 0 0 0 0 0 0 ];
Y(3,:) =[Y3 Y5 Y6 0 0 0 0 0 0 0 0 0 ];
Y(4,:) =[0 0 0 Y1 Y2 Y3 0 0 0 0 0 0 ];
Y(5,:) =[0 0 0 Y2 Y4 Y5 0 0 0 0 0 0 ];
```

```
Y(6,:) =[0 0 0 Y3 Y5 Y6 0 0 0 0 0 0 ];
Y(7,:) =[0 0 0 0 0 0 Y1 Y2 Y3 0 0 0 ];
Y(8,:) =[0 0 0 0 0 0 Y2 Y4 Y5 0 0 0 ];
Y(9,:) =[0 0 0 0 0 0 Y3 Y5 Y6 0 0 0 ];
Y(10,:) =[0 0 0 0 0 0 0 0 0 Y1 Y2 Y3 ];
Y(11,:) =[0 0 0 0 0 0 0 0 0 Y2 Y4 Y5 ];
Y(12,:) =[0 0 0 0 0 0 0 0 0 Y3 Y5 Y6 ];
%%%%%%%%%%%%%%%%%%%%%%%%%%%%%%%%%%%%%%%%%%%%%%%
IL=ISerror'-(Y*VSerror');
ILA4=IL(1);
ILB4=IL(2);
ILC4=IL(3);
ILA5=IL(4);
ILB5=IL(5);
ILC5=IL(6);
ILA6=IL(7);
ILB6=IL(8);
ILC6=IL(9);
ILA8=IL(10);
ILB8=IL(11);
ILC8=IL(12);

  I=[ILA4 ILB4 ILC4 0 0 0;
     0  ILA4 0 ILB4 ILC4 0;
    0 0  ILA4 0 ILB4 ILC4;
    ILA5 ILB5 ILC5 0 0 0;
     0  ILA5 0 ILB5 ILC5 0;
    0 0  ILA5 0 ILB5 ILC5;
    ILA6 ILB6 ILC6 0 0 0;
     0  ILA6 0 ILB6 ILC6 0;
    0 0  ILA6 0 ILB6 ILC6;
    ILA8 ILB8 ILC8 0 0 0;
     0  ILA8 0 ILB8 ILC8 0;
    0 0  ILA8 0 ILB8 ILC8;
    ];
%VRerror=VR+stdn.*VR.*randn(length(VR),1);
for ii=1:length(VR)
[VRr(ii),VRm(ii)]= coverty(real(VR(ii)),imag(VR(ii)),stdmag);
VRerror(ii)=VRr(ii)+1i*VRm(ii);
end

VZ=VSerror-VRerror;
%VZ=reshape(VZ,length(VZ),1);
%%%
CovR2=Rcov2;
Lcho=chol(CovR2,'lower');
VzerN=(Lcho)\VZ';
IerN=(Lcho)\I;

%zresults=mltsY3M(IerN,VzerN,0.03,1);
zresults=mltsY3M(IerN,VzerN,0.03,1);
```

```
zbeta(:,ij)=zresults.beta;
zmag=abs(zbeta);
zang=angle(zbeta)*180/pi;
zmat=[zbeta(1,ij) zbeta(2,ij) zbeta(3,ij);zbeta(2,ij) zbeta(4,ij) zbeta(5,ij);zbeta(3,ij)
zbeta(5,ij) zbeta(6,ij)];
zbet012=A012\(zmat*A012);
zeromag(ij)=abs(zbet012(1,1))
zeroang(ij)=(180/pi)*angle(zbet012(1,1))
%%%%%%%%%%%%%%%%%%%%%%%%%%%%%%%%%%%%%%%%
zposmag(ij)=abs(zbet012(2,2))
zposang(ij)=(180/pi)*angle(zbet012(2,2))
zave=(zave+zbeta(:,ij));
end
zfinalmag=mean(zmag');
zfinalang=mean(zang');
zfinalmag
zfinalang
zave=zave/mc;
for iu=1:6
zstd(iu)=std(real(zbeta(iu,:)))+1i*std(imag(zbeta(iu,:)));
end
zavemat=[zave(1) zave(2) zave(3);zave(2) zave(4) zave(5);zave(3) zave(5) zave(6)]
zstdmat=[zstd(1) zstd(2) zstd(3);zstd(2) zstd(4) zstd(5);zstd(3) zstd(5) zstd(6)]
zave012=A012\(zavemat*A012)
zstd012=A012\(zstdmat*A012)
%%%%%%%%%%%%%%%%%%%%%%%%%%%%%%%%%%%%%%%%%%%%%%%%%%%%%%%%%%%%
avezeromag=mean(zeromag);
stdzeromag=std(zeromag);

avezeroang=mean(zeroang);
stdzeroang=std(zeroang);

aveposmag=mean(zposmag);
stdposmag=std(zposmag);

aveposang=mean(zposang);
stdposang=std(zposang);

aveposmag
stdposmag

aveposang
stdposang

avezeromag
stdzeromag

avezeroang
stdzeroang
```